Prepared for:

DG Rijkswaterstaat,

Rijksinstituut voor Kust en Zee | RIKZ

Description of improvements in the UNIBEST-TC model

Upgrade of UNIBEST-TC Version 2.04 to 2.10

D.J.R. Walstra en H.J. Steetzel

Research Report

July 2003

Z3412

WL | delft hydraulics

Prepared for:

DG Rijkswaterstaat,

Rijksinstituut voor Kust en Zee | RIKZ

Description of improvements in the UNIBEST-TC model

Upgrade of UNIBEST-TC Version 2.04 to 2.10

D.J.R. Walstra en H.J. Steetzel

Research Report

July 2003

Z3412

CLIENT: DG Rijkswaterstaat
Rijks-Instituut voor Kust en Zee | RIKZ

TITLE: Description of improvements in the Unibest-TC model; Upgrade of Unibest-TC Version 2.04 to Version 2.10

ABSTRACT:

This report describes the implementation and subsequent testing of several new expressions into UNIBEST-TC, a process based profile model predicting the morphological profile development under the combined forcing of waves and tidal longshore currents. This study is carried out in the framework of the 'strategic cooperation' between RIKZ and WL | DELFT HYDRAULICS (VOP2002 Project 2).

The implementations have been verified by comparing results obtained with both the upgraded and the original version of UNIBEST-TC with results from the engineering transport point model TRANSPOR2000 and with laboratory tests in the Delta flume (LIP11D experiments: Test 1A, 1B and 1C) part of the UNIBEST-TC Testbank (Roelvink, 2000 and Walstra et al., 2001).

Unfortunately despite the improvements suggested and implemented in UNIBEST-TC in this study it thought that site-specific calibrations will still be necessary. Moreover, the limited verification runs have shown that the sediment transports in the improved UNIBEST-TC model have changed considerably. This implies that application of the new model to sites investigated with previous UNIBEST-TC model versions will require complete new calibrations. However, this is an inevitable process which has explicitly been identified in the VOP-project as the Development – Testing – Evaluation cycle.

The improvements and results presented in this report should be seen as a first step in integrating the DUROSTA approach into UNIBEST-TC. It was shown that both model generally give similar solutions which is, considering the different wave and transport models, somewhat surprising.

REFERENCES: Opdracht RKZ-1214

VER.	ORIGINATOR		DATE	REMARKS	REVIEW		APPROVED BY	
1.0	D.J.R. Walstra		1 July 2003	Final	L.C. van Rijn		A. Roelfzema	

PROJECT IDENTIFICATION: Z3412

KEYWORDS: Unibest-TC, TRANSPOR2000, Profile model, Dune erosion

NUMBER OF PAGES 87

CONFIDENTIAL: ☐ YES, until (date) ☒ NO

STATUS: ☐ PRELIMINARY ☐ DRAFT ☒ FINAL

Contents

Summary

This report describes the implementation and subsequent testing of several new expressions into UNIBEST-TC, a process based profile model predicting the morphological profile development under the combined forcing of waves and tidal longshore currents. This study is carried out in the framework of the 'strategic cooperation' between RIKZ and WL | DELFT HYDRAULICS (VOP2002 Project 2).

The following items were implemented successfully:
1. Upgrade of the transport module using the TRANSPOR2000 formulations (Van Rijn, 2000).
2. Implementation of the Isobe-Horikawa approach to model the near-bed orbital velocities (Grasmeijer and Van Rijn, 1998).
3. Inclusion of wave related suspended sediment transport (Houwman and Ruessink, 1996).
4. Upgrade of the near bed velocities used to determine the bed load transports following Reniers et al. (2003).
5. Harmonisation of the wave dissipation in the wave boundary layer in the flow module.
6. Implementation of a variable γ expression (wave height over water depth ratio in B&J wave model) following Ruessink et al. (2003).
7. Implementation of the extrapolations methods of DUROSTA (Steetzel, 1993) in UNIBEST-TC following the suggestions of Walstra et al. (2001).
8. A number of small modifications that have been carried out in the past year (summarised in Section 2.5)

The implementations listed above constitute the upgrade of UNIBEST-TC from Version 2.04 to Version 2.10.

The implementations have been verified by comparing results obtained with both the upgraded and the original version of UNIBEST-TC with results from the engineering transport point model TRANSPOR2000 and with laboratory tests in the Delta flume (LIP11D experiments: Test 1A, 1B and 1C) part of the UNIBEST-TC Testbank (Roelvink, 2000 and Walstra et al., 2001).

The main findings are summarised below:
- The upgrade of UNIBEST-TC' transport model to the TRANSPOR2000 formulations (Van Rijn (2000) and the implementation of the Isobe-Horikawa non-linear wave theory have resulted in identical results compared to the TRANSPOR2000 point model.
- The modification of the long wave effects on the bed load can have a significant effect on the resulting bed load transport. Especially, in the surf zone where wave breaking is most intense (e.g. near bars) the bed load transport was much too sensitive to the long wave motion in case of relative low waves. The considered simulations showed that the new approach resulted in a dramatic decrease of the seaward transport for LIP11D Test 1C on top of bars and could even cause a shift from offshore to onshore transports.
- The inclusion of wave related suspended transports is imperative for an accurate prediction of the total suspended sediment transport. In the considered cases the wave

related suspended transport are dominant or of the same order of magnitude compared to the offshore directed undertow related suspended transport.

- Comparison of the Isobe-Horikawa and Rienecker&Fenton non-linear wave theories showed that the onshore peak velocities had a surprisingly similar cross-shore distribution. However, the offshore peaks were significantly under-predicted by the Rienecker&Fenton model. The resulting bed load transports showed that with Isobe-Horikawa a better qualitative agreement was obtained for the total transports.
- The implementation of the DUROSTA functionality to model dune erosion has shown that the DUROSTA concept is an improvement to the existing formulation of UNIBEST-TC. The verification study for a number of large scale flume experiments showed that in most cases the behaviour of the beach/dune area was comparable to DUROSTA results. However, the significant wave run-up, which is vital for accurate predictions, had to be limited to the offshore wave height in UNIBEST-TC. The discrepancies between both models are thought to be mainly due to:
  1. the different approaches in both models to determine the transition point (i.e. last wet point) at which the dune erosion formulations are valid,
  2. the 'lack' of (numerical) swash in the region near the waterline,
  3. the determination of the characteristic slope (in DUROSTA this parameter and the transition point are determined exactly whereas in UNIBEST-TC these are determined on the computational grid which can cause relative large differences).

The knowledge of cross-shore processes is still very limited. This lack of knowledge is mainly caused by the inability to accurately predict the cross-shore distribution of the breaking wave forces and the associated sediment transport. As a result, usually site-specific calibrations have to be carried out. Unfortunately despite the improvements suggested and implemented in UNIBEST-TC in this study it thought that site-specific calibrations will still be necessary. Moreover, the limited verification runs have shown that the sediment transports in the improved UNIBEST-TC model have changed considerably. This implies that application of the new model to sites investigated with previous UNIBEST-TC model versions will require complete new calibrations. However, this is an inevitable process which has explicitly been identified in the VOP-project as the Development – Testing – Evaluation cycle (see e.g. Walstra et al., 2001).

The improvements and results presented in this report should be seen as a first step in integrating the DUROSTA approach into UNIBEST-TC. It was shown that both model generally give similar solutions which is, considering the different wave and transport models, somewhat surprising. The differences in model outcomes have been summarised above and lead to recommendations to solve the remaining discrepancies between both models regarding the treatment of dune erosion. It has to be noted however that the aim is not to find an exact match between both models, but to extend the DUROSTA approach implemented in UNIBEST-TC to the same level as in the DUROSTA model.

It is therefore recommended to initiate a verification study which addresses important processes on which the knowledge is limited or are known to be modelled inaccurately by the upgraded UNIBEST-TC model. In addition, to extend the modelling of the dry part of the profile in UNIBEST-TC to the same level as the original DUROSTA model a detailed comparison of both models is necessary. Although it is difficult to assess beforehand which improvements will have the greatest influence on the results it is our opinion that the following issues should be dealt with first (in order of importance):

1. The position of the transition zone should be synchronised. It is recommended to implement the DUROSTA method which uses a quarter of the local wave length from the water line to assess the transition point.
2. The calculation of the significant wave run-up should be improved. It is not clear at this stage why the run up has to be limited to the offshore wave height in UNIBEST-TC.
3. In DUROSTA the above parameters are determined exactly and are not coupled to the applied numerical grid as in UNIBEST-TC. Considering the large transport gradients present in the inner surf zone it is imperative to implement this in UNIBEST-TC as well.
4. The above also hold for the determination of the characteristic slope which is used to determine the wave run-up. This expression should also be compared in detail with results from the DUROSTA model.

Subsequently a study should be undertaken to investigates the performance of the improved Unibest-TC model to simulate the dry part of the beach for other hydraulic conditions. In the present study the model has been applied only to investigate the effect of storm conditions. The effect of mild conditions, which might generate even onshore-directed transport have not yet been investigated. Such an elaboration seems a very logical step, since this will extend and improve the model’s applicability to simulate coastal behaviour for the medium term and thus make it a more useful instrument to assess the effect of large-scale (beach) nourishments.

The evaluation of the model should be based on aggregated parameters such as beach width, dune volume, etc to provide coastal authorities insight in the performance and the applicability of the model as a support tool for coastal policy issues.

1 Introduction

1.1 General

This study is aimed at implementing a number of improvements in WL|Delft Hydraulics' UNIBEST-TC model. The items that have been improved are based on weak points identified in various discussions between WL | Delft Hydraulics and RIKZ some of which are listed below.

1. The landward migration of breaker bars during calm weather and the behaviour of the shoreface are not properly modelled owing to an insufficient accuracy of the prediction of net effects of the cross-shore transport mechanisms.
2. There is a clear need for a new 'engineering' sand transport formulation, in which also the wave related suspended sediment transport is taken into account (*e.g.* TRANSPOR2000)
3. Modelling the wave-group bounded long waves and especially the phase difference between the long waves and the wave group, which influences the rate of sediment transport, should be paid attention to.
4. The coherence between the different modules of the UNIBEST-TC program is not optimal. For example, no relation exists between the viscosity profile and the diffusivity profile. In relation with this point, the expressions for bottom roughness (including input parameters) are not uniform.
5. The wave model is unable to accurately predict the rapid decrease of waves over bars.
6. The calculation of wave asymmetry can be improved, e.g. by implementation of the Isobe-Horikawa method.
7. The advection type description implemented in 2000 (van Kessel, 2000) has been compared with DUROSTA simulations in Walstra et al. (2001). This study showed that that both models yielded comparable results for cases where the dune eroded over its complete height. However, UNIBEST-TC was unable to represent a partial erosion of the dune.

These weak points have resulted in the implementation of the following improved or new expressions in UNIBEST-TC:
1. Upgrade of the transport module using the TRANSPOR2000 formulations (Van Rijn, 2000).
2. Implementation of the Isobe-Horikawa approach to model the near-bed orbital velocities (Grasmeijer and Van Rijn, 1998).
3. Inclusion of wave related suspended sediment transport (Houwman and Ruessink, 1996).
4. Upgrade of the near bed velocities used to determine the bed load transports following Reniers et al. (2003).
5. Harmonisation of the wave dissipation in the wave boundary layer in the flow module.
6. Implementation of a variable γ expression (wave height over water depth ratio in B&J wave model) following Ruessink et al. (2003).
7. Implementation of the extrapolations methods of DUROSTA (Steetzel, 1993) in UNIBEST-TC following the suggestions of Walstra et al. (2001).

8. A number of small modifications that have been carried out in the past year (summarised in Section 2.5)

The implementations listed above constitute the upgrade of UNIBEST-TC from Version 2.04 to Version 2.10.

This study is carried out in the framework of the ‘strategic cooperation’ between RIKZ and WL (VOP2002 Project 2).

1.2 Methodology

The upgrade to the TRANSPOR2000 transport model and the implementation of the Isobe-Horikawa non-lineair wave model were already partly carried out in a previous study (Van Kessel, 2000) which constituted the upgrade from Version 2.03 to Version 2.04. However in this study the comparison with Van Rijn’s TRANSPOR2000 point model resulted in unacceptable large differences. These were partly caused by the fact that not all formulations were updated and the fact that the test cases used for the comparison were unsuitable for comparison with the point model due to wave decay.

In this study version 2.04 was reviewed thoroughly and updated were necessary. Next, the Items 2 to 6 were implemented and tested. The description of the formulations and the verification results can be found in Chapter 2.

The implementation of the extrapolations methods of DUROSTA (Steetzel, 1993) in UNIBEST-TC following the suggestions of Walstra et al. (2001) were first carried out in Version 2.03 (TRANSPOR1993 transport model) so that a comparison could be made with earlier results (Walstra et al. 2001). In Chapter 3 a description is given of the extrapolation methods transferred from DUROSTA to UNIBEST-TC. Furthermore, a detailed comparison is made for a large number of dune erosion experiments in large wave flumes. In this comparison the DUROSTA results are compared with the upgraded UNIBEST-TC model.

2 Upgrade of UNIBEST-TC

2.1 Introduction

The upgrade to the TRANSPOR2000 transport model and the implementation of the Isobe-Horikawa non-lineair wave model were already partly carried out in a previous study (Van Kessel, 2000) which constitutes the upgrade from Version 2.03 to Version 2.04. However in this study the comparison with Van Rijn's TRANSPOR2000 point model resulted in unacceptable large differences. These were partly caused by the fact that not all formulations were updated and the fact that the test cases used for the comparison were unsuitable for comparison with the point model due to wave decay.

In this chapter first an improvement of the Battjes&Janssen model is described by introducing a cross-shore varying γ (a wave height-to-depth ratio) in Section 2.2. Next, the upgraded bed transport model and suspended transport model are described in Sections 2.3 and 2.4, respectively. Finally the upgraded model is verified in Section 2.5.

2.2 Wave model

Since its introduction in 1978, the Battjes and Janssen model has proven to be a popular framework for estimating the cross-shore root-mean-square wave height H_{rms} transformation of random breaking waves in shallow water. Previous model tests have shown that wave heights in the bar trough of single bar systems and in the inner troughs of multiple bar systems are over predicted by up to 60% when the settings for the free model parameter γ (a wave height-to-depth ratio) are used according to Battjes and Stive (1985). In a study, partly supported by this project, a new functional form for γ is derived empirically by an inverse modelling of γ from a high-resolution (in the cross-shore) 300 hours H_{rms} data set collected at Duck, NC, USA. We find that, in contrast to the standard setting, γ is not cross-shore constant, but depends systematically on the product of the local wave number k and water depth h:

$$\gamma = 0.29 + 0.76kh \tag{2.1}$$

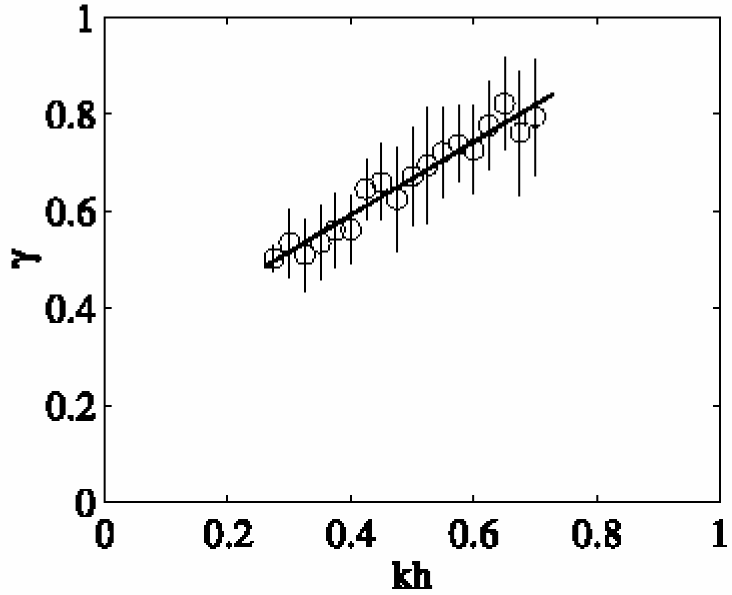

Figure 2.1 Average (circles) and standard deviation (vertical bars) of γ versus *kh* based on all estimates with a wave dissipation higher than 15 N/ms. The solid line is the least squares linear fit, Eq. (2.1).

Model verification with other data at Duck, and data collected at Egmond and Terschelling (Netherlands), spanning a total of about 1600 hours, shows that cross-shore H_{rms} profiles modelled with the locally varying γ are indeed in better agreement with measurements than model predictions using the cross-shore constant γ. In particular, model accuracy in inner bar troughs increases by up to 80%. Additional verifications with data collected on planar laboratory beaches show the new functional form of γ to be applicable to non-barred beaches as well. Eq. (2.1) has been implemented in UNIBEST-TC.

This work was published in the Journal of Coastal Engineering:

> Ruessink, B.G., Walstra, D.J.R. and Southgate, H.N., 2003. Calibration and verification of a parametric wave model on barred beaches. *Journal of Coastal Engineering 1051 (2003) 1-11.*

This publication can be found in Appendix B.

2.3 Bed transport

The net bed-load transport rate in conditions with uniform bed material is obtained by time-averaging (over the wave period T) of the instantaneous transport rate using a bed-load transport formula (quasi-steady approach), as follows:

$$q_b = \frac{1}{T}\int q_{b,t}\,dt \qquad (2.2)$$

with: $q_{b,t} = f($ instantaneous hydrodynamic and sediment transport parameters).

The applied bed-load transport formula is a parameterization of a detailed grain saltation model representing the basic forces acting on a bed-load particle for steady flow (Van Rijn, 1984a, 1993). This approach is generalized to the regime of combined current and wave conditions by using the concept of the instantaneous bed-shear stress. The instantaneous bed-load transport rate (kg/s/m) is related to the instantaneous bed-shear stress, which is based on the instantaneous velocity vector (including both wave-related and current-related components) defined at a small height above the bed. The formula applied, reads as:

$$q_b(t) = \gamma \rho_s D_*^{-0.3} \left(\frac{\tau'_{b,cw}}{\rho} \right)^{0.5} \left(\frac{\tau'_{b,cw} - \tau_{b,cr}}{\tau_{b,cr}} \right)^{\eta} \tag{2.3}$$

in which: $\tau'_{b,cw}$ is the instantaneous grain-related bed-shear stress due to both currents and waves, $\tau_{b,cr}$ the critical bed-shear stress according to Shields, ρ_s the sediment density, ρ the fluid density, d_{50} the particle size, D_* the dimensionless particle size, $\tau_{b,cr}$ is the critical bed-shear stress according to Shields, γ and η are constants (0.5 and 1.0, respectively).

The instantaneous grain-related bed-shear stress due to both currents and waves is written as:

$$\tau'_{b,cw} = 0.5 \rho f'_{cw} u^2_{\delta,cw} \tag{2.4}$$

where $u_{\delta,cw}$ is the time-dependent (intra-wave) near-bottom horizontal velocity vector of the combined wave-current motion at the top of the wave boundary layer and f'_{cw} is the grain friction coefficient due to currents and waves:

$$f'_{cw} = \alpha \beta f'_c + (1-\alpha) f'_w \tag{2.5}$$

where f'_c is the current-related grain friction coefficient, f'_w is the wave-related grain friction coefficient, α is the coefficient related to relative strength of wave and current motion, β is the wave-current-interaction coefficient (Appendix B, Van Rijn, 1993). The expression for f'_c reads:

$$f'_c = 0.24 \log^{-2} \left(\frac{12h}{k_{s,grain}} \right) \tag{2.6}$$

The grain roughness is assumed to be $k_{s,grain}=\varepsilon d_{90}$ with $\varepsilon=3$ for $d_{50}<0.5$ mm; $\varepsilon=1$ for $d_{50}>1$ mm and $\varepsilon=3$ to 1 for intermediate values (van Rijn, 1993). The expression for f'_w reads:

$$f'_w = \exp\left[-6 + 5.2 \left(\frac{\hat{A}_\delta}{3D_{90}} \right)^{-0.19} \right] \tag{2.7}$$

where $\hat{A}_\delta$ is the near bed peak orbital excursion according to lineair wave theory.

The bed-load transport is assumed to be mainly affected by the grain roughness, but the overall bed-form roughness also has some (weak) influence on the bed-load transport in case of combined steady and oscillatory flow because of its effect on the near-bed velocity profile. Analysis of sensitivity computations for combined steady and oscillatory flow shows that the bed-load transport is reduced by about 15% for an increase of the bed-form roughness by a factor of 5 ($k_{s,c}$= 0.05 m in stead of 0.01 m).

Eq. (2.3) yields slightly modified transports compared to the Van Rijn (1993) formulations, as the difference between both formulations comes from updated values for γ and η. These were derived by calibrating Eq. (2.3) on new datasets (Van Rijn, 2000).

The instantaneous cross- and longshore transport components are obtained from:

$$q_{bx} = \frac{u_{\delta,cw,x}}{\left|u_{\delta,cw}\right|}\left|q_b\right| \qquad q_{by} = \frac{u_{\delta,cw,y}}{\left|u_{\delta,cw}\right|}\left|q_b\right| \tag{2.8}$$

in which $u_{\delta,cw,x}$, $u_{\delta,cw,y}$ and q_b are respectively the time-dependent (intra-wave) near-bottom horizontal velocity vector and the bed-load transport vector of the combined wave-current motion.

In the previous versions of UNIBEST-TC the near-bed velocity (orbital motion) due to non-linear short waves and long waves related to wave groups was used in Eq. (2.4):

$$u_{\delta,cw} = u_{\delta,c} + u_{\delta,sw} + u_{\delta,lw} \tag{2.9}$$

in which $u_{\delta,c}$ is the averaged velocity at 1 cm above the bed, $u_{\delta,sw}$ the near bed orbital velocity due to short waves and $u_{\delta,lw}$ is the long wave component (all in m/s).

However this is conceptually incorrect because, as stated by Reniers et al. (2003), the calibration of the bed load formulation was based on comparison with measurements ignoring the explicit infragravity wave contribution in the stirring. Therefore the Reniers et al. (2003) approach is followed which assumes that the additional stirring of sediment by the infragravity motions is not explicitly taken into account, but instead is assumed to be implicit in the near bed orbital motion. This implies that the intra-wave velocity signal is used to determine the instantaneous bed load transport in Eq.(2.4):

$$u'_{\delta,cw} = u_{\delta,c} + u_{\delta,sw} \tag{2.10}$$

whereas the advection, Eq. (2.8), is based on the complete near bed velocity signal including long wave effects according to Eq. (2.9).

In UNIBEST-TC three options have been introduced to determine the velocity signals used for the bed-load transport via a new parameter SWLONG:

- SWLONG=1: Original implementation ($u_{\delta,cw}$ used for stirring and advection following Eq. (2.9)),
- SWLONG=2: Improved implementation ($u'_{\delta,cw}$ used for stirring, Eq. (2.10), and $u_{\delta,cw}$ for advection, Eq. (2.9)),
- SWLONG=3: No long wave effect ($u'_{\delta,cw}$, Eq. (2.10) used for stirring and advection).

The net wave-averaged bed-load transport rate is obtained by averaging of the time-dependent transport vector $q_b(t) = (q_{bx}, q_{by})$ over the duration of the imposed near bottom velocity time series.

2.4 Suspended Transport

2.4.1 General

The suspended sediment transport rate (q_s) can be computed from the vertical distribution of fluid velocities and sediment concentrations, as follows:

$$q_s = \int_a^{h+\eta} VCdz \tag{2.11}$$

in which:

V	=	local instantaneous fluid velocity at height z above bed (m/s)
C	=	local instantaneous sediment concentration at height z above bed (kg/m^3)
h	=	water depth (to mean surface level), (m)
η	=	water surface elevation (m)
a	=	thickness of bed-load layer (m)

Defining:

$$V = v + \tilde{v} \text{ and } C = c + \tilde{c} \tag{2.12}$$

in which:

v	=	time and space-averaged fluid velocity at height z (m/s)
c	=	time and space-averaged concentration at height z (kg/m^3)
$\tilde{v}$	=	oscillating fluid component (including turbulent component), (m/s)
$\tilde{c}$	=	oscillating concentration component (including turbulent component), (kg/m^3)

Substituting Eq. (2.12) in Eq. (2.11) and averaging over time and space yields:

$$\overline{q}_s = \int_a^h vc\ dz + \int_a^h \overline{\tilde{v}\tilde{c}}\ dz = \overline{q}_{s,c} + \overline{q}_{s,w} \tag{2.13}$$

in which:

$\overline{q}_{s,c} = \int_a^h vc dz$ time-averaged current-related sediment transport rate (kg/sm)

$\overline{q}_{s,w} = \int_a^h \overline{\tilde{v}\tilde{c}} dz$ time-averaged wave-related sediment transport rate (kg/sm)

The current-related suspended sediment transport is defined as the transport of sediment particles by the time-averaged (mean) current velocities (longshore currents, rip currents, undertow currents). The current velocities and the sediment concentrations are affected by the wave motion. It is known that the wave motion reduces the current velocities near the bed and strongly increases the near-bed concentrations due to its stirring action. The wave-related suspended sediment transport is defined as the transport of sediment particles by the oscillating fluid components (cross-shore orbital motion). In the previous versions of UNIBEST-TC based on the TRANSPOR1993 formula, the wave related suspended transport was not included. In the present version an engineering approach is implemented which is described in Section 2.4.3. First, the current related transport formulations are given in the next sub-section.

Note that in UNIBEST-TC the transport rates include pores (porosity 40%) in volume per unit time and width (m^2/s):

$$q_s = \frac{\int_a^h vc\, dz}{(1-p)\rho_s} \tag{2.14}$$

2.4.2 Current-Related Suspended Transport Formulation

The time-averaged convection-diffusion equation is applied to compute the equilibrium concentration profile in steady flow and reads:

$$w_{s,m} c + \varphi_d \varepsilon_{s,cw} \frac{dc}{dz} = 0 \tag{2.15}$$

in which:

$w_{s,m}$ = fall velocity of suspended sediment in a fluid-sediment mixture (m/s)
$\varepsilon_{s,cw}$ = sediment mixing coefficient for combined current and waves (m^2/s)
c = time-averaged concentration at height z above the bed (kg/m^3)
φ_d = damping factor dependent on the concentration (-)

Here, it is assumed that Eq. (2.15) is also valid for wave-related mixing. The computation of the fall velocity $w_{s,m}$ and the turbulence damping factor φ_d are dealt with in Sub-Section 2.4.2.1 . The procedure for computation of the mixing coefficient $\varepsilon_{s,cw}$ is described in Sub-Section 2.4.2.2.

The convection-diffusion equation is solved by numerical integration from a near-bed reference level a to the water surface. At the reference level a concentration-type boundary condition is used. This reference concentration is given in Sub-Section 2.4.2.3.

2.4.2.1 Sediment fall velocity and turbulence damping

The fall velocity of a sediment particle is computed according to Van Rijn (1993):

$$\begin{aligned}
w_s &= \frac{\Delta g d_s^2}{18\nu} && , \; 1 \; \mu m < d_s \leq 100\,\mu m \\
w_s &= \frac{10\nu}{d_s}\left[\left(1+\frac{0.01\Delta g d_s^3}{\nu^2}\right)^2 - 1\right] && , \; 100 \; \mu m < d_s \leq 1000\,\mu m \\
w_s &= 1.1\left(\Delta g d_s\right)^{0.5} && , \; 1000 \; \mu m < d_s
\end{aligned} \tag{2.16}$$

Here d_s is the diameter of the suspended sediment, and is a user-defined property (DSS parameter). Van Rijn (1986) concluded on the basis of measurements that d_s should be in the range of 60 to 100% of the diameter of the median bed material size d_{50}. The kinematic viscosity ν is computed according to Van Rijn (1993).

In high concentration mixtures, the fall velocity of a single particle is reduced due to the presence of other particles. In order to account for this hindered settling effect, the fall velocity in a fluid-sediment mixture is determined as a function of the sediment concentration c (kg/m^3) and the particle fall velocity w_s:

$$w_{s,m} = \left(1 - \frac{c}{\rho_s}\right)^5 w_s \tag{2.17}$$

The damping factor φ_d represents the influence of the sediment particles on the turbulence structure of the fluid. This effect becomes increasingly important for high sediment concentrations which result in stratification and hence damping of turbulence. The following relation is used (see Van Rijn, 1993):

$$\varphi_d = 1 + \left(\frac{c}{c_0}\right)^{0.8} - 2\left(\frac{c}{c_0}\right)^{0.4} \tag{2.18}$$

in which c_0 is the maximum concentration and c is the actual concentration. The maximum volume concentration is set to 0.65 which amounts to a maximum concentration c_0 of approximately 1700 kg/m^3.

2.4.2.2 Sediment mixing coefficient

Measurements in wave flumes show the presence of suspended sediment particles from the bed up to the water surface. The largest concentrations are found close to the bed where the diffusivity is large due to ripple-generated eddies. Further away from the bed the sediment concentrations decrease rapidly because eddies dissolve rather rapidly traveling upwards.

Based on analysis of measured concentration profiles, the following characteristics were observed (Van Rijn, 1993):

- approximately constant mixing coefficient $\varepsilon_{s,w,bed}$ in a layer ($z \leq \delta_s$) near the bed,
- approximately constant mixing coefficient $\varepsilon_{s,w,max}$ in the upper half ($z \geq 0.5\ h$) of the water depth,
- approximately linear variation of the mixing coefficient for $\delta_s < z < 0.5\ h$.

For the current mixing coefficient, a constant mixing is assumed in the upper half of the water column which decreases in a parabolic shape to zero in the lower half of the column.

A sketch of the resulting shape of the mixing coefficients is given in Figure 2.2 below:

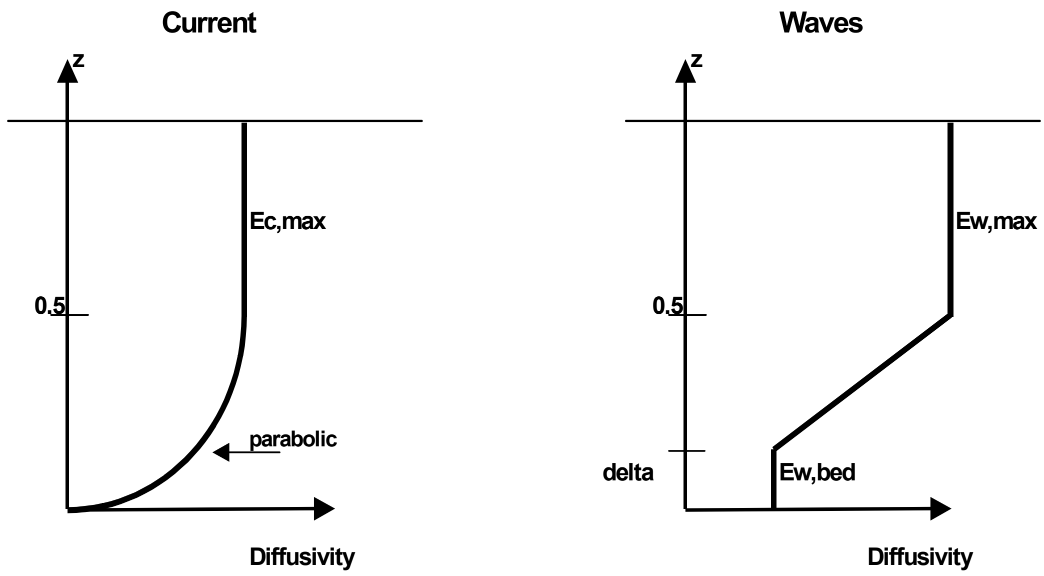

Figure 2.2 Vertical mixing distributions.

For combined current and wave conditions the sediment mixing coefficient is modeled as:

$$\varepsilon_{s,cw} = \sqrt{\varepsilon_{s,w}^2 + \varepsilon_{s,c}^2} \tag{2.19}$$

in which:

$\varepsilon_{s,w}$ wave-related mixing coefficient (m^2/s)
$\varepsilon_{s,c}$ current-related mixing coefficient due to longshore current and undertow (m^2/s)

The formulation for the wave-related mixing coefficient reads:

$$\begin{array}{ll} z \le \delta_s & \varepsilon_{s,w} = \varepsilon_{s,w,bed} \\ z \ge 0.5h & \varepsilon_{s,w} = \varepsilon_{s,w,\max} \\ \delta_s < z < 0.5h & \varepsilon_{s,w} = \varepsilon_{s,w,bed} + \left(\varepsilon_{s,w,\max} - \varepsilon_{s,w,bed}\right)\left(\dfrac{z-\delta_s}{0.5h-\delta_s}\right) \end{array} \tag{2.20}$$

Equation (2.20) is also used in TRANSPOR1993. However, the thickness δ_s of the near-bed sediment mixing layer, the mixing coefficient $\varepsilon_{s,w,bed}$ in the near-bed layer and the mixing coefficient $\varepsilon_{s,w,max}$ in the upper layer have been updated.

The thickness δ_s reads:

$$\delta_s = \max\left(5\gamma_{br}\delta_w, 10\gamma_{br}k_{s,w}\right) \ \ with \ \ 0.1 \le \delta_s \le 0.5 \tag{2.21}$$

with:

- δ_s thickness of effective near-bed sediment mixing layer (m),
- δ_w thickness of wave boundary layer (m)
- $k_{s,w}$ wave-related bed roughness (m)
- γ_{br} empirical coefficient related to wave breaking (-)

The expression for γ_{br} is:

$$\begin{array}{ll} \gamma_{br} = 1 + \left(\dfrac{H_s}{h} - 0.4\right)^{0.5} & for \ \dfrac{H_s}{h} > 0.4 \\ \gamma_{br} = 1 & for \ \dfrac{H_s}{h} \le 0.4 \end{array} \tag{2.22}$$

The mixing coefficient in upper layer reads:

$$\varepsilon_{s,w,\max} = 0.035\gamma_{br}\frac{H_s h}{T_p} \ \ with \ \varepsilon_{s,w,\max} = 0.05\, m^2/s \tag{2.23}$$

in which T_p is the peak period of the wave spectrum. The minimum value for $\varepsilon_{s,w,max}$ is the value of $\varepsilon_{s,w,bed}$.

For the mixing coefficient in the near-bed layer the following expression is used:

$$\varepsilon_{s,w,bed} = 0.018\beta_w\delta_s\hat{U}_\delta \tag{2.24}$$

in which $\hat{U}_\delta$ is the near-bed peak orbital velocity and β_w is a coefficient which reads:

$$\beta_w = 1 + 2\left(\frac{w_s}{u_{*,w}}\right)^2 \ \ with \ \beta_w \le 1.5 \tag{2.25}$$

in which w_s is the fall velocity of suspended sand and $u_{*,w}$ is the wave-related bed-shear velocity.

In Van Rijn (2000) it was stated that "The near-bed mixing parameter $\varepsilon_{s,w,bed}$ was found to be dependent on the particle velocity (size), based on analysis of sand concentration profiles of experiments with bed material in the range of 0.1 to 0.3 mm (Van Rijn, 1993). The near-bed mixing appears to increase with increasing particle size, which may be an indication of the dominant influence of centrifugal forces acting on the particles due to strong turbulence-induced vortex motions close to the bed resulting in an increase of the effective mixing of sediment particles. This effect is modelled by the β_w coefficient. As no information is available for bed materials larger than about 0.3 mm, the application of Eq. (2.25) for these conditions is highly uncertain. More research is necessary for accurate prediction of the wave-induced suspended transport for relatively coarse materials (>0.3 mm; coarse sand and gravel beds)."

The expression for the current-related mixing coefficient $\varepsilon_{s,c}$ has not been changed.

2.4.2.3 Reference Concentration

Numerical solution of the advection-diffusion equation Eq. (2.15) requires the specification of the concentration at a certain elevation above the bed which is referred to as the reference concentration, see Figure 2.3.

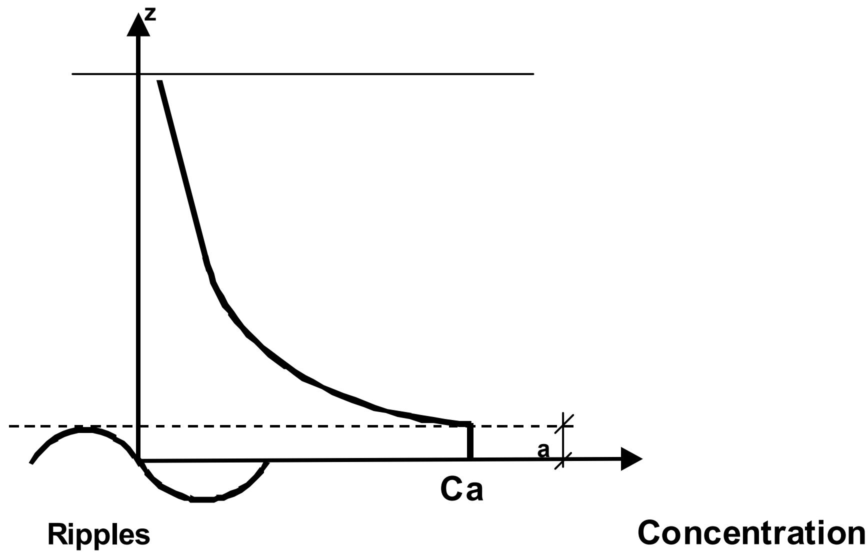

Figure 2.3 Reference Concentration, c_a

The reference concentration (volume) is given by:

$$c_a = 0.015 \frac{d_{50}}{a} \frac{T^{1.5}}{D_*^{0.3}} \quad with\ c_a \leq 0.05 \qquad (2.26)$$

in which D_* is the dimensionless particle parameter (-), T is the dimensionless bed-shear stress parameter (-) and a is a reference level (m) given by the maximum value of the current-related roughness $k_{s,c}$ and wave-related roughness $k_{s,w}$, with a minimum value of 0.02 m.

The bed shear stress parameter is defined as follows:

$$T = \frac{\tau'_{b,cw} - \tau_{b,cr}}{\tau_{b,cr}} \tag{2.27}$$

in which: $\tau'_{b,cw}$ is the time-averaged effective bed-shear stress (N/m²), $\tau_{b,cr}$ is the time-averaged critical bed-shear stress according to Shields (N/m²).

The time-averaged critical shear stress is computed as:

$$\tau_{b,cr} = (\rho_s - \rho)\, g d_{50} \theta_{cr} \tag{2.28}$$

with θ_{cr} being the critical shields number. Note that no bed slope correction is applied to the critical shear stress, as opposed to the critical shear stress for the bed load formula.

The magnitude of the time-averaged bed-shear stress, which is independent of the angle between the wave- and current direction, is given by:

$$\tau'_{b,cw} = \tau'_{b,c} + \tau'_{b,w} \tag{2.29}$$

in which: $\tau'_{b,c}$ is the effective current-related bed-shear stress (N/m²) and $\tau'_{b,w}$ is the effective wave-related bed-shear stress (N/m²):

$$\tau'_{b,c} = \mu_c \alpha_{cw} \tau_{b,c} \tag{2.30}$$

$$\tau'_{b,w} = \mu_{w,a} \tau_{b,w} \tag{2.31}$$

In these equations $\mu_{w,a}$ is an efficiency factor and α_{cw} is the wave-current interaction factor.

The wave-related efficiency factor $\mu_{w,a}$ is an important parameter, as it strongly affects the reference concentration near the bed. This parameter will depends on the bed form and bed roughness characteristics, but the functional relationship involved is not yet known. Therefore, the $\mu_{w,a}$ factor has been used as a calibration parameter to get a better estimate of the near-bed concentration (Van Rijn, 2000). As the bed forms are related to the relative wave height (ripples for small values of H_s/h and plane bed for large values of H_s/h), the $\mu_{w,a}$ factor is supposed to be related to the relative wave height. Based on analysis of experimental data Van Rijn (2000) modified the $\mu_{w,a}$ factor into:

$$\mu_{w,a} = 0.125\left(1.5 - \frac{H_s}{h}\right)^2 \quad with \ \mu_{w,a} \geq 0.063 \tag{2.32}$$

This expression yields a better description of the reference concentration for relatively small wave heights in the ripple regime.

2.4.3 Wave-Related Suspended Transport Formulation

The approach in TRANSPOR2000 is to determine the wave-related suspended transport (Van Rijn, 2000) by assuming an instantaneous response of the suspended sand concentrations (c) and transport ($q_{s,w}$) to the near-bed orbital velocity. The method was introduced by Houwman and Ruessink (1996) and reads:

$$q_{s,w} = \gamma \left(\frac{U_{on}^4 - U_{off}^4}{U_{on}^3 + U_{off}^3} \right) \int c dz \qquad (2.33)$$

with $U_{on}=U_{\delta f}$ is the near-bed peak orbital velocity in the wave direction, $U_{off}=U_{\delta b}$ is the near-bed peak orbital velocity against the wave direction, c is the time-averaged concentration and γ is a phase lag function.

This approach is valid for the near-bed layer (say 1 to 5 times the wave boundary layer thickness), but at higher levels a delayed response of the sand concentrations (phase lag effects) will be more realistic, particularly for fine sediments. For very fine sediment the wave-related suspended transport may even be opposite to the wave propagation direction.

Phase lag effects are supposed to be accounted for by the γ-function. As phase lag effects are related to the wave conditions, sand size and bed geometry, the γ-function is supposed to be a complicated function of the former parameters (yielding negative values for very fine sand). A detailed discussion of phase lag effects and functions is given by Dohmen-Janssen (1999).

Simulation of the wave-related suspended transport with Eq. (2.33) requires the computation of the time-averaged sand concentration profile according to Eq. (2.15) and a vertical integration of the time-averaged sand concentration profile. Based on the considerations above, the integration is taken over a near-bed layer with a thickness equal to 0.5 m, assuming that the suspended sand above this layer is not much effected by the high-frequency wave motion with periods in the range of T= 5 to 10 s. This assumption is satisfied if the fall time of a suspended sand particle over a distance of 0.5 m is much larger than the wave period (T_{fall}= 0.5/w_s yielding about 25 s for d= 0.2 mm with w_s= 0.02 m/s). Furthermore, the data of the Delta flume (Chung and Grasmeijer, 1999) show that most of the wave-related suspended transport occurs in the near-bed layer with a thickness of about 0.5 m (10 to 20 times the ripple height).

Chung and Grasmeijer (1999) have determined the γ-function by fitting of Eq. (2.33) to measured wave-related transport rates. The peak onshore and offshore orbital velocities as well as the time-averaged sand concentrations were taken from measured data. Amazingly, the γ-function was found to be a constant value of about 0.2 for all test results (relative standard error of about 30 %). Any influence of the wave conditions and/or the sand size on the γ-function could not be detected, implying relatively small phase lag effects in the considered data sets. It is noted that the γ-value of 0.2 is based on data with rather pronounced ripples observed in a large scale 2D wave tank. The γ-value may be considerably smaller (say between 0.1 and 0.2) for field conditions with less pronounced

3D-ripples (Grasmeijer et al., 2000). The γ-value can be set by the user (ASFAC parameter) and has a default value of 0.20.

The near bed peak orbital velocities are determined by following Grasmeijer and Van Rijn (1998) which is a modified Isobe-Horikawa (1982) approach or the method of Rienecker and Fenton (1981). The latter was already available in UNIBEST-TC (details can be found in the technical reference manual: Bosboom et al., 1997). As part of the upgrade to the TRANSPOR2000 formula in UNIBEST-TC, the modified Isobe-Horikawa approach has been implemented in the UNIBEST-TC model. The method is described in Appendix A. The user can select between the non-linear short wave theories with the SWASYM parameter (0 = Rienecker&Fenton and 1 = Isobe-Horikawa).

2.5 Miscellaneous

This section describes small improvements to the model and pre- and postprocessing software.

Improvements to UNIBEST-TC model:
- Fixed error with fixed layer that caused erosion through fixed layer.
- Added ZUV parameter which specifies height above the bed for output of velocities in DAF-file (default is 0.10 m).
- Added output of variable gamma (Ruessink et al., 2003), last considered x coordinate and associated water depth to mp1-file (ASCII-output).
- Added reference concentration, relative wave height, suspended wave transport, onshore peak orbital velocity and offshore peak orbital velocity to DAF-file.
- Synchronised bottom wave dissipation for streaming in flow model. Expression is now consistent with wave model.
- Extended the calculation of the longshore current SWTIDE parameter:
  - SWTIDE=1 : Original expression based on Chezy
  - SWTIDE=2 : dh/dy directly imposed
  - SWTIDE=3 : Longshore velocity imposed as boundary condition (in combination with x-coordinate). dh/dy is determined via iteration of flow module to the specified longshore velocity.

Improvements to Pre-processor, Pre-TC:
- Overall updating of colour schemes applied in the program. The Windows API is now followed which avoids ugly colour combinations.
- Extended input sections and made them compatible with extensions of the model (ZUV, SWTIDE, SWASYM, ZDRY and SWLONG parameters).
- For selection of ASCII output, the parameters are automatically updated with parameters listed in viz-tc.ini located in the “windows” directory.

Improvements to visualisation program VIZ-TC:
- The last time step of data on DAF-file is time averaged over the simulation. Viz-TC indicated this by adding an extra time step. To avoid confusion the averaged data is now indicated as “Averaged”.

Improvements to animation program ANI-TC:

- Increased number of profiles that can be animated to 10000 (was 2000).

2.6 Model testing and evaluation

To check the implementation of the new formulations a limited verification of the upgraded UNIBEST-TC model is carried out. The verification is aimed at testing the four major improvements implemented in the UNIBEST-TC model:

- Upgrade to TRANSPOR2000 transport formula;
- Modification of long wave effects on bed load transport;
- Inclusion of wave related suspended sediment transport;
- Implementation of the Isobe-Horikawa non-lineair wave theory for the near bed orbital velocities.

The verification is sub-divided into:

- An evaluation of the TRANSPOR2000 formula implemented in UNIBEST-TC. This is performed by comparing concentration profiles of UNIBEST-TC with van Rijn's TRANSPOR2000 point model which is discussed in Sub-Section 2.6.1.
- An evaluation of the implemented improvements using LIP11D Tests 1A, 1B and 1C included in the UNIBEST-TC Testbank. These datasets consist of high quality data on waves, hydrodynamics, sediments and morphology and can be used to make a first assessment of the results of the improved model. This evaluation can be found in Sub-sections 2.6.2 to 2.6.4.

2.6.1 Comparison between UNIBEST-TC and TRANSPOR2000

A comparison between the upgraded UNIBEST-TC model with the original TRANSPOR2000 point model is made to test the implementation of the new transport formulations which included modifications to:

- the reference concentration,
- the parametric wave related sediment mixing profiles,
- modification of the bed load transport formulation.

In addition the implementation of the non-lineair wave theory of Isobe-Horikawa is verified via a comparison of the near bed orbital velocities.

The comparison is made for six cases in 5 m water depth with non-breaking waves. Varied model input comprises the longshore velocities (0.5 and 1.0 m/s), wave height (H_{rms} 0.7, 1.0 and 1.4 m) and roughness heights (r_c=r_w 0.01, 0.03 and 0.05 m). The focus will be on the longshore sediment transport as the cross-shore flow is computed differently in both models. The basic settings are listed in Table 2.1 below.

Table 2.1 Overview of basic settings.

Parameter	**Description**	**Value**
h	water depth (m)	5.0
U_{long}	longshore velocity (m/s)	0.5
H_{rms}	RMS wave height (m)	0.7
T_p	Peak wave period (s)	7.0
α	wave direction (°)	0 (shore normal)
R_c	current related roughness height (m)	0.05
R_w	wave related roughness height (m)	0.05
D_{50}	mean particle diameter (μm)	200
D_{90}	90 percentile particle diamter (μm)	300
D_{ss}	mean diameter of suspended sediment (μm)	200
Te	water temperature (°C)	15
Sa	salinity (‰)	30

In Figure 2.4 to Figure 2.9 the longshore velocity, concentrations and longshore transport profiles are compared. As a reference the results for the UNIBEST-TC version with TRANSPOR1993 is also included.

It can be seen that the concentration profiles show a more or less exact agreement with TRANSPOR2000. The small differences in the transports mainly originate from the flow profiles and are not related to the transport model.

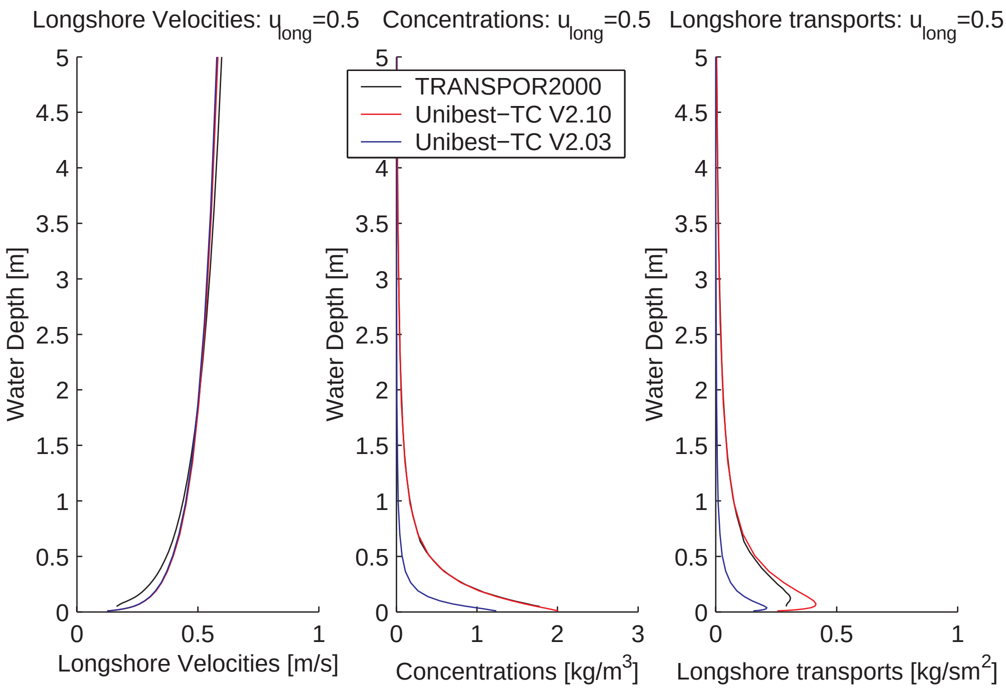

Figure 2.4 Comparison between TRANSPOR2000 and UNIBEST-TC (U_{long}=0.5 m/s, R_c/R_w=0.05 m, H_{rms}=0.7 m).

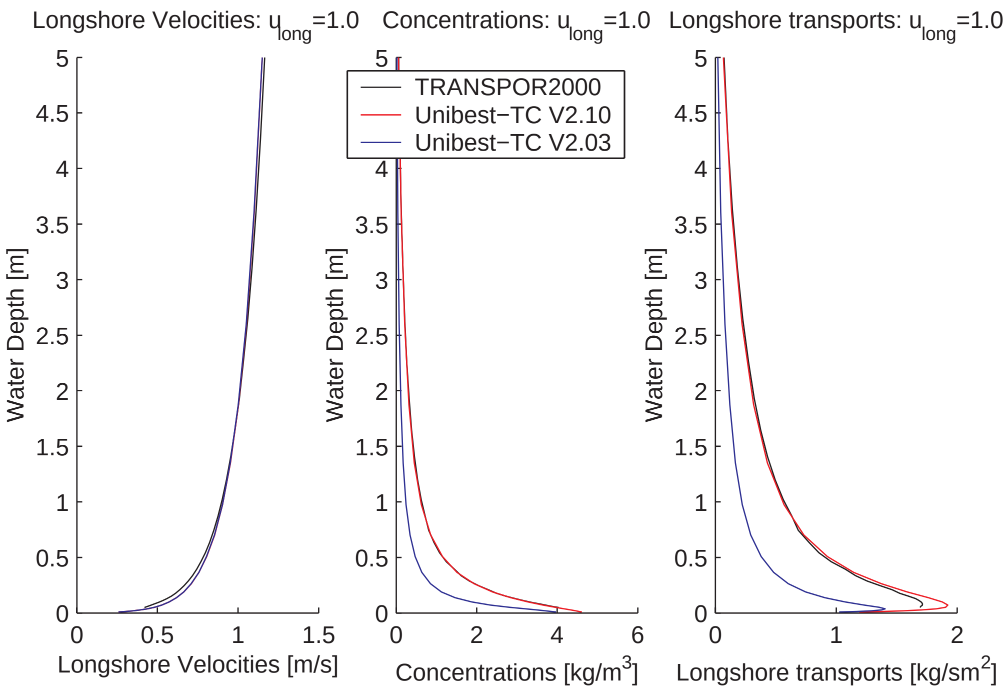

Figure 2.5 Comparison between TRANSPOR2000 and UNIBEST-TC (U_{long}=1.0 m/s).

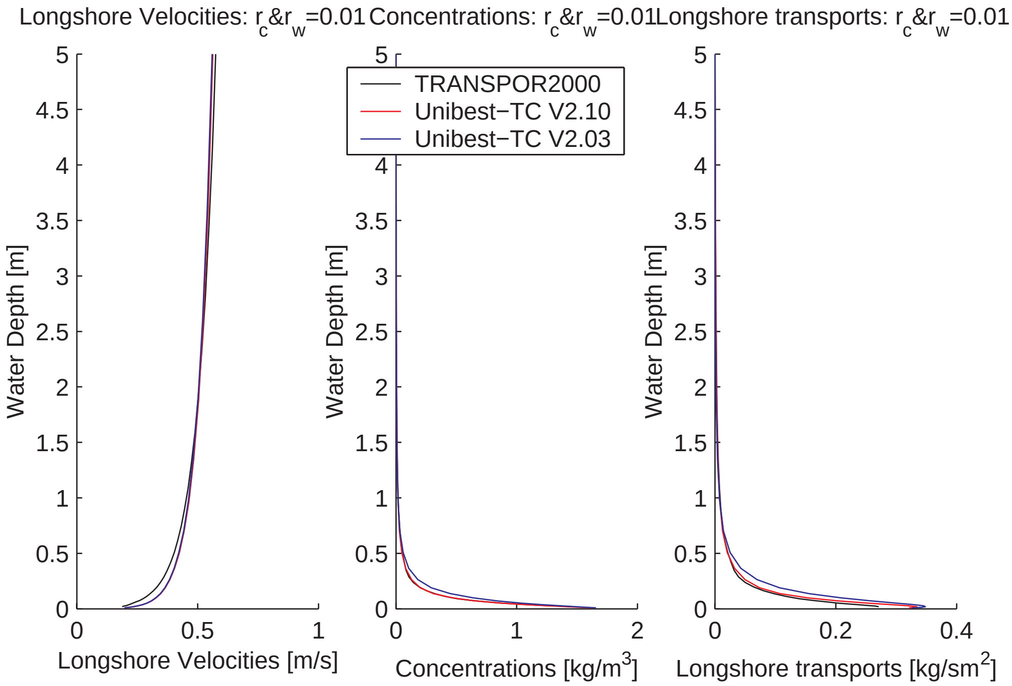

Figure 2.6 Comparison between TRANSPOR2000 and UNIBEST-TC (R_c/R_W=0.01 m).

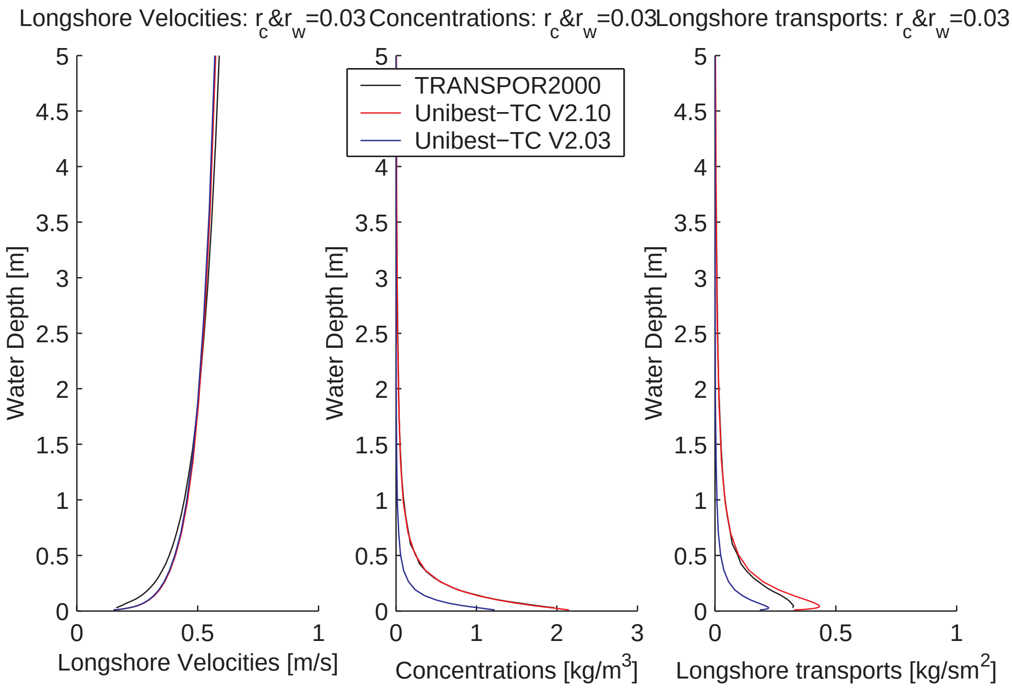

Figure 2.7 Comparison between TRANSPOR2000 and UNIBEST-TC (R_c/R_W=0.03 m).

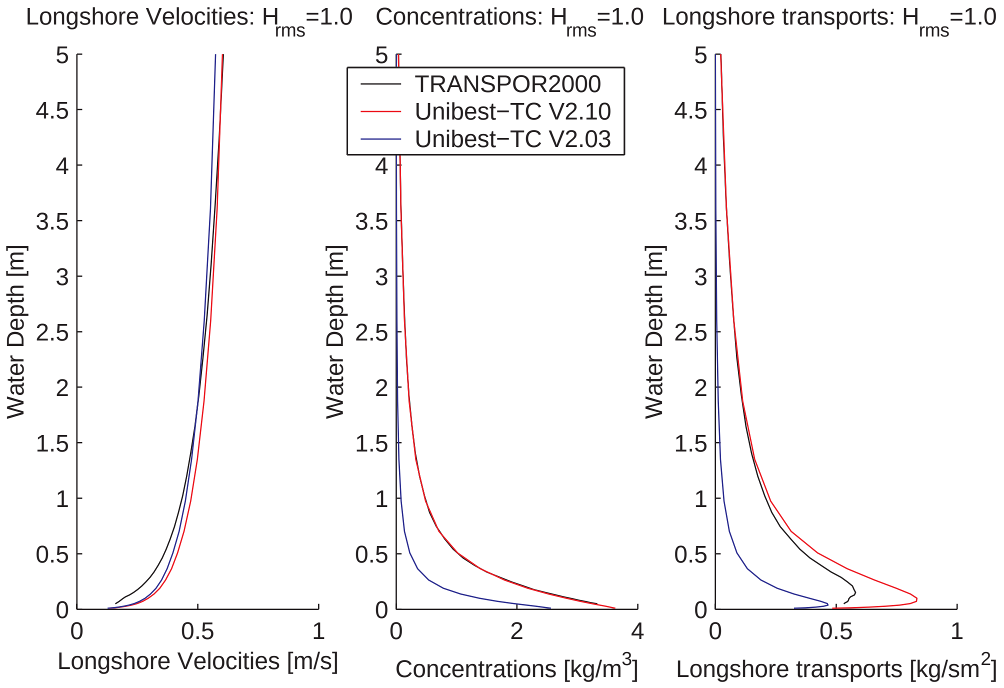

Figure 2.8 Comparison between TRANSPOR2000 and UNIBEST-TC (H_{rms}=1.0 m).

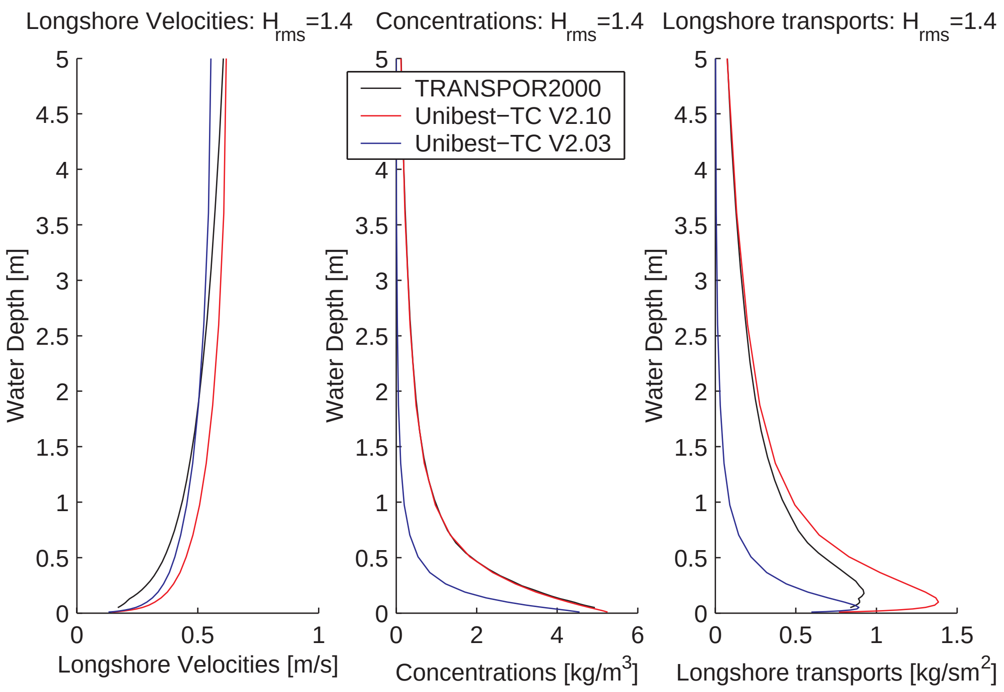

Figure 2.9 Comparison between TRANSPOR2000 and UNIBEST-TC (H_{rms}=1.4 m).

In Figure 2.10 the near bed orbital velocities generated by the Isobe-Horikawa model for both models are compared. It can be seen that the peak onshore (U_{on}) and offshore (U_{off}) velocities are the same (these are the result of the Isobe-Horikawa approach).

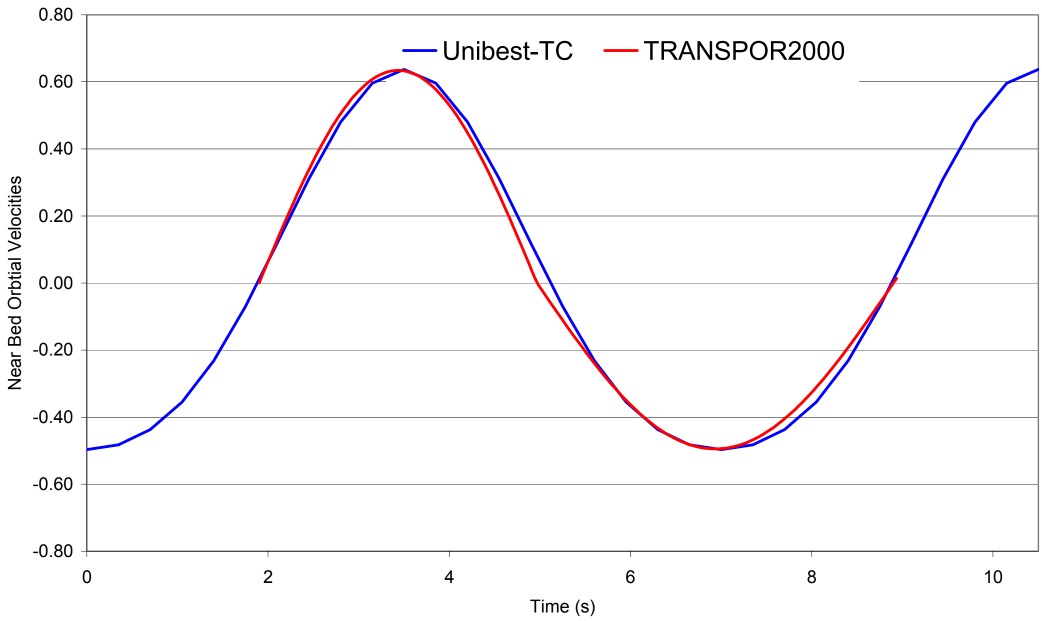

Figure 2.10 Comparison of the near bed orbital velocities based on Isobe-Horikawa for UNIBEST-TC and TRANSPOR2000.

The time series that is constructed by both models is somewhat different. In UNIBEST-TC these are constructed according to:

$$u(t) = z_1 \cos \omega t + z_2 \cos 2\omega t \tag{2.34}$$

where z_1 and z_2 are computed as:

$$\begin{aligned} z_1 &= \frac{U_{on} + U_{off}}{2} \\ z_2 &= \frac{U_{on} - U_{off}}{2} \end{aligned} \tag{2.35}$$

whereas in TRANSPOR2000 the time series is constructed by an onshore part and offshore part separately:

$$\begin{aligned} &\textit{in wave direction}: \\ &u(t) = u_{on} \sin\left(\frac{\pi}{T_{on}} t\right) \\ &\textit{opposite wave direction}: \\ &u(t) = u_{off} \sin\left(\frac{\pi}{T_{off}} (t - T_{on})\right) \end{aligned} \tag{2.36}$$

in which:

$$T_{on} = \frac{U_{off}}{U_{on} + U_{off}} T_p \tag{2.37}$$

and

$$T_{off} = T_p - T_{on} \tag{2.38}$$

The approach followed in UNIBEST-TC is probably more consistent as it is a continuous time series which is not the case for the TRANSPOR2000 approach. However the difference between both time series is small and has not a significant influence on the resulting bed load transport.

2.6.2 UNIBEST-TC (TRANSPOR1993) vs. UNIBEST-TC (TRANSPOR2000)

A first step is to compare the old model UNIBEST-TC model with TRANSPOR1993 and the upgraded model with TRANSPOR2000. To that end the results of three simulations are compared in which Rienecker&Fenton non-lineair wave model is used (each setting is applied on the three LIP11D experiments):

1. UNIBEST-TC with TRANSPOR1993 (wave related suspended sediment not included in model),
2. UNIBEST-TC with TRANSPOR2000 and no wave related suspended transport (ASFAC=0),
3. UNIBEST-TC with TRANSPOR2000 and wave related suspended transport included (ASFAC=0.2).

The basic model input for Test 1A to 1C is summarised in Table 2.2 below.

In the third plot of Figure 2.14 to Figure 2.14 the total suspended transports are compared for Test 1A to Test 1C. It can be seen that the differences between TRANSPOR1993 and TRANSPOR2000 are limited (compare blue and red line). However, the effect of the wave related suspended transport is significant and results in a reduced (Tests 1A and 1B) or onshore total transport (Test 1C). The bed-load transports, depicted in the fourth plot show that the new expression results in a lower onshore transports outside the breaker zone for three tests. The total transports (bottom plots) show an improved overall agreement with the measured total transports. Note that the measured total transports are derived from an integration of the differences between the initial and final profile. This implies that the measured total transports are in fact time-averaged transports over the duration of the experiment.

In Figure 2.15 the undertow profile are compared for Test 1C, to illustrate some changes that have been made in the upgraded UNIBEST-TC model regarding the effects of streaming on the velocity profiles. Streaming is included in parameterised way which is based on the wave dissipation in the wave boundary layer. In the previous versions of UNIBEST-TC the wave dissipation in the wave boundary layer was computed separately by the flow module in stead of using the bottom dissipation determined by the wave module. The expression in the flow module resulted in a significant over-estimation of the bottom dissipation of wave energy especially in deeper water. In the upgraded version this inconsistency was removed by using the bottom dissipation determined in the wave module. It can be seen that especially in deeper water the streaming effect has reduced significantly.

In Figure 2.16 the concentration profiles for Test 1C are compared. From this comparison it is obvious that the new transport formulations do not lead to an improvement of the concentration profiles and hence the suspended transports. This mainly due to the fact that the new formulations have been derived from field measurements. Application of this formula with a varying roughness across the profile can improve the concentrations considerably as was shown by Van Rijn et al. (2003).

To objectively assess the model performance for the various model settings, the Brier Skill Scores have been determined for the predicted total transport for all simulations. The original UNIBEST-TC model with TRANSPOR1993 is used as the base line prediction. The Brier Skill Score is a relative skill score which determines the performance relative to the base line prediction. A negative score implies a worse prediction than the base line, a positive score a better prediction. A score of one implies a perfect match with the measurements.

In Figure 2.11 the Brier Skill Scores for both runs are compared which confirm the findings based on the visual inspection. The inclusion of the suspended wave related transport (ASFAC=0.2) results in a significant improvement (compare scores for both settings).

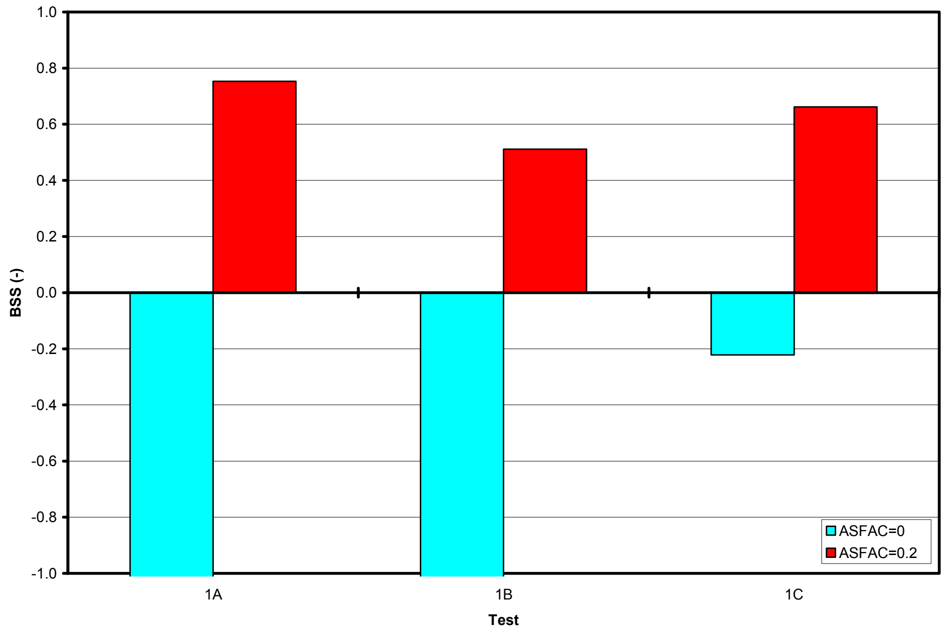

Figure 2.11 Brier Skill Scores for the total transports (UNIBEST-TC with TRANSPOR1993 is used as the base line prediction.

Table 2.2 Overview of model settings for LIP11D Tests 1A, 1B and 1C.

Parameter	Description	1A	1B	1C
h	water depth (m)	Dean profile	end profile from 1A	end profile from 1B
H_{rms}	RMS wave height (m)	0.66	0.86	0.41
T_p	Peak wave period (s)	5.0	5.0	8.0
R_c	current related roughness height (m)	0.03	0.03	0.03
R_w	wave related roughness height (m)	0.03	0.03	0.03
D_{50}	mean particle diamter (μm)	200	200	200
D_{90}	90 percentile particle diamter (μm)	300	300	300
D_{ss}	mean diameter of suspended sediment (μm)	170	170	170
γ	asymmetry factor for wave related suspended transport	0.2	0.2	0.2
Te	water temperature (°C)	15	15	15
Sa	salinity (‰)	0	0	0

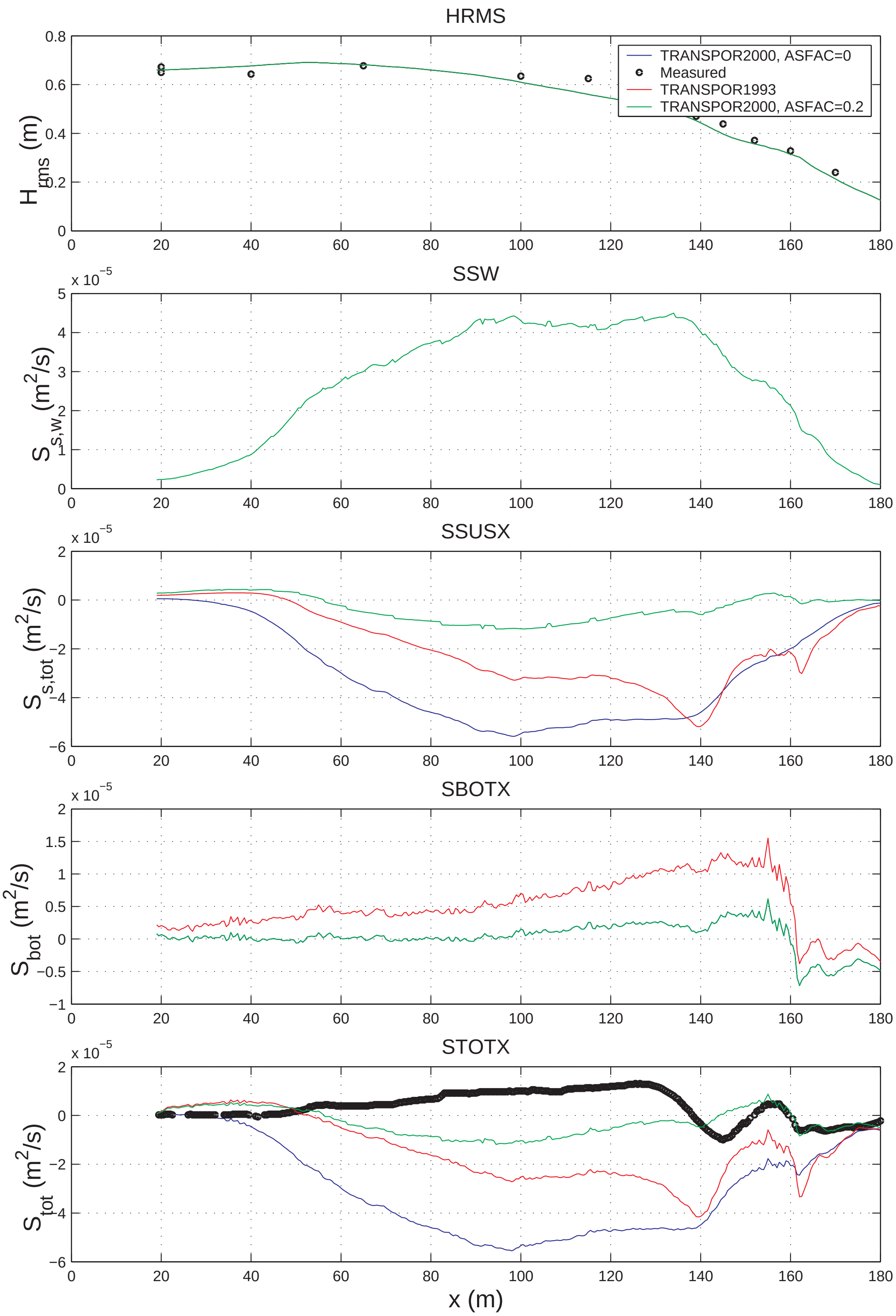

Figure 2.12 Investigation of new transport formulations and effect of wave related suspended transport for LIP11D Test 1A.

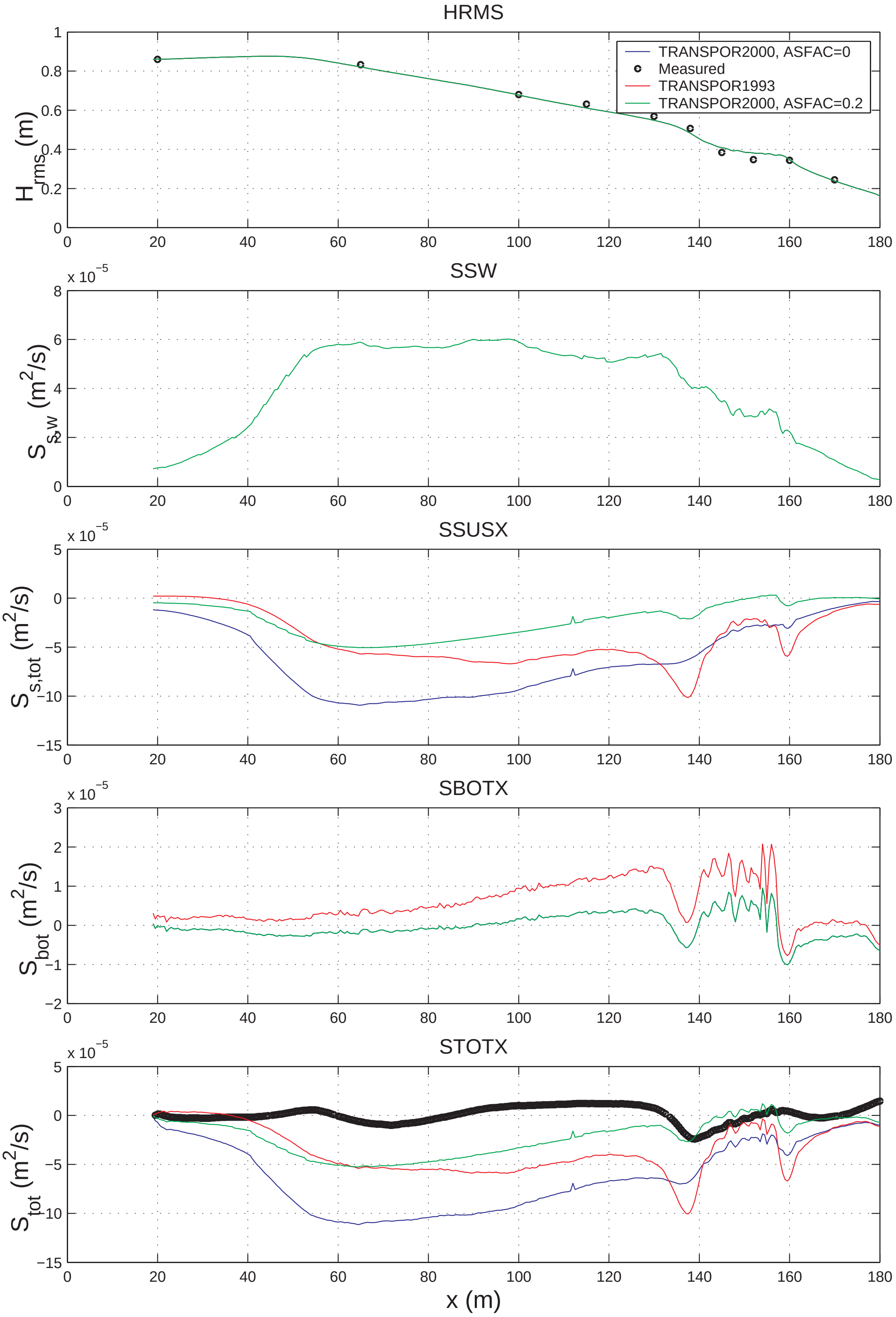

Figure 2.13 Investigation of new transport formulations and effect of wave related suspended transport for LIP11D Test 1B.

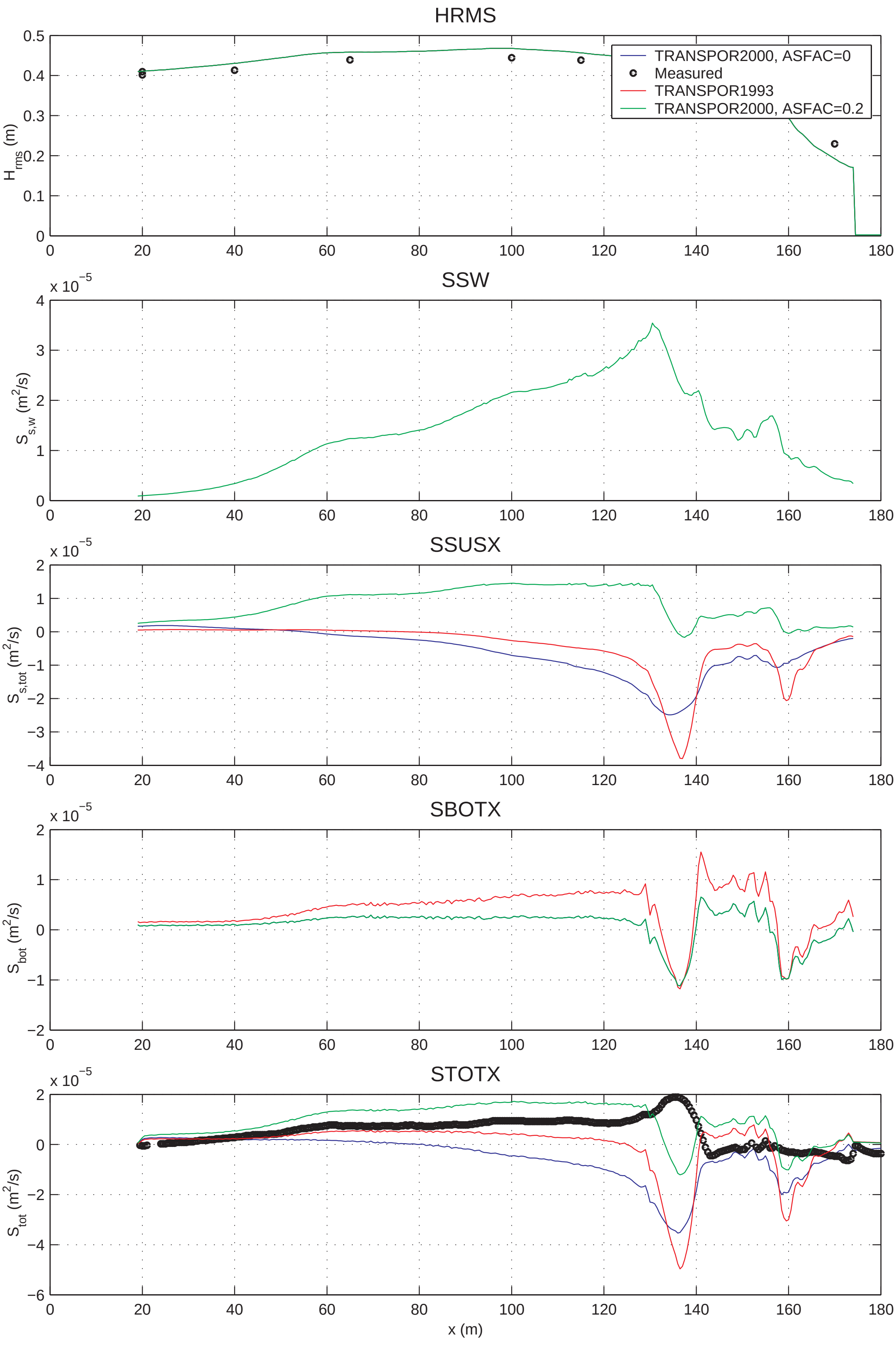

Figure 2.14 Investigation of new transport formulations and effect of wave related suspended transport for LIP11D Test 1C.

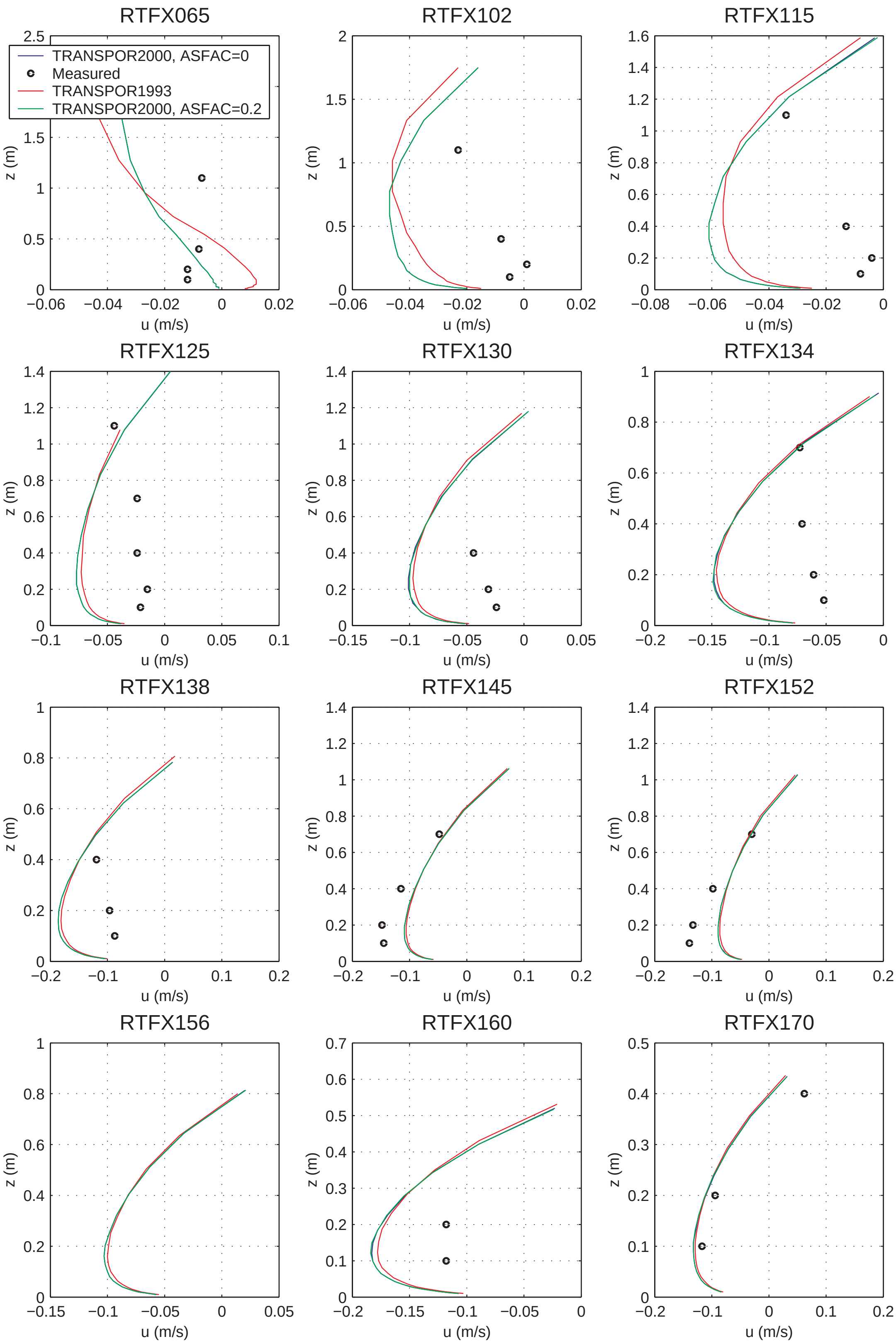

Figure 2.15 Comparison of undertow profiles for LIP11D Test 1C.

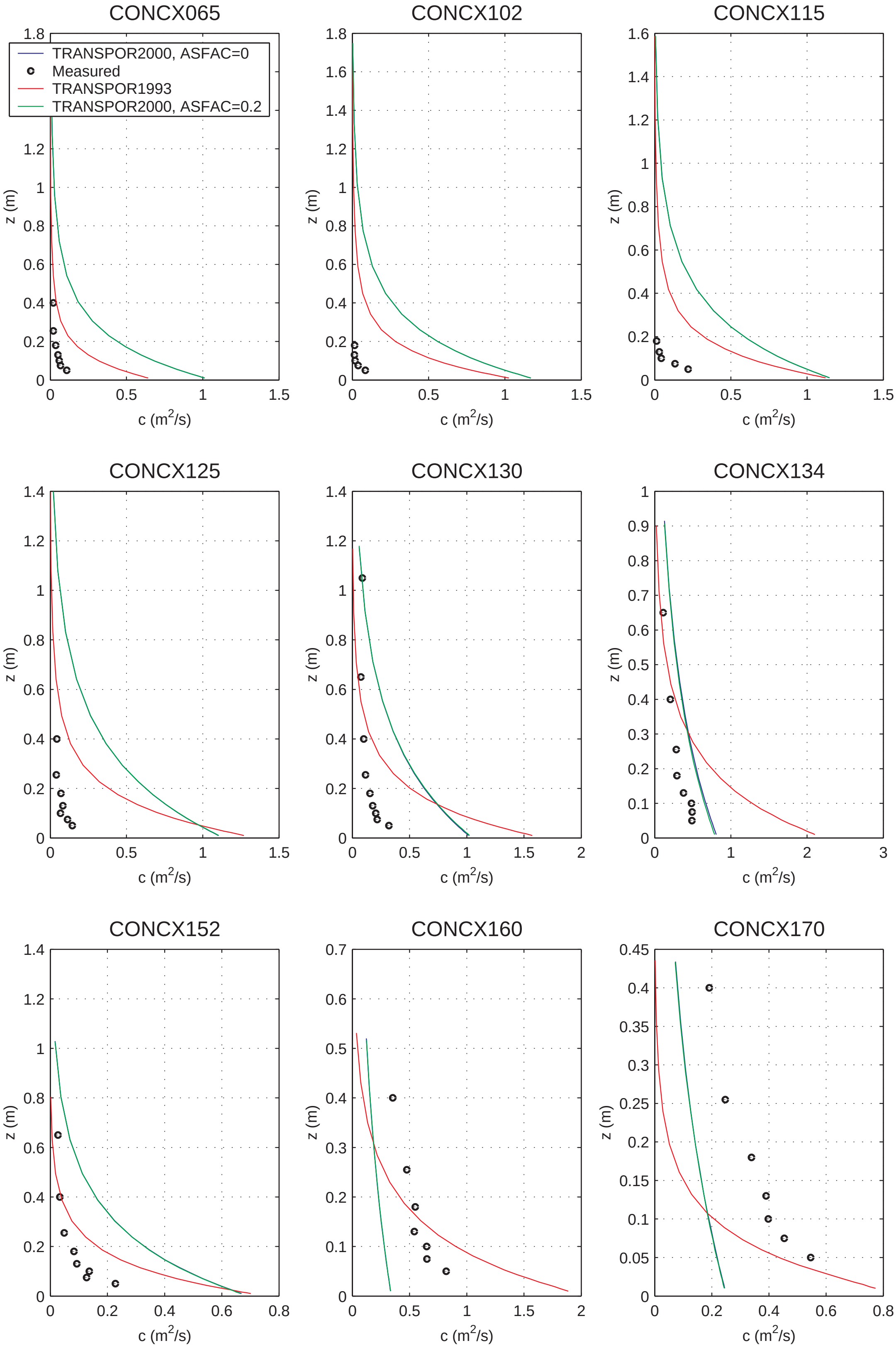

Figure 2.16 Comparison of concentration profiles for LIP11D Test 1C.

2.6.3 Long wave effects on bed load transport

In UNIBEST-TC three options have been introduced to determine the velocity signals used for the bed-load transport via a new parameter SWLONG:

- SWLONG=1: Original implementation ($u_{\delta,cw}$ used for stirring and advection following Eq. (2.9)),
- SWLONG=2: Improved implementation ($u'_{\delta,cw}$ used for stirring, Eq. (2.10), and $u_{\delta,cw}$ for advection, Eq. (2.9)),
- SWLONG=3: No long wave effect ($u'_{\delta,cw}$, Eq. (2.10) used for stirring and advection).

In Figure 2.19 to Figure 2.21 the results for the three SWLONG options are shown. It can be seen that the original approach results in a significant influence of the long wave effects on the bed load transport for Test 1C (second plot in Figure 2.21). Especially in the area where wave breaking is most intense (x=130 m – 140 m). The non-lineair reaction of the bed load transport formula yields an unrealistic offshore bed load transport near the bar area (see also the total transport plot). The modification results in an improved prediction of the bed load transport if the total transports are compared with the measured values. For Tests 1A and 1B, the sensitivity of the bed load is not as dramatic. This is to be expected as the short wave near bed velocity signal is much higher than for Test 1C (and the relative contribution of long waves is significantly reduced).

The Brier Skill Scores are shown in Figure 2.17 from which it becomes obvious that the effect of SWLONG is only significant for Test 1C. As this test used relative low waves which are responsible for bar formation and onshore transports this indicates the relevance of this improvement for field conditions.

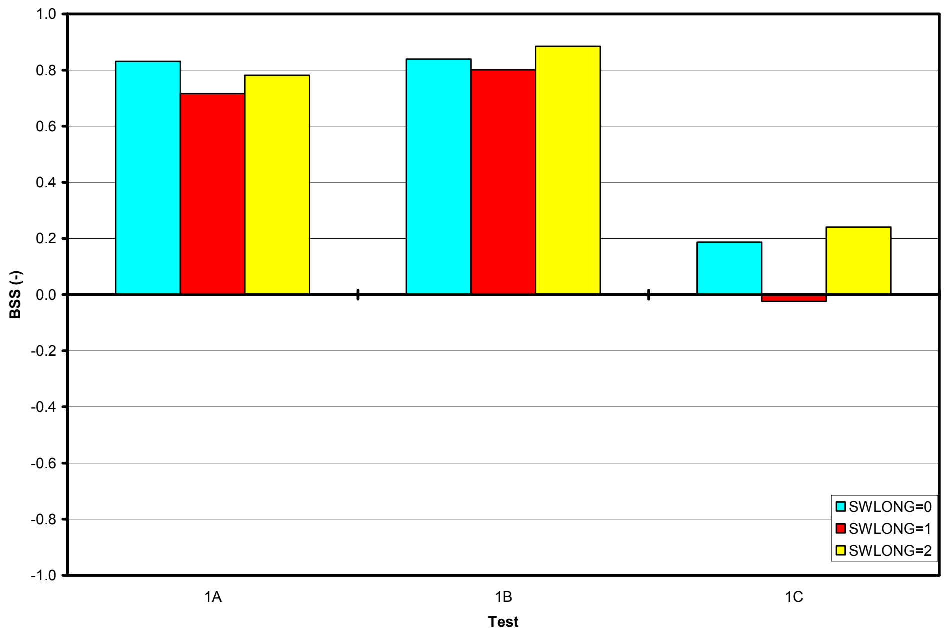

Figure 2.17 Brier Skill Scores for the total transports (UNIBEST-TC with TRANSPOR1993 is used as the base line prediction.

2.6.4 Comparison of Rienecker&Fenton and Isobe-Horikawa

Two runs were made for Tests 1A to 1C in which the non-lineair near-bed orbital velocities were determined by using either the Isobe-Horikawa and Rienecker&Fenton approach. In Figure 2.22 to Figure 2.24 the results for both model runs are compared. The peak orbital velocities in onshore direction are comparable as can be seen in the second plot (UBWF) of each figure. However the offshore directed peak is severely under-estimated by Rienecker&Fenton in all tests (see third plot, UBWB). However, this has a relative small effect on the wave related suspended transports as shown in the fourth plot (SSW) of the figures. The total suspended transport is onshore directed (Test 1C) or reduced considerably for both theories and implies that the onshore wave related suspended transport in all the investigated tests can not be ignored.

In all cases the cross-shore bed-load transport distribution determined by both approaches show significant differences. For all cases Rienecker&Fenton predicts onshore bed load transports over the complete profile. However, with Isobe-Horikawa offshore transports are predicted in the surf zone (see sixth plots, SBOTX). The total transports are compared in the bottom plots (STOTX). It can be seen that the both approaches are unable to reproduce the measured total transports satisfactory. However, Isobe-Horikawa shows a better qualitative agreement. Especially, the change from onshore to offshore transport at the bar (~ x=130-140 m) is reproduced with Isobe-Horikawa and not with Rienecker&Fenton.

The findings are not completely supported by the Brier Skill Scores shown in Figure 2.18. These indicate that the differences between both wave theories is limited for Tests 1A and 1B and for Test 1C Rienecker&Fenton performs better. The mixed picture emphasises that more research is needed on this subject.

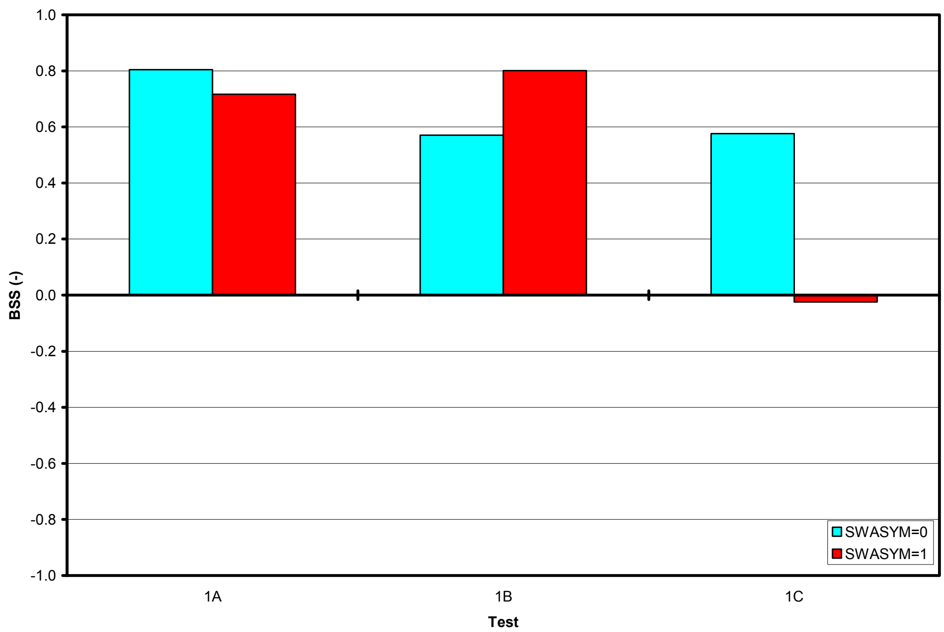

Figure 2.18 Brier Skill Scores for the total transports (UNIBEST-TC with TRANSPOR1993 is used as the base line prediction.

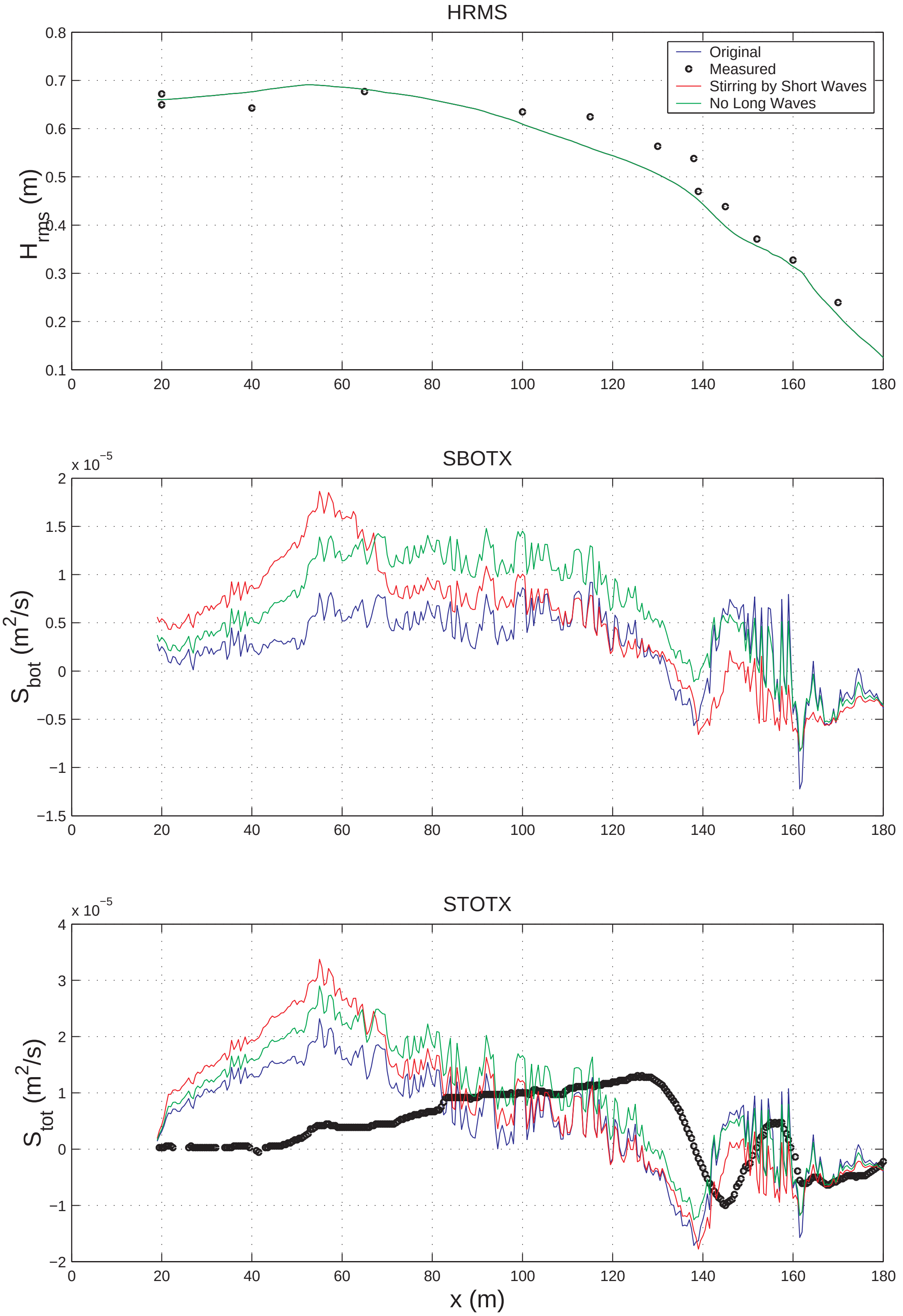

Figure 2.19 Investigation of the long wave effects on the bed load transport for Test 1A.

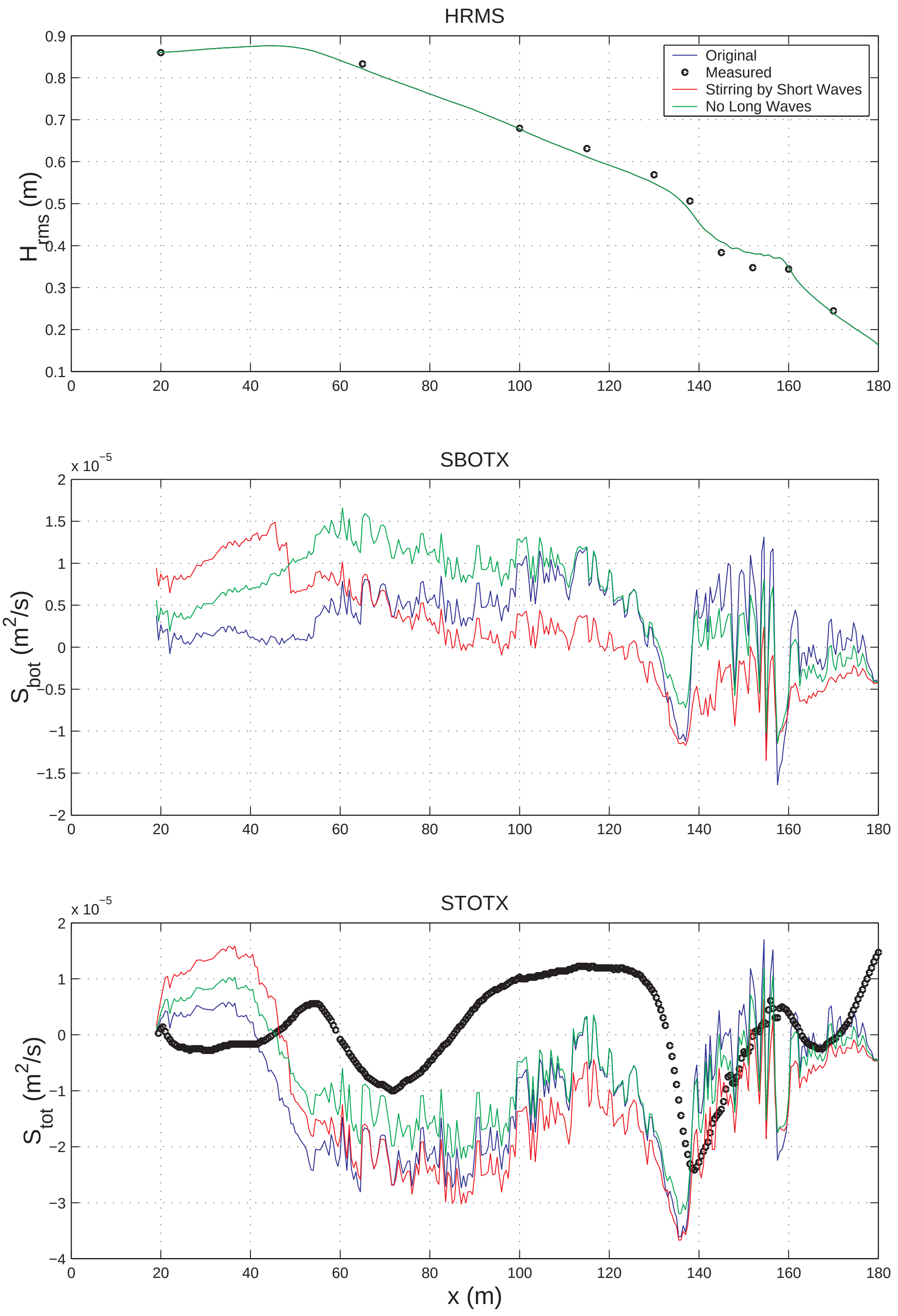

Figure 2.20 Investigation of the long wave effects on the bed load transport for Test 1B.

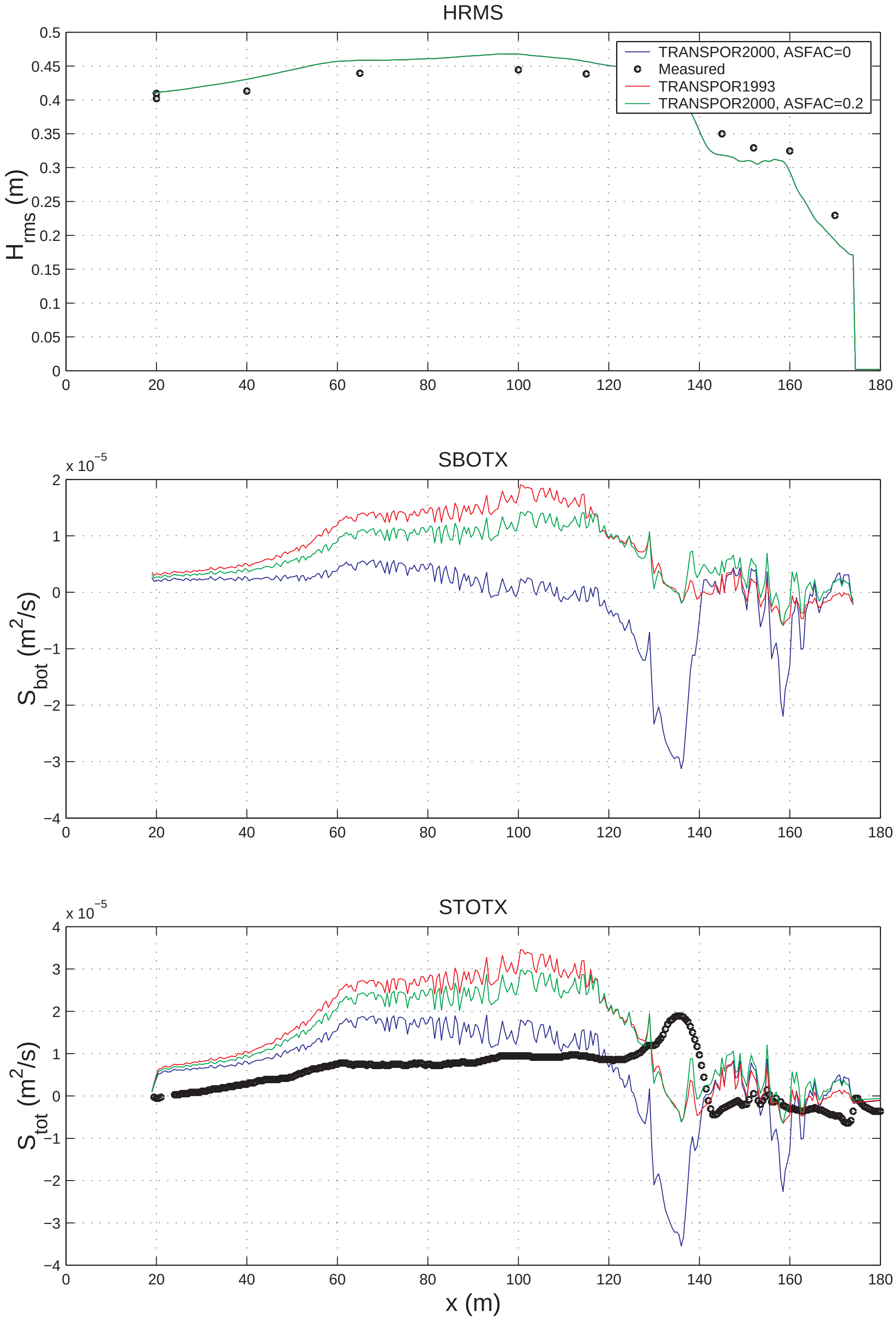

Figure 2.21 Investigation of the long wave effects on the bed load transport for Test 1C.

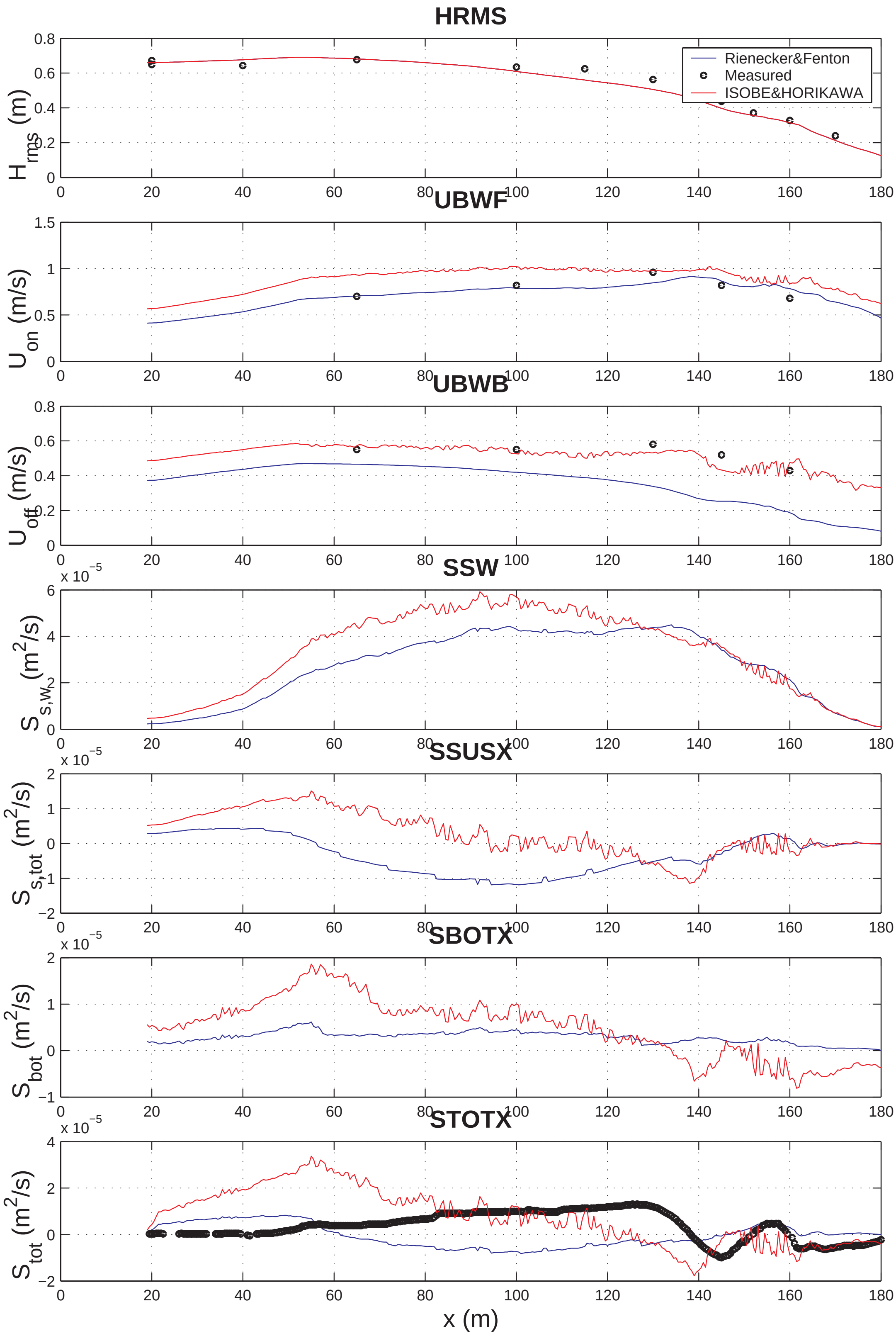

Figure 2.22 Investigation of the non-lineair wave theory for Test 1A.

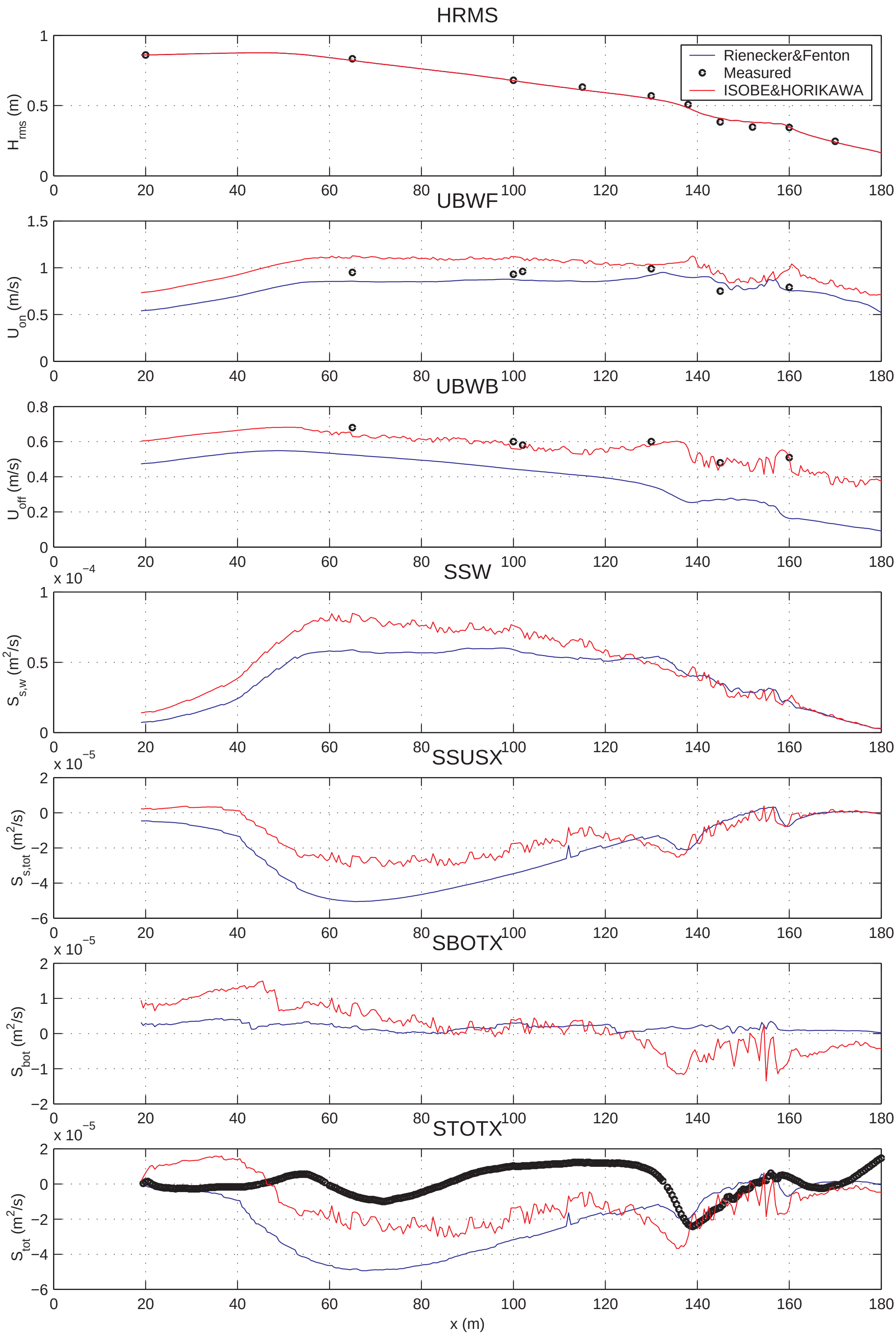

Figure 2.23 Investigation of the non-lineair wave theory for Test 1B.

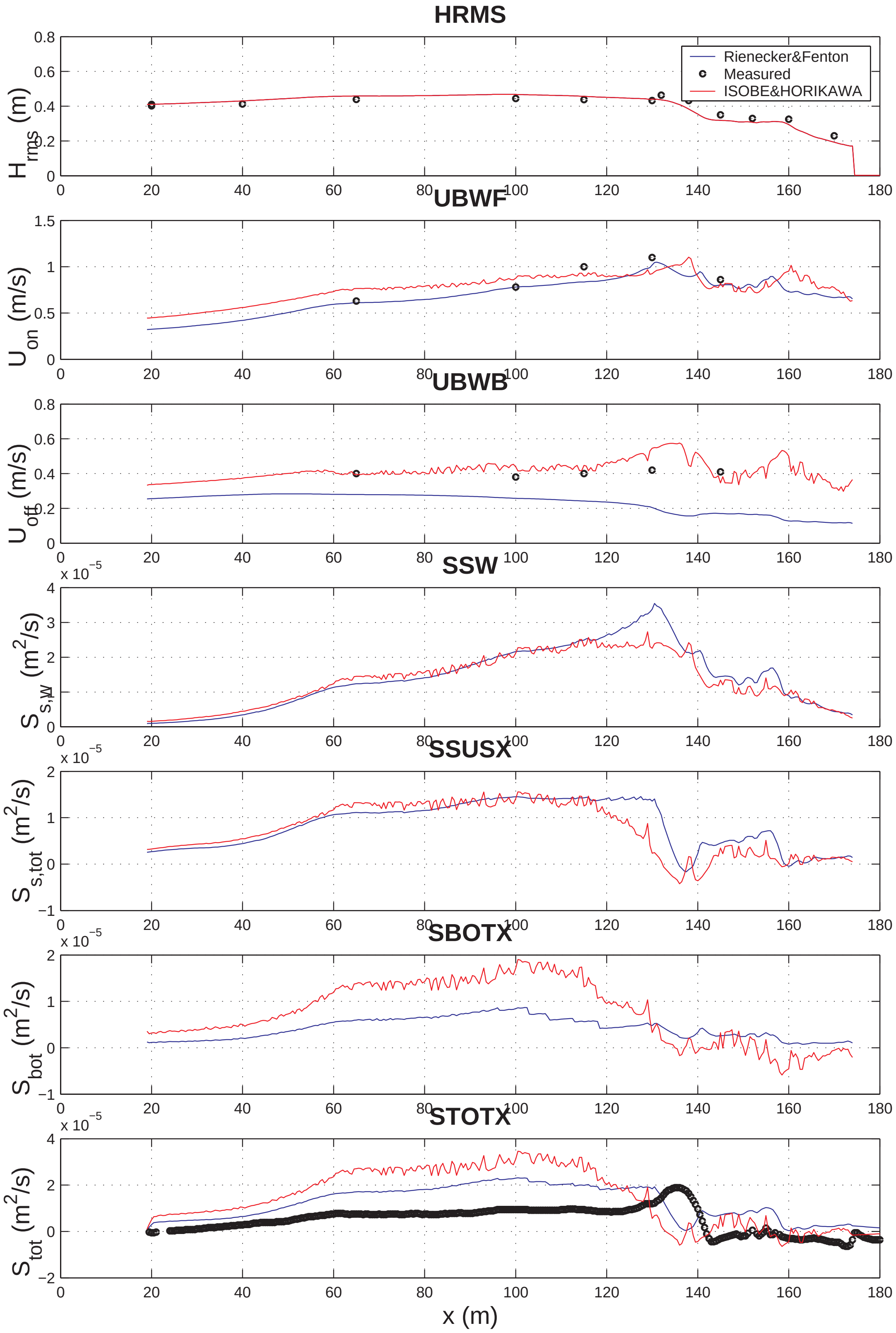

Figure 2.24 Investigation of the non-lineair wave theory for Test 1C.

2.7 Conclusions and Recommendations

2.7.1 Conclusions

Within this project a number of improvements have been implemented in an upgraded UNIBEST-TC model (Version 2.10):

- Upgrade to TRANSPOR2000 transport formula.
- Modification of long wave effects on bed load transport by assuming the orbital velocities to determine the sediment stirring and applying the complete velocity signal (including long wave motion) for the advection of the stirred up sediment.
- Inclusion of wave related suspended sediment transport.
- Implementation of the Isobe-Horikawa non-lineair wave theory for the near bed orbital velocities.

The implementation of these items was verified via a limited number of verification runs which showed that:

- the upgrade to TRANSPOR2000 has been successful and resulted in identical concentration profiles with van Rijn's TRANSPOR2000 point model.
- the Isobe-Horikawa non-lineair wave theory in UNIBEST-TC yielded identical peak orbital velocities in onshore and offshore direction. The method to construct the intra wave time series differs slightly from the method applied in TRANSPOR2000. However it is thought that the UNIBEST-TC approach, which results in a continuous signal is more realistic.
- The modification of the long wave effects on the bed load can have a significant effect on the resulting bed load transport. Especially, in the surf zone where wave breaking is most intense (e.g. near bars) the bed load transport was much to sensitive to the long wave motion. The considered simulations showed that the new approach resulted in a dramatic decrease of the seaward transport for LIP11D Test 1C on top of bars and could even cause a shift from offshore to onshore transports.
- The inclusion of wave related suspended transports is imperative for an accurate prediction of the total suspended sediment transport. In the considered cases the wave related suspended transport are dominant or of the same order of magnitude compared to the offshore directed undertow related suspended transport.
- Comparison of the Isobe-Horikawa and Rienecker&Fenton non-lineair wave theories showed that the onshore peak velocities had a surprisingly similar cross-shore distribution. However, the offshore peaks were significantly under-predicted by the Rienecker&Fenton model.
- The resulting bed load transports showed that with Isobe-Horikawa a better qualitative agreement was obtained.

2.7.2 Recommendations

The knowledge of cross-shore processes is still very limited. This lack of knowledge is mainly caused by the inability to accurately predict the cross-shore distribution of the breaking wave forces and the associated sediment transport. As a result, usually site-specific calibrations have to be carried out. Unfortunately despite the improvements suggested and implemented in UNIBEST-TC in this study it thought that site-specific calibrations will still be necessary. Moreover, the limited verification runs have shown that the sediment transports in the improved UNIBEST-TC model have changed considerably. This implies that application of the new model to sites investigated with previous UNIBEST-TC model versions will require a complete new calibration. This is part of the development – testing – evaluation cycle which plays a central role in the VOP-project (see e.g. Walstra et al., 2001).

It is therefore recommended to initiate a verification study which addresses important processes on which the knowledge is limited or are known to be modelled inaccurately. The following processes are identified:

1. Roller model,
   The roller model facilitates the delayed response of the undertow and water level set-up to the depth-induced wave height decay. Already the original Battjes and Janssen (1978) paper identifies this problem. Accurate prediction of this delay is essential for accurate modelling of the water set-up and undertow and consequently the predicted profile development
2. Undertow (or return current),
   The undertow is mainly determined by two processes: the wave induced mass flux and the surface shear stress induced by the breaking waves. In both processes the roller model plays a vital part. However, the application of lineair wave theory to derive wave characteristics such as energy fluxes and shear stresses is questionable. Some studies (e.g. Dally and Brown, 1996) have shown that non-lineair wave theories (e.g. Dean's Stream Function Theory) improve the predictions considerably. However, all such studies have been performed for regular waves, extension to random waves is probably possible but not trivial.
3. Wave asymmetry (and its effect on suspended and bed load transports),
   Wave asymmetry in UNIBEST-TC can now be modelled by two different non-lineair wave theories (cf. Rienecker&Fenton and Isobe-Horikawa). The comparisons presented in this study show that both models can have significant different outcomes. More study is needed to interpret the results and verify the models. This should lead to more insight into the quality of the wave asymmetry predictions and its effect on the sediment transport rates and the sub-sequent morphological profile development.
4. Long wave effects,
   Long wave effects are modelled in a parametric way in UNIBEST-TC. The comparisons of different methods has shown that dramatic differences can occur. Further study is needed to arrive at a more comprehensive modelling of long wave effects.
5. Profile development (bar, beach. and dune development)
   As the morphological profile development is determined by the processes listed above it is essential to investigate the effects of modifications of the implemented processes. Especially the prediction in the upper part of the profile (swash zone, beach and dune) needs further attention (see also the next chapter).

In the UNIBEST-TC Testbank a number of comprehensive studies are available which can be used to perform such a verification study:

1. LIP11D Experiment (large flume, detailed hydrodynamics and morphology, short time scale)
   This experiment can be used to perform a detailed study on all items listed above. The dataset included detailed hydrodynamic measurements such as wave characteristics, current and transport measurements along the bottom profile.
2. Coast3D – Egmond (field, short time scale, detailed hydrodynamics and morphology)

This is a very comprehensive dataset which can be used to study undertow, wave asymmetry and profile development in proto type conditions. The time scale of this dataset is about a month.

3. Duck – Onshore and offshore events (short time scale detailed hydrodynamics and morphology)
   This dataset can be used as the Egmond Coast3D dataset. However, an important extension is the fact that clear onshore and offshore events are available in this dataset. These can provide insight into the relevance of the various transport processes under different forcing conditions.
4. Egmond – LT (long term morphology: time scale is 20 years, but no hydrodynamics)
   This dataset can be used to determine the long term effects.

3 Implementation of the DUROSTA approach

3.1 General background

One of the main problems in mathematical cross-shore transport modelling is the treatment of the beach boundary condition. Without special measures, the local cross-shore transport discontinuity will yield an unfavourable and incorrect profile development at this location. In previous studies it was shown that by an advection description of the dry beach profile a reasonable prediction of dune erosion was established with UNIBEST-TC (see Gootjes, 2000 and Walstra et al. 2001). However, the Walstra et al. (2001) also showed that the dune erosion predicted by UNIBEST-TC was always uniformly distributed over the dune. Especially for the GWK-experiments this yielded an unrealistic over-estimation of dune erosion in the upper part of the profile.

In the present study, the approach followed by the DUROSTA model to extrapolate the sediment transport over the dry beach and dune is implemented in UNIBEST-TC. The mathematical dune erosion model DUROSTA is described (Steetzel, 1993).

In dune erosion modelling, the actual cross-shore transport rates in especially the beach and dune area are of utmost importance. As a consequence, special attention has to be given to the treatment of the beach boundary condition. The aim of the dune erosion model (Steetzel, 1993) was especially to assess the amount of erosion from above the maximum storm surge level and subsequently to determine the landward extent of the erosion.

Since only extreme eroding events are of interest, only seaward directed transport has been taken into account in the DUROSTA-model.

3.2 General procedure in the DUROSTA-model

The general procedure for the improvement of the beach boundary condition and the subsequent bottom modification consists of three subsequent steps, namely:

1. The modification of the cross-shore transport distribution in the area near and above the waterline;
2. The computation of the bed level changes in the beach/dune area;
3. The application of additional (numerical) swash near the waterline.

These steps are briefly described in the following sub-sections.

3.2.1 Modified cross-shore transport distribution

The basic idea is that the transport formulation applied in the numerical model yields acceptable results for relatively deeper water. In the region near the water line, this is (by definition) not the case. The first step is to define a so-called transition point. Seaward of this position, the transport formulations are assumed to be valid. Landward of this position, additional corrections have to be taken into account.

The magnitude of the cross-shore transport rate in the transition point is referred to as the reference transport rate. It should be noted that, in case of the DUROSTA-model, this reference transport rate is always offshore directed whereas in UNIBEST-TC an onshore transport can occur.

The transport rate in any point landward of the transition point is expressed as a fraction of the reference transport rate, depending on the local bed level. For a specific position in the beach-dune area, the fraction of the reference transport is assumed to be related to both the relative bed level and the relative wave run-up. The combination of a relatively high bed level and a relatively small wave attack (and thus small wave run-up) has to yield a minor fraction as a result. The actual fraction of the transport at a certain bed level (the relative vertical transport distribution) is assumed to be related to the relative volume of water (the so-called relative conflict volume) which passes this level. In the transition point this fraction equals 100%.

The absolute horizontal cross-shore transport distribution in the area landward of the transition point can now be assessed from the product of the reference transport rate and the relative conflict volume.

3.2.2 Bed changes in dune area

Applying the corrected cross/shore transport distribution and an adequate time step, the bed level changes can be assessed. Near the dune face the bed level correction must be such that only the dune face itself is eroding. In the DUROSTA-model, a modified numerical scheme is used in this region.

3.2.3 Local swash

In order to mitigate the effect of bottom irregularities in the area between the transition point and the waterline, some additional numerical swash is applied.

In the framework of the present study attention has been paid only to the assessment of a corrected transport distribution in the beach/dune area. A special treatment of the bottom change assessment procedure in the dune area in the present UNIBEST-TC model seems difficult. Also the application of additional numerical swash in this region has not been considered.

In the next section, the assessment of the modified cross-shore transport distribution is elaborated in more detail.

3.3 Modified cross-shore transport distribution

The basic idea is to relate the relative cross-shore transport rate at a certain vertical level to the relative amount of water, which exceeds this level due to wave run-up on the beach/dune slope.

3.3.1 Transition point and reference transport rate

The first step is to define a so-called transition point. Seaward of this position, the basic transport formulations are assumed to be valid. Landward of this position, additional corrections have to be taken into account.

In the DUROSTA-model, this position is chosen in such a way that the distance between the waterline and this transition point is equal to a quarter of the local wavelength. In this way the assessment of the location of this transition point is independent of the actual schematisation in terms of grid positions etc. The magnitude of the cross-shore transport rate in the transition point is referred to as the reference transport rate. In the UNIBEST-TC model the location of the transition point is assessed using:

$$h_{\min} = g\left(\frac{T_p}{T_{dry}}\right)^2 \tag{3.1}$$

The T_{dry} parameter has to be specified by the user.

No modifications have been made regarding this item.

3.3.2 Significant wave run-up level

The transport rate in any point landward of the transition point is expressed as a fraction of the reference transport rate, depending on the local bed level. For a specific position in the beach-dune area, the fraction of the reference transport is assumed to be related to both the relative bed level and the relative wave run-up. The combination of a relatively high bed level and a relatively small wave attack (and thus small wave run-up) has to yield a minor fraction as a result.

The significant wave run-up level is computed from:

$$Z_s = 0.5\, T_p \sqrt{gH_s}\, \tan(\alpha) \tag{3.2}$$

in which:

- Z_s significant run-up above the mean water level (m)
- T_p wave peak period (s)
- H_s significant wave height (m)
- $\tan(\alpha)$ mean slope of the dune face (between transition point and wave run-up level)

For the wave height the offshore wave height has been used (just like in the DUROSTA-model).

Starting at the transition point, the area for which the mean slope is computed, is extended in landward direction until the run-up position is exceeded. In the present version of the UNIBEST-TC code, the maximum run-up level is limited to the offshore wave height.

The next step is to assume a Rayleigh-distribution for the run-up levels.

The chance that the a specific run-up level Z is exceeded can thus be computed from:

$$P(Z > Z) = \exp\left[-2\left(\frac{Z}{Z_s}\right)\right] \tag{3.3}$$

In which:

P the probability of exceedance (-)
Z a specific level (m)
Z_s significant run-up above the mean water level (m)

3.3.3 Conflict volume

The actual fraction of the transport at a certain level above the waterline is assumed to be related to the relative volume of water (the so-called relative conflict volume) which passes this level. Assuming a triangular shaped water tongue, the volume of water above a specific crest level can be expressed as:

$$A = C_A \left(Z - Z_c\right)^2 \tag{3.4}$$

in which:

A the trespassing water volume (m^3/m^1)
C_A a dimensionless constant (-)
Z a specific run-up level (m)
Z_c a specific crest level (m)

The chance of occurrence of a specific run-up-level can be computed from:

$$p(Z = z) = \frac{4}{Z_s}\frac{z}{Z_s}\exp\left[-2\left(\frac{z}{Z_s}\right)^2\right] \tag{3.5}$$

In which:

p the chance of occurrence of a specific run-up level (-)
z a specific level (m)
Z_s the significant run-up above the mean water level (m)

The time-averaged integrated trespassing volume above a specific crest level can be computed from:

$$A_{mean}\left(Z_c\right) = \int_{z=Z_c}^{\infty} p\ A\ dz \tag{3.6}$$

or:

$$A_{mean}(Z_c) = \int_{z=Z_c}^{\infty} C_A\left(z - Z_c\right)^2 \frac{4}{Z_s}\frac{z}{Z_s}\exp\left[-2\left(\frac{z}{Z_s}\right)^2\right]dz \tag{3.7}$$

This expression yields the time-averaged amount of water trespassing a specific crest level.

3.3.4 Relative conflict volume

For the assessment of the transport rate, especially the relative volume RCV is relevant. Thus:

$$RCV = \frac{A_{mean}(Z_c)}{A_{mean}(0)} \tag{3.8}$$

The absolute horizontal cross-shore transport distribution in the area landward of the transition point can now be assessed from the product of the reference transport rate and the relative conflict volume (RCV). After some elaboration it can be found that the magnitude of the relative conflict volume can be assessed from a function:

$$RCV = \exp\left(-\sigma^2\right) - \sqrt{2\pi}\ R_z\ \left[1 - erf(\sigma)\right] \tag{3.9}$$

In which:

$$\sigma = \sqrt{2}\ R_z \tag{3.10}$$

The relative level is computed from:

$$R_z = \frac{Z_c}{Z_s} \tag{3.11}$$

Use is made of the so-called ERF-function which is defined as:

$$erf\left(\sigma\right) = \frac{2}{\pi}\int_0^{\sigma}\exp\left(-x^2\right)dx \tag{3.12}$$

In the mathematical model an approximation for the computation of the ERF-function has been used.

3.3.5 Cross-shore transport distribution

The modified transport rate in the area landward of the transition point is computed from the product of the reference transport rate (in the transition point) and the local value of the RCV-value according to:

$$q_{x,i} = RCV\left(\frac{Z_i}{Z_s}\right)q_{ref} \tag{3.13}$$

3.4 Results of computations

UNIBEST-TC's improved capability to model dune erosion has been assessed by intercomparing UNIBEST-TC predicted profile evolution against DUROSTA results, both obtained from modelling the 10 representative flume experiments described in Walstra et al. (2001), which is included in Appendix C. As a reference the Walstra et al. (2001) results are also included. DUROSTA was run with the standard parameter settings according to Steetzel (1993). UNIBEST-TC settings were according to the Walstra et al. (2001) settings in which the model was calibrated based on test M1263-T1. GAMMA was set to 0.85 (in accordance with the DUROSTA settings) and the current-related roughness parameters RKVAL (flow model) and R_c (transport model) were both lowered to 0.005 m. Standard settings were applied for the roller model (BETD = 0.10), while the concept of breaker delay was turned off (F_LAM = 0, cf. Roelvink et al., 1995). No bar damping mechanisms (modification of sub-aqueous angle of natural repose, cf. Bosboom et al, 1997) were applied. The parameter settings thus obtained were consistently applied to all 10 test cases. For reasons of stability, different grid layouts and numerical time steps were applied for the various runs (Table 3.1).

Table 3.1 Overview of numerical model settings. dt represents the time step, Dxsea the model extension at the seaward boundary, dx1 (dx2) the cross-shore step size at the deep (shallow) part of the profile and Ndx1 and Ndx2 the number of dx1 and dx2 respectively.

Test	Time step dt (days)	Δx_{sea}	Computational grid			
			dx1 (m)	N_{dx1} (-)	dx2 (m)	N_{dx2} (-)
GWK-A9	0.002	-	1	140	0.50	220
GWK-B2	0.002	-	1	130	0.50	216
GWK-C2	0.002	-	1	130	0.50	216
GWK-H2	0.002	-	1	130	0.50	216
M1263-T1	0.0001	-	1	100	0.50	200
M1263-T2	0.0005	-	1	100	0.50	200
M1263-T3	0.0005	20	1	100	0.50	240
M1263-T4	0.0005	90	1	290	-	-
M1263-T5	0.0002	90	1	290	-	-
M1792-T1	0.00025	-	1	230	-	-

3.4.1 Experiment #01: M1797, Test T1

This experiment is characterised by dramatic dune erosion and the entire profile is experiencing significant accretion (Figure 3.1). Both UNIBEST-TC models under-estimate the erosion volume, but the accretion in the lower parts of the profile is modelled accurately by DUROSTA and the original UNIBEST-TC 'Vertical' approach. In the simulation with the upgraded UNIBEST-TC model the wave run-up had to be restricted to the offshore significant wave height. Probably, the presence of time-varying boundary conditions enhances the effect of the too pronounced erosion at the waterline position. In order to overcome this (rather crude) correction, a more detailed elaboration of the wave run-up procedure is required. In combination with an improved definition of the transition point and an improved method to assess the characteristic slope the results will probably improve.

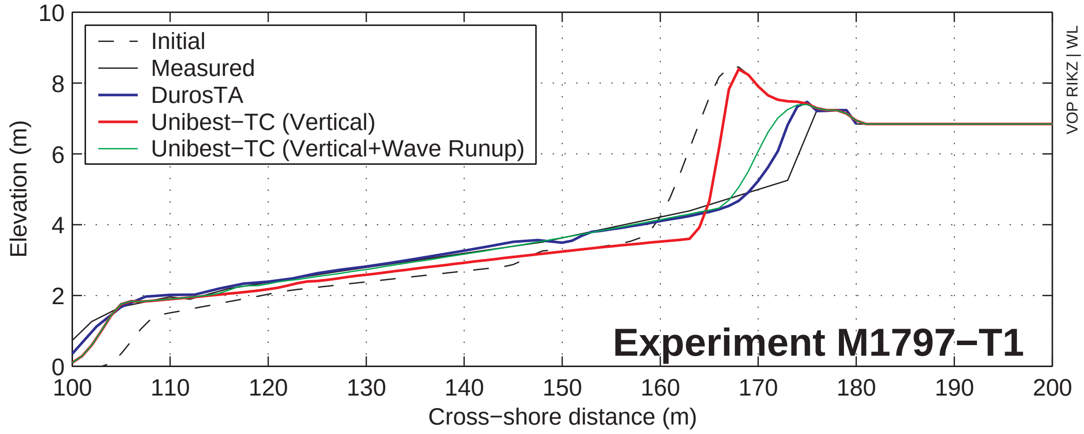

Figure 3.1 Overview of profiles for test T1 of the M1797-series.

3.4.2 Experiments #02 - #06: M1263, Test T1- Test T5

Test 1

Both models show comparable results, but UNIBEST-TC under-estimates the dune erosion and as a consequence the accretion on the beach and inner surf zone is also under-estimated (Figure 3.2). However the seaward extent of the accretion is comparable for both models and agrees well with the measurements. The beach slope is also reproduced well. The effect of the improved dune erosion in UNIBEST-TC is limited.

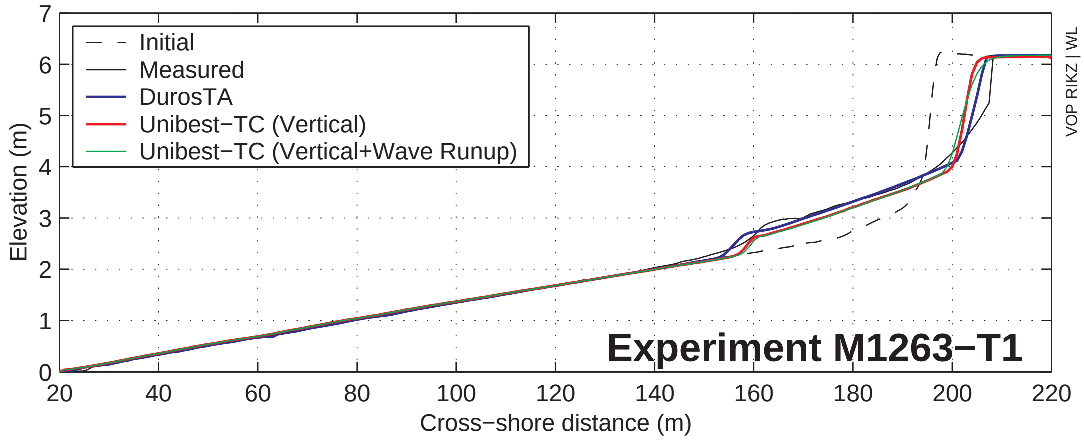

Figure 3.2 Overview of profiles for test T1 of the M1263-III-series.

Test 2

Results are consistent with Test 1: under-estimation of dune erosion and accretion. Shoreward extents of accretion and beach slope are comparable and agree well with measurements (Figure 3.3). Again the improvements lead to a somewhat steeper dune front in UNIBEST-TC.

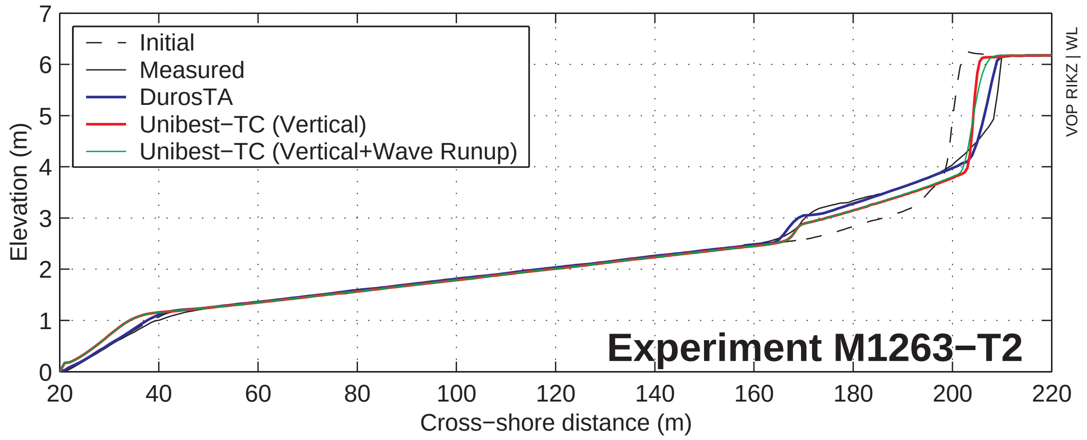

Figure 3.3 Overview of profiles for test T2 of the M1263-III-series.

Test 3

Both models show almost the exact same final profile (Figure 3.4). Compared to the measurements the dune erosion is under-estimated and does not show the discontinuity at the dune foot. The accretion in the inner surf zone shows very good agreement. The UNIBEST-TC run with wave run-up under-estimates the dune erosion. Especially the erosion in the upper part of the dune is under-estimated.

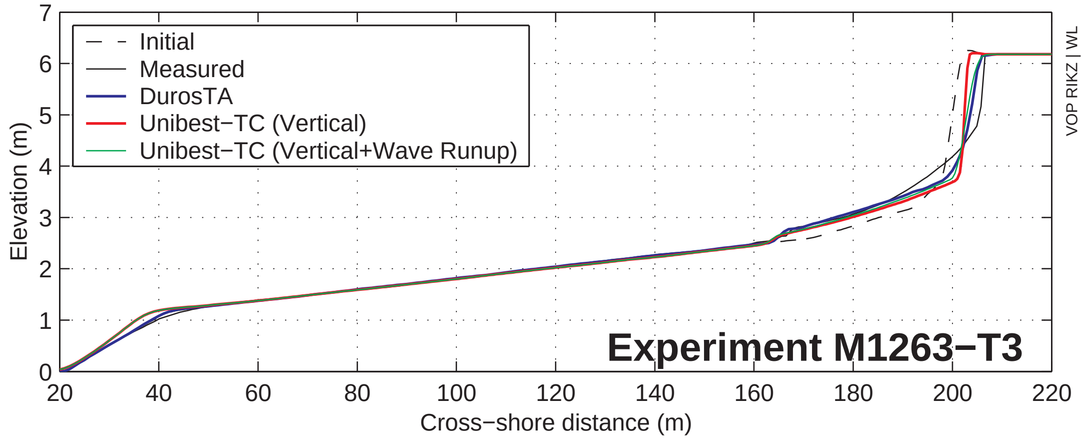

Figure 3.4 Overview of profiles for test T3 of the M1263-III-series.

Test 4

In contrast to Tests 1 and 2, the improved UNIBEST-TC model now shows an excellent agreement with DUROSTA profile (Figure 3.5). However, the accretion at the beach and the inner surf zone is predicted better by DUROSTA. The UNIBEST-TC final profiles (both 'Vertical' and 'Vertical+Wave Run-up') is too flat and expands too far seaward, with as a consequence an under-estimation the absolute accretion levels in this area.

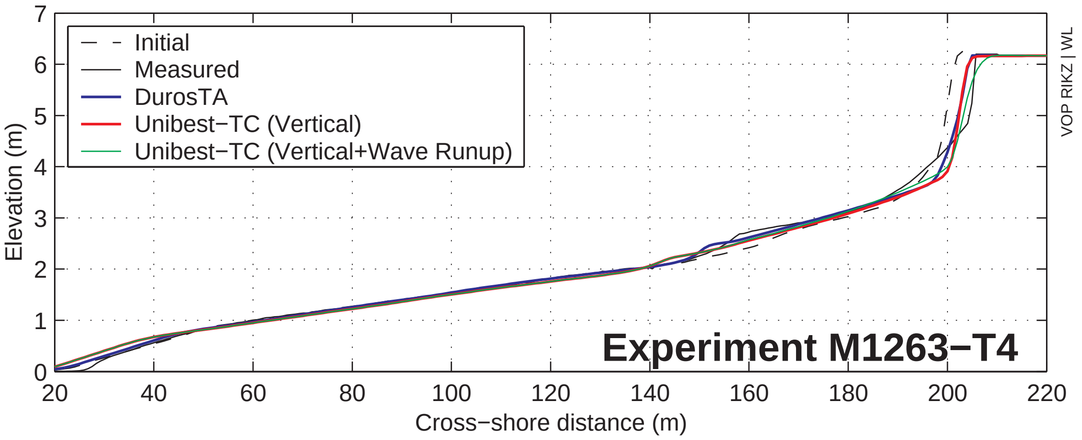

Figure 3.5 Overview of profiles for test T4 of the M1263-III-series.

Test 5

For this test both models show considerable differences. Similar to Tests 1 and 2 UNIBEST-TC under-estimates the dune erosion whereas DUROSTA slightly over-estimates the dune retreat (Figure 3.6). The deposition area is too large for both models and the slope is somewhat flatter which results increased errors near the dune foot.

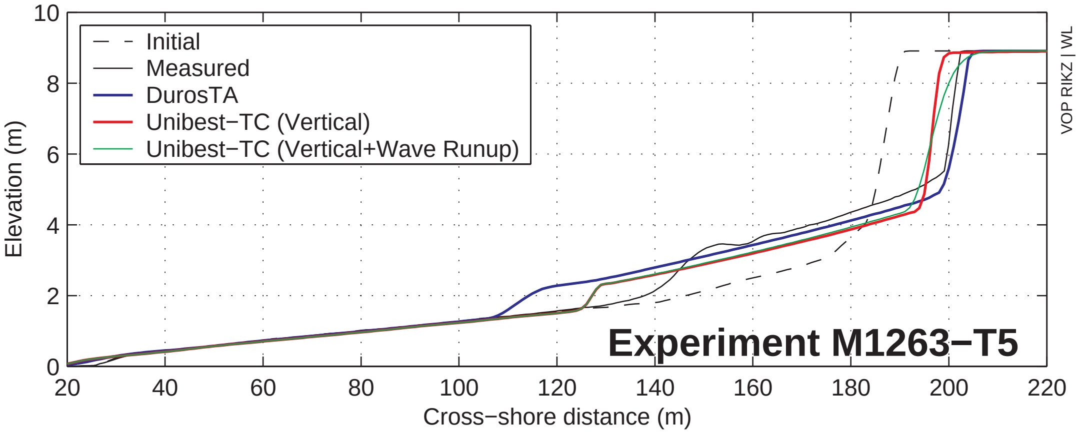

Figure 3.6 Overview of profiles for test T5 of the M1263-III-series.

3.4.3 Experiments #07 - #10: GWK1998, Tests A9, B2, C2 and H2

During the experiments the beach profile tends to develop a less steep profile and yields erosion near the waterline. The eroded material settles in the nearshore area and a relatively flat beach slope is obtained. Both models consistently predict the deposition of eroded material too far seaward for all 4 test cases. The computational results for DUROSTA are in line with the experiments, looking at the amount of erosion near the waterline and the beach slope after the experiments.

If we look in more detail at the results of the GWK-tests (viz. A9, B2, C2 and H2), the effect of the modification of the boundary treatment is very obvious in the upgraded UNIBEST-TC model. Instead of a gradual erosion of the dune slope (see 'UNIBEST-TC (Vertical)' results) the erosion is now concentrated in a restricted zone near the waterline.

Although the overall resemblance is much better for the modified version, the model seems to yield relatively too much erosion at the waterline position. This reason for this is not clear. It might be due to:

1. the fact that the area in which the cross-shore transport modification is valid is too narrow (in DUROSTA the 'quarter of the local wave length' is used to assess the position of the transition point),
2. the 'lack' of (numerical) swash in the region near the waterline or
3. the computational scheme.

In order to sort this out, a more detailed elaboration is required.

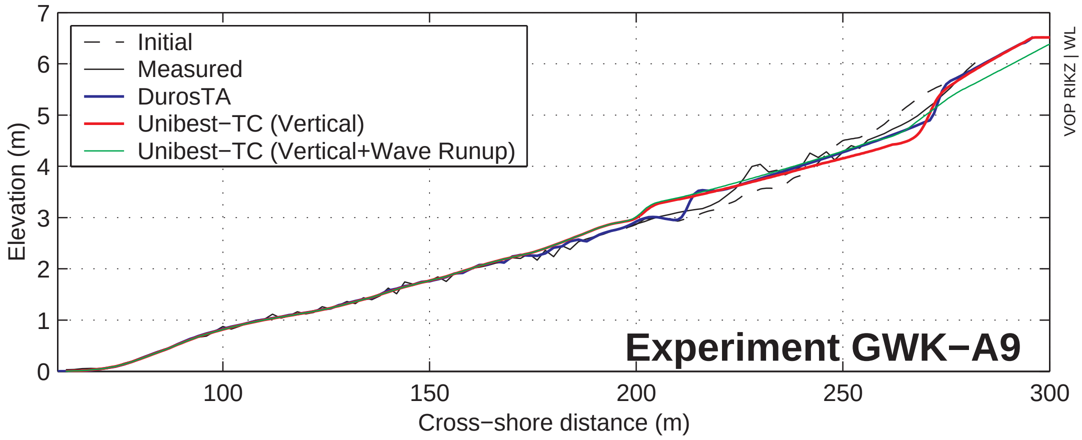

Figure 3.7 Overview of profiles for test A9 of the GWK-series.

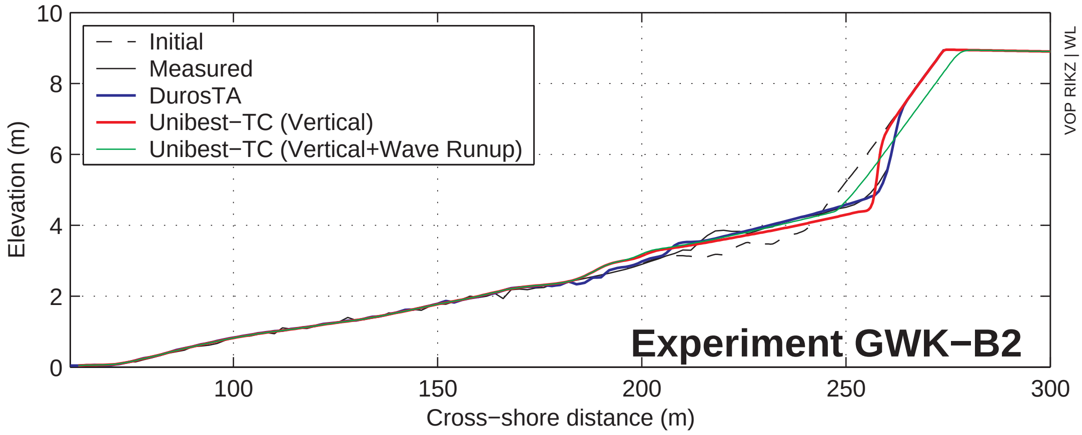

Figure 3.8 Overview of profiles for test B2 of the GWK-series.

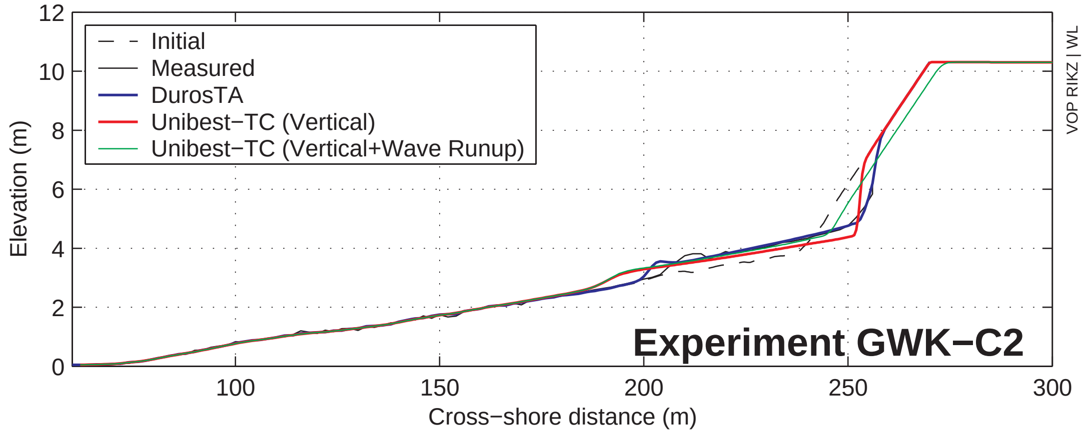

Figure 3.9 Overview of profiles for test C2 of the GWK-series.

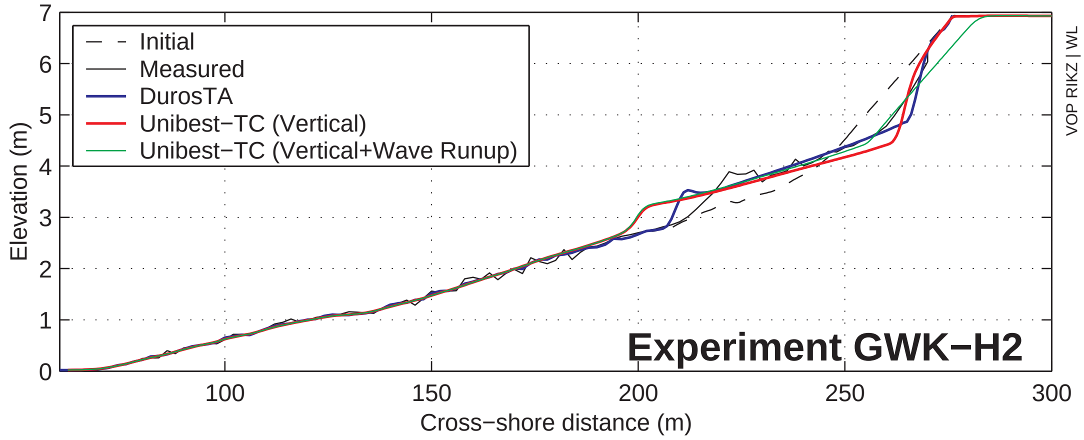

Figure 3.10 Overview of profiles for test H2 of the GWK-series.

3.5 Conclusions and Recommendations

3.5.1 Conclusions

From the results of the computations it can be observed that in most cases the behaviour of the beach/dune area is comparable to the DUROSTA-case. The erosion of the dune face is restricted to the area of the wave run-up and therefore independent of the width or height of the dune.

If we look in more detail at the results of the GWK-tests (viz. A9, B2, C2 and H2), the effect of the modification of the boundary treatment is very obvious. Instead of a gradual erosion of the dune slope (see 'UNIBEST-TC (Vertical)' results) the erosion is now concentrated in a restricted zone near the waterline.

Although the overall resemblance is much better for the modified version, the model seems to yield relatively too much erosion at the waterline position. This reason for this is not clear. It might be due to:

1. the fact that the area in which the cross-shore transport modification is valid is too narrow (in DUROSTA the ‘quarter of the local wave length’ is used to assess the position of the transition point),
2. the ’lack’ of (numerical) swash in the region near the waterline or
3. the computational scheme.

More or less the same results hold for the M1263-tests where the vertical erosion at the waterline position is overestimated also. Due to the relatively severe wave attack, the improvement of the modification is less clear. The overall resemblance is however reasonable.

It should be noted that especially for these tests, the computed estimate of the significant wave run-up had to be restricted to the offshore significant wave height. In order to overcome this (rather crude) correction, a more detailed elaboration of the wave run-up procedure is required. In combination with an improved definition of the transition point and an improved method to assess the characteristic slope the results will probably improve.

The latter problem seems even more prevailing in the M1797-case. Probably, the presence of time-varying boundary conditions enhances the effect of the too pronounced erosion at the waterline position.

3.5.2 Recommendations

The improvements and results presented in this report should be seen as a first step in integrating the DUROSTA approach into UNIBEST-TC. It was shown that both model generally give similar solutions which is, considering the different wave and transport models, somewhat surprising. The differences in model outcomes have been summarised above and lead to recommendations to solve the remaining discrepancies between both models regarding the treatment of dune erosion. It has to be noted however that the aim is not to find an exact match between both models, but to extend the DUROSTA approach implemented in UNIBEST-TC to the same level as in the DUROSTA model.

To extend the modelling of the dune erosion in UNIBEST-TC to the same level as the original DUROSTA model a detailed comparison of both models is necessary. Although it is difficult to assess beforehand which improvements will have the greatest influence on the results it is our opinion that the following issues should be dealt with first (in order of importance):
1. The position of the transition zone should be synchronised. It is recommended to implement the DUROSTA method which uses a quarter of the local wave length from the water line to assess the transition point.
2. The calculation of the significant wave run-up should be improved. It is not clear at this stage why the run-up has to be limited to the offshore wave height in UNIBEST-TC.
3. In DUROSTA the above parameters are determined exactly and are not coupled to the applied numerical grid as in UNIBEST-TC. Considering the large transport gradients present in the inner surf zone it is imperative to implement this in UNIBEST-TC as well.
4. The above also hold for the determination of the characteristic slope which is used to determine the wave run-up. This expression should also be compared in detail with results from the DUROSTA model.

Next, it is recommended to perform a detailed comparison study along the lines presented in this study. However such an extended comparison should be focussed on parameters which are relevant for coastal authorities (such as decrease in dune volume) and should also include some field cases.

Additional improvements that could be considered are:

- It is expected that implementation of a DUROSTA alike time stepping method, involving a varying time step based on the simulated profile changes, will result in a more robust model.

Subsequently a study should be undertaken to investigates the performance of the improved Unibest-TC model to simulate the dry part of the beach for other hydraulic conditions. In the present study the model has been applied only to investigate the effect of storm conditions. The effect of mild conditions, which might generate even onshore-directed transport have not yet been investigated. Such an elaboration seems a very logical step, since this will extend and improve the model's applicability to simulate coastal behaviour for the medium term and thus make it a more useful instrument to assess the effect of large-scale (beach) nourishments.

The evaluation of the model should be based on aggregated parameters such as beach width, dune volume, etc to provide coastal authorities insight in the performance and the applicability of the model as a support tool for coastal policy issues.

4 References

Battjes, J.A., and J.P.F.M. Janssen, 1978. Energy loss and set-up due to breaking in random waves. Proc. 16th Int. Conf. on Coastal Eng., ASCE, pp. 569-587.

Battjes, J.A., and M.J.F. Stive, 1985. Calibration and verification of a dissipation model for random breaking waves. J. Geophys. Res., 90(C5): 9159-9167.

Bosboom, J., Aarninkhof, S.G.J., Reniers, A.J.H.M., Roelvink, J.A. and Walstra, D.J.R. (1997). UNIBEST-TC 2.0. Overview of model formulations. Delft Hydraulics report H2305.42

Chung, D.H. and Grasmeijer, B.T. , 1999. Analysis of sand transport under regular and irregular waves in large-scale wave flume. Report R99-05, Dep. of Physical Geography, Univ. of Utrecht, The Netherlands

Dette, H.H., Peters, K. and Newe, J., 1998a, Large wave flume experiments '96/97, equilibrium profile with different beach slopes, Rep. No. 825 Leichtweiss Inst., Techn. Univ. Braunschweig.

Dette, H.H., Peters, K. and Newe, J., 1998b, Large wave flume experiments '96/97experiments on beach erosion and stability, Rep. No. 830 Leichtweiss Inst., Techn. Univ. Braunschweig.

Dohmen-Janssen, M., 1999. Grain size influence on sediment transport in oscillatory sheet flow. Doc. Thesis. Dep. of Civil Engineering, Univ. of Twente, The Netherlands

Gootjes, G. (2000). Dunes as a source of sediment for DELFT3D-MOR. WL | delft hydraulics report no. Z2534.

Grasmeijer, B.T. and Van Rijn, L.C., 1998. Breaker bar formation and migration. Proc. ICCE., Copenhagen, Denmark

Grasmeijer, B.T. , Van Rijn, L.C., Elgar, S. and Gallagher, E., 2000. Verification of a cross-shore profile model using field data. Proc. 27th ICCE., Sydney Australia

Houwman, K.T. and Ruessink, B.G., 1996. Sediment transport in the vicinity of the shoreface nourishment of Terschelling. Dep. of Physical Geography. Univ. of Utrecht, The Netherlands

Isobe, M, Horikawa, K., 1982. Study on water particle velocities of shoaling and breaking waves. *Coastal Eng. in Japan*, 25, pp. 109–123

Hotta, S. and M. Mizuguchi, 1980. A field study of waves in the surf zone. Coastal Engineering in Japan, vol. XXIII, Japan Soc. of Civil Engineers, Tokyo.

Kessel van, T., 2000. Unibest V204 documentation. WL | Delft Hydraulics report Z2899.40.

Reniers, A.J.H.M., J.A. Roelvink and D.J.R. Walstra, 1995. Validation study of UNIBEST-TC; validation against the LIP 11D experiment, Report H2130, DELFT HYDRAULICS.

Reniers, A.J.H.M., J.A. Roelvink and E.B. Thornton, 2003. Morphodynamic modeling of an embayed beach under wave forcing. Submitted to JGR.

Rienecker, M.M. and J.D. Fenton, 1981. A Fourier approximation method for steady water waves. J. Fluid Mech., vol. 104, pp. 119-137.

Roelvink J.A. and M.J.F. Stive, 1989. Bar-generating cross-shore flow mechanisms on a beach. J. Geophys. Res., Vol. 94, no. C4, pp. 4785-4800.

Roelvink, J.A., Th.J.G.P. Meijer, K. Houwman, R. Bakker and R. Spanhoff, 1995: Field validation and application of a coastal profile model. Int. Proc. Coastal Dynamics 1995, pp. 818-828.

Ruessink, B.G., 1998. The temporal and spatial variability of infragravity energy in a barred nearshore zone. Continental Shelf Research 18 (1998), pp. 586-605.

Ruessink, B.G., 2000. An emperical energetics-based formulation for the cross-shore suspended sediment transport by bound infragravity waves. Journal of Coastal Res., Vol. 16, No. 2.

Ruessink, B.G., Walstra, D.J.R. and Southgate, H., 2002. Modeling of wave breaking on barred beaches. In press.

Steetzel, H.J., 1990. Golfhoogteafname tijdens extreme condities (Wave height decay during extreme hydraulic conditions). Research report H298, Part II (in Dutch).

Steetzel, H.J., 1993. Cross shore transport during storm surges. PhD. thesis WL | delft hydraulics, ISBN 90-9006345-5

Steetzel, H.J., 1999. Parameter review and sensitivity analysis DUROSTA-model; Initiation of a new guideline for the assessment of the safety of the Dutch dune coast. Alkyon Hydraulic Consultancy & Research, Rep. A116.

Van Rijn, L.C., 1984a. Sediment transport, Part I: Bed load transport. Journal of Hydraulic Engineering, ASCE, Vol. 110. No. 10.

Van Rijn, L.C., 1986. Mathematical modelling of suspended sediment transport in nonuniform flows. Journal of Hydraulic Engineering, ASCE, Vol. 112, No. 6

Van Rijn, L.C., 1993. Principles of sediment transport in rivers, estuaries and coastal seas. Aqua Publications, Amsterdam, The Netherlands.

Van Rijn, L.C., 2000. General view on sand transport by currents and waves: data analysis and engineering modelling for uniform and graded sand (TRANSPOR2000 and CROSMOR2000 models). Report Z2899.20/Z2099.30/Z2824.30, WL | Delft Hydraulics.

Walstra, D.J.R., M. van Koningsveld, S.G.J. Aarninkhof, 2001. Methodological approach to model development for UNIBEST-TC, WL | Delft Hydraulics report Z3148.10.

WL | Delft Hydraulics, 1982. Duinafslag tijdens superstormvloed, Noorderstrand Schouwen (Dune erosion during a super storm surge, Noorderstrand Schouwen). Research report M1797 (in Dutch).

WL | Delft Hydraulics, 1984. Schaalserie duinafslag, proeven op grote schaal in de Deltagoot (Scale series on dune erosion, large scale tests in the Delta Flume). Research report M1263, Part III (in Dutch).

A Modified Isobe-Horikawa method for non-linear orbital velocities near the bed

This method is descibed in: “Breaker bar formation and migration” by Grasmeijer and Van Rijn, ICCE 1998, Copenhagen, Denmark. However based on new calibration studies some of the formulations have been updated recently.

The high-frequency near-bed orbital velocities (low-frequency effects are neglected) are computed using a modification of the method of Isobe and Horikawa (1982). The method of Isobe and Horikawa method is a parameterisation of fifth-order Stokes wave theory and third-order cnoidal wave theory which can be used over a wide range of wave conditions. In the original formulation the near-bed value of û (defined as: $u_{on} + u_{off}$) is derived from deep water wave conditions as follows:

$$\hat{u} = 2.r.u_{linear} \tag{A1}$$

with:

$$r_3 = -27.3\log_{10}\left(\frac{H_0}{L_0}\right) - 16.3 \tag{A2}$$

$$r_2 = 1.28 \tag{A3}$$

$$r_1 = 1 \tag{A4}$$

$$r = r_1 - r_2 \exp\left\{-r_3 \frac{h}{L_0}\right\} \tag{A5}$$

u_{linear} = peak near-bed velocity computed using linear wave theory (m/s), H_0 = deep water wave height (m), L_0 = deep water wave length (m), h = local water depth (m).

The method has been modified by improving the r-factor using the local wave conditions (instead of the deep water wave height) to determine the near-bed value of û. The r-factor was found by calibration using laboratory and field data with random waves (see Table A1). This resulted in:

$$r = 1 - 3.2\left(\frac{H}{L}\right)^{065}\left(\frac{H}{L}\right)^{3.4\frac{h}{L}} \tag{A6a}$$

with: H = local wave height (m), L = local wave length (m), u_{linear} = near-bed velocity computed using linear waves theory.

In 2001, Eq. (A6a) was revised into:

$$r=0.75-0.1\tanh(2.5(H/L)-1.4) \tag{A6b}$$

The basic data are given in Table A1.

Description	Testnumber	h (m)	H_{m0} (m)	T_p (s)
Field: Terschelling, The Netherlands	Fop05330	9.0	1.89	8.0
	Fop17352	9.4	0.37	17.1
	Fop17576	10.5	4.20	10.2
	Fra05330	5.6	1.87	8.0
	Fra17576	7.7	3.42	9.7
	Fre05330	4.1	1.70	8.1
	Fre17352	5.4	0.37	16.5
Field: Egmond aan Zee, The Netherlands	1B_04430	1.9	0.76	6.1
Lab: small scale flume Delft Univ. of Techn.	TUDB2_01	0.60	0.18	2.2
	TUDB2_05	0.31	0.17	2.2
	TUDB2_07	0.51	0.15	2.2
Field: Muriwai, New Zealand	Muriwai2	1.83	0.92	19.7
Field: Skallingen, Denmark	Sk304_08	1.8	0.80	11.0
	Sk310_01	2.6	1.49	8.8
Lab: Delta Flume Lip11D WL Delft Hydraulics	1A0203_02	2.31	0.92	5.0
	1A0203_07	0.91	0.62	5.0
	1B0213_02	2.30	1.19	5.0
	1B0213_07	0.89	0.57	5.0
	1C0204_02	2.25	0.63	8.0
	1C0204_03	1.77	0.63	8.0
	1C0204_05	1.16	0.63	8.0
	1C0204_11	1.59	0.63	8.0

Table A1 *Basic data of measurements used in calibration of r-factor.*

Measured signals of surface elevation and horizontal orbital velocity near the bed were analysed using spectral analysis. High- and low-frequency oscillations were separated (by filtering) at a period of 2 times the wave spectrum peak period, T_p. The high-frequency signals were separated into shorter time series each containing 10-15 individual waves. Each of the short time series was defined as one single wave class with one representative wave height, wave period, crest velocity near the bed, and trough velocity near the bed. The mean values were chosen to represent the wave class. A comparison between measured and computed values of û is presented in Figure A1. The broken lines indicate a 20% error band.

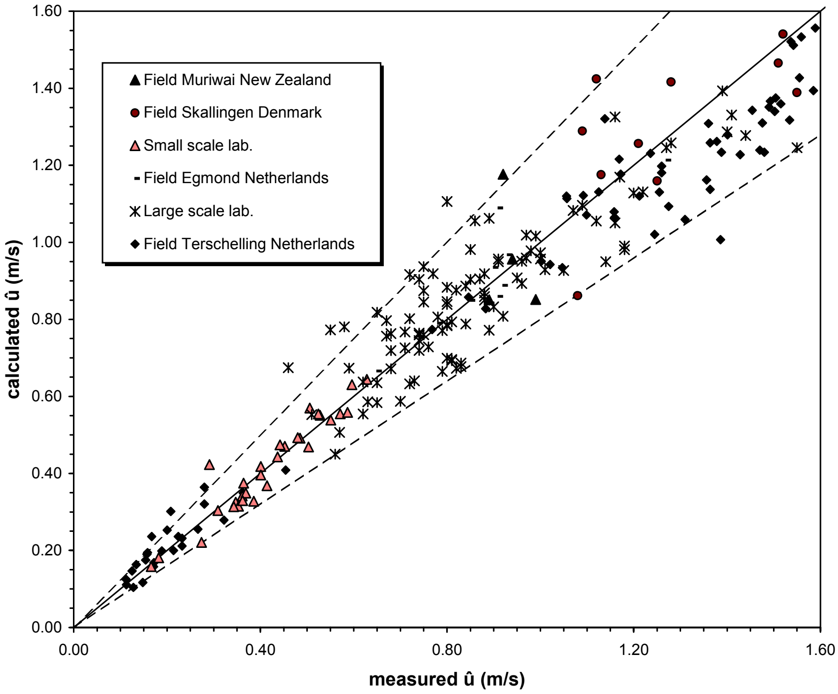

Figure A1. *Comparison between measured and computed values of near-bed orbital velocity û defined as* $u_{on} + u_{off}$.

The following formulae, Eq.(A7)-Eq.(A14), were derived to account for the asymmetry of the velocity profile (Isobe and Horikawa, 1982). Eq.(A7)-Eq.(A12) is a parameterisation of fifth-order Stokes wave theory and third-order cnoidal wave theory. Eq.(A13) and Eq.(A14) were introduced to take into account the deformation of the velocity profile due to bottom slope.

$$\left(\frac{u_{on}}{\hat{u}}\right)_a = \lambda_1 + \lambda_2\left(\frac{\hat{u}}{\sqrt{gh}}\right) + \lambda_3 \exp\left(-\lambda_4\left(\frac{\hat{u}}{\sqrt{gh}}\right)\right) \tag{A7}$$

with:

$$\lambda_1 = 0.5 - \lambda_3 \tag{A8}$$

$$\lambda_2 = \lambda_3\lambda_4 + \lambda_5 \tag{A9}$$

$$\lambda_3 = \frac{(0.5 - \lambda_5)}{\lambda_4 - 1 + \exp(-\lambda_4)} \tag{A10}$$

$$\lambda_4 = \begin{cases} -15 + 1.35\left(T\sqrt{\frac{g}{h}}\right), & T\sqrt{\frac{g}{h}} \le 15 \\ -2.7 + 0.53\left(T\sqrt{\frac{g}{h}}\right), & T\sqrt{\frac{g}{h}} > 15 \end{cases} \tag{A11}$$

$$\lambda_5 = \begin{cases} 0.0032\left(T\sqrt{\frac{g}{h}}\right)^2 + 0.000080\left(T\sqrt{\frac{g}{h}}\right)^3, & T\sqrt{\frac{g}{h}} \le 30 \\ 0.0056\left(T\sqrt{\frac{g}{h}}\right)^2 - 0.000040\left(T\sqrt{\frac{g}{h}}\right)^3, & T\sqrt{\frac{g}{h}} > 30 \end{cases} \tag{A12}$$

$$\left(\frac{u_{on}}{\hat{u}}\right)_{modified} = 0.5 + \left(\left(\frac{u_{on}}{\hat{u}}\right)_{max} - 0.5\right)\tanh\left(\frac{\left(\frac{u_{on}}{\hat{u}}\right)_a - 0.5}{\left(\frac{u_{on}}{\hat{u}}\right)_{max} - 0.5}\right) \tag{A13}$$

with:

$$\left(\frac{u_{on}}{\hat{u}}\right)_{max} = 0.62 + \frac{0.003}{\text{bed slope}} \tag{A14}$$

A comparison between preliminary computations using the present model and laboratory tests showed that the influence of the bed slope might be less pronounced. The following relation gave more realistic results:

$$\left(\frac{u_{on}}{\hat{u}}\right)_{max} = 0.62 + \frac{0.001}{\text{bed slope}} \tag{A15a}$$

In 2001, Eq. (A15a) was revised into:

$(u_{on}/\hat{u})_{max}$=-2.5(h/L)+0.85 ` (A15b)

with:

$(u_{on}/\hat{u})_a=(u_{on}/\hat{u})_{max}$	if $(u_{on}/\hat{u})_a>(u_{on}/\hat{u})_{max}$
$(u_{on}/\hat{u})_{max}=0.75$	if $(u_{on}/\hat{u})_a>0.75$
$(u_{on}/\hat{u})_{max}=0.62$	if $(u_{on}/\hat{u})_a<0.62$

The offshore-directed peak orbital velocity follows from: $u_{off}= \hat{u} - u_{on}$

The present model includes a sinusoidal distribution of the instantaneous velocities during the forward and backward phase of the wave cycle. The duration period of each phase is corrected to obtain zero net flow over the full cycle (in contrast to the original approach of Isobe and Horikawa).

B Improved wave modelling based on a cross-varying wave height over water depth ratio

ARTICLE IN PRESS

Available online at www.sciencedirect.com

SCIENCE DIRECT®

Coastal Engineering 1051 (2003) 1–11

Coastal Engineering
An International Journal for Coastal, Harbour and Offshore Engineers

www.elsevier.com/locate/coastaleng

Calibration and verification of a parametric wave model on barred beaches

B.G. Ruessink[a,*], D.J.R. Walstra[a], H.N. Southgate

[a] *WL|Delft Hydraulics, Marine and Coastal Management, P.O. Box 177, 2600 MH Delft, The Netherlands*

Received 31 May 2002; accepted 29 January 2003

Abstract

Since its introduction in 1978, the Battjes and Janssen model has proven to be a popular framework for estimating the cross-shore root-mean-square wave height H_{rms} transformation of random breaking waves in shallow water. Previous model tests have shown that wave heights in the bar trough of single bar systems and in the inner troughs of multiple bar systems are overpredicted by up to 60% when standard settings for the free model parameter γ (a wave height-to-depth ratio) are used. In this paper, a new functional form for γ is derived empirically by an inverse modelling of γ from a high-resolution (in the cross-shore) 300-h H_{rms} data set collected at Duck, NC, USA. We find that, in contrast to the standard setting, γ is not cross-shore constant, but depends systematically on the product of the local wavenumber k and water depth h. Model verification with other data at Duck, and data collected at Egmond and Terschelling (Netherlands), spanning a total of about 1600 h, shows that cross-shore H_{rms} profiles modelled with the locally varying γ are indeed in better agreement with measurements than model predictions using the cross-shore constant γ. In particular, model accuracy in inner bar troughs increases by up to 80%. Additional verifications with data collected on planar laboratory beaches show the new functional form of γ to be applicable to non-barred beaches as well. Our optimum γ cannot be compared directly to field and laboratory measurements of height-to-depth ratios and we do not know of a physical mechanism why γ should depend positively on kh.

Keywords: Wave breaking; Inverse modelling; Height-to-depth ratio; Sandbars

1. Introduction

In 1978, Battjes and Janssen presented a nowadays commonly applied model to estimate the cross-shore transformation of random breaking waves in shallow water. The model is a parametric model based on the wave energy balance, transforming a single representative wave height (the root-mean-square wave height, H_{rms}) with a constant period (the peak period T_{p}) and a representative wave angle (the peak or (energy-weighted) mean direction $\bar{\theta}$) through the surf zone. The breaking-induced dissipation is computed as the product of energy dissipation S in a single breaking wave and the probability of occurrence of breaking Q, where Battjes and Janssen (1978) described S on the basis of a bore-type dissipation model and adopted a clipped-Rayleigh probability density function (pdf) to estimate Q. The only free model parameter, γ, indi-

* Corresponding author. Now at Department of Physical Geography, Institute for Marine and Atmospheric Research Utrecht, Utrecht University, P.O. Box 80115, 3508 TC Utrecht, The Netherlands. Tel.: +31-30-2532405; fax: +31-30-2531145.

E-mail address: g.ruessink@geog.uu.nl (B.G. Ruessink).

0378-3839/03/$ - see front matter
doi:10.1016/S0378-3839(03)00023-1

cates a breaker height-to-depth ratio. Using mainly small-scale laboratory data, Battjes and Stive (1985) determined that γ, assumed to be cross-shore constant, depends weakly on the deep-water wave steepness s_d as

$$\gamma = 0.5 + 0.4\tanh(33 s_d). \quad (1)$$

Although H_{rms} predictions using Eq. (1) (henceforth γ predicted with Eq. (1) will be denoted as γ_{BS85}) are generally in good agreement with observations on planar (i.e., constant slope) beaches, model–data agreement for single-bar systems or for the innermost bar in multiple bar systems is usually less fair (e.g., Rivero et al., 1994; Southgate, 1995; Ruessink et al., 2001). Ruessink et al. (2001), for instance, found systematic H_{rms} overpredictions of up to 60% in the inner bar trough of the double-barred beach at Egmond aan Zee (Netherlands), but far better model–data agreement (without systematic overpredictions) in the outer bar trough. We realize that predictions of wave heights are generally good (even in multiple barred situations) in comparison with predictions of Q, radiation-stress related quantities (such as alongshore currents and undertow), and sediment transport (and thus morphological change). However, wave height predictions are usually the first step in morphodynamic process-based modelling, and errors in these predictions feed in directly to most subsequent computations. From this viewpoint, we feel that an improvement in wave height predictions on barred beaches is warranted.

Various attempts to improve H_{rms} predictions on non-planar beaches have been presented in the literature. One such attempt is the replacement of the clipped-Rayleigh distribution by a Rayleigh or Weibull distribution (e.g., Gerritsen, 1980; Roelvink, 1993; Baldock et al., 1998), as natural wave height distributions do not conform to a truncated distribution. However, the cross-shore evolution of H_{rms} in the surf zone is generally found to be rather insensitive to the choice of a particular distribution (Roelvink, 1993; Baldock et al., 1998). Only on steep slopes (>1:10) H_{rms} predictions based on the Rayleigh distribution (using γ_{BS85}) may outperform those based on the clipped-Rayleigh distribution (Baldock et al., 1998). A physics-based attempt has been to implement breaking-wave persistence in the Q formulation (Southgate and Wallace, 1994). These authors separated Q in a fraction of newly breaking waves and a fraction of breaking waves that persisted from seaward locations. The main purpose was to improve predictions of Q rather than wave heights. Another possible explanation for lower observed than modelled wave heights landward of bars is that it is a feature of the data analysis procedure. When surface elevation data is analysed spectrally, it is usual to truncate the analysed frequency range to exclude low frequencies. However, it is well known that the wave breaking process commonly involves transfer of energy from primary to low frequencies resulting in the generation of infragravity waves. This transfer of energy is not normally included in surf zone models (except when the main purpose is to model the generation of infragravity waves), so the modelled wave heights will tend to be larger than those measured in the field. However, this transfer of energy to low frequencies is a relatively small effect and would generally not be large enough to explain the observed discrepancies between measured and modelled wave heights landward of bars. In addition, this transfer of energy also occurs on planar beaches for which γ_{BS85} generally results in accurate H_{rms} predictions.

In this paper, we propose an empirical improvement to Battjes and Janssen (1978)-based cross-shore wave height modelling by implementing a new functional form for γ (i.e., other than Eq. (1)). The inverse modelling of the wave energy balance from detailed H_{rms} observations across a subtidal bar at Duck, NC, USA shows (Section 3) that γ is not a cross-shore constant but depends systematically on kh, where k is the local wave number. Verification against data from Egmond and Terschelling (Netherlands) subsequently shows that inner-trough H_{rms} predictions indeed improve and that outer-bar H_{rms} predications are about the same as those based on γ_{BS85} (Section 4). Additional verifications against laboratory wave data show the new empirical form for γ to be applicable to planar beaches as well (Section 5).

2. Model formulation

The applied model, a parametric model based on the wave energy balance, is the Battjes and Janssen (1978) wave transformation model in which, as proposed by

Baldock et al. (1998), the clipped-Rayleigh distribution is replaced by a Rayleigh distribution. For shore parallel depth contours, the energy balance reads

$$\frac{\mathrm{d}}{\mathrm{d}x}\left(\frac{1}{8}\rho g H_{\mathrm{rms}}^2 c_{\mathrm{g}} \cos\bar{\theta}\right) = -D, \tag{2}$$

where x is the cross-shore coordinate, positive onshore, ρ is the water density, g is the gravitational acceleration

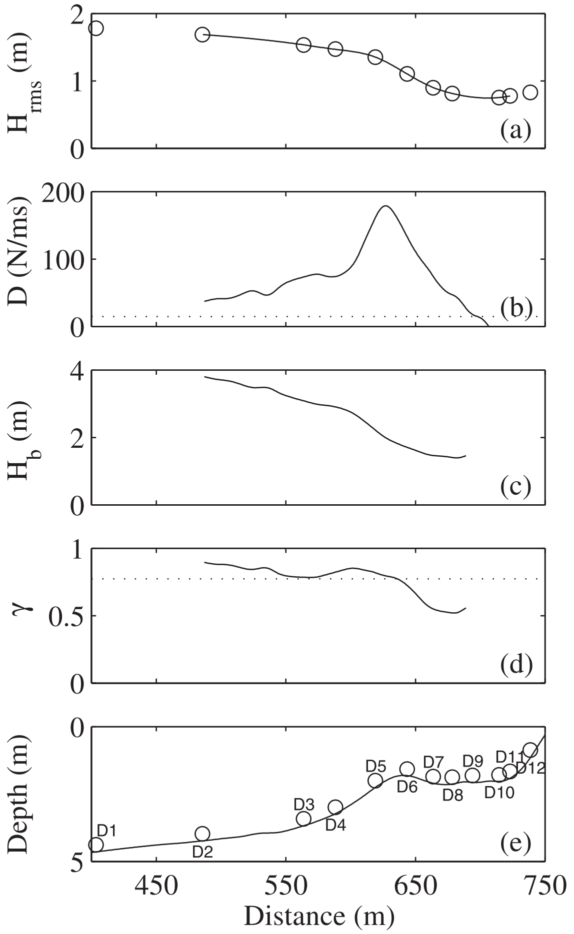

Fig. 1. Cross-shore distribution of (a) root-mean-square wave height H_{rms} (measured, circles; cubic spline, solid line), and inversely modelled (b) breaking-induced dissipation D, (c) maximum wave height H_{b}, and (d) breaking parameter γ, on September 22, 1994, 06:00 EST. (e) Depth relative to mean sea level on September 21, 1994 and instrument locations. The dotted line in (b) is the threshold $D = 15$ N/ms below which γ estimates were not retained. The dotted line in (d) is γ_{BS85}. Distance is relative to the offshore sensor in 8-m depth.

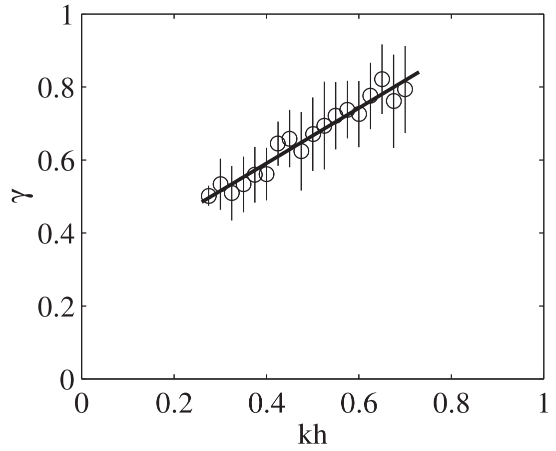

Fig. 2. Average (circles) and standard deviation (vertical bars) of γ versus kh based on all estimates with D>15 N/ms. The solid line is the least squares linear fit, Eq. (5).

and c_{g} is the group velocity evaluated at the representative wave period. Following Baldock et al. (1998), D is

$$D = \frac{\alpha}{4}\frac{1}{T_{\mathrm{p}}}\rho g \exp\left[-\left(\frac{H_{\mathrm{b}}}{H_{\mathrm{rms}}}\right)^2\right](H_{\mathrm{b}}^2 + H_{\mathrm{rms}}^2), \tag{3}$$

in which α is a proportionality constant of order one and H_{b} is the breaker height, given by Battjes and Janssen (1978)

$$H_{\mathrm{b}} = \frac{0.88}{k}\tanh\left(\frac{\gamma}{0.88}kh\right). \tag{4}$$

Here, k is the wave number of the representative period, h is the water depth ($= d + \zeta$, where d is depth and ζ is (tidal) water level with respect to mean sea level). Note that in the limit for deep water ($kh \to \infty$), Eq. (4) reduces to $H_{\mathrm{b}} = 0.88/k$, implying steepness-limited breaking, whereas in shallow ($kh \to 0$), Eq. (4) reduces

Table 1
Offshore wave conditions for H_{rms} verification data sets

Site	H_{rms} (m)	T_{p} (s)	$\bar{\theta}$ (deg)	N
Duck	0.29–2.19	4.5–7.0	−30 to 50	270
Egmond	0.46–3.90	4.8–10.5	−45 to 45	508
Terschelling	0.12–1.83	3.0–12.8	−30 to 30	816

N: number of observations.

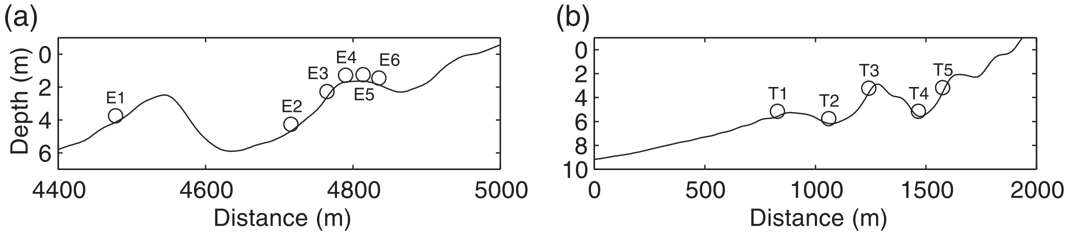

Fig. 3. Depth relative to mean sea level versus cross-shore distance and instrument locations at (a) Egmond on 19 October 1998 and (b) Terschelling in April 1994. Distance is relative to the location of the offshore sensor.

to $H_b = \gamma h$, corresponding to depth-limited breaking. Baldock et al. (1998) used γ_{BS85} as standard setting for γ. The wave model is solved here on a fourth-order Runge–Kutta scheme with adaptive step size control using the observed bathymetry, and offshore values of H_{rms}, T_p, $\bar{\theta}$ and ζ. Linear wave theory is used to calculate c_g and k, and Snell's law is used to determine $\bar{\theta}(x)$.

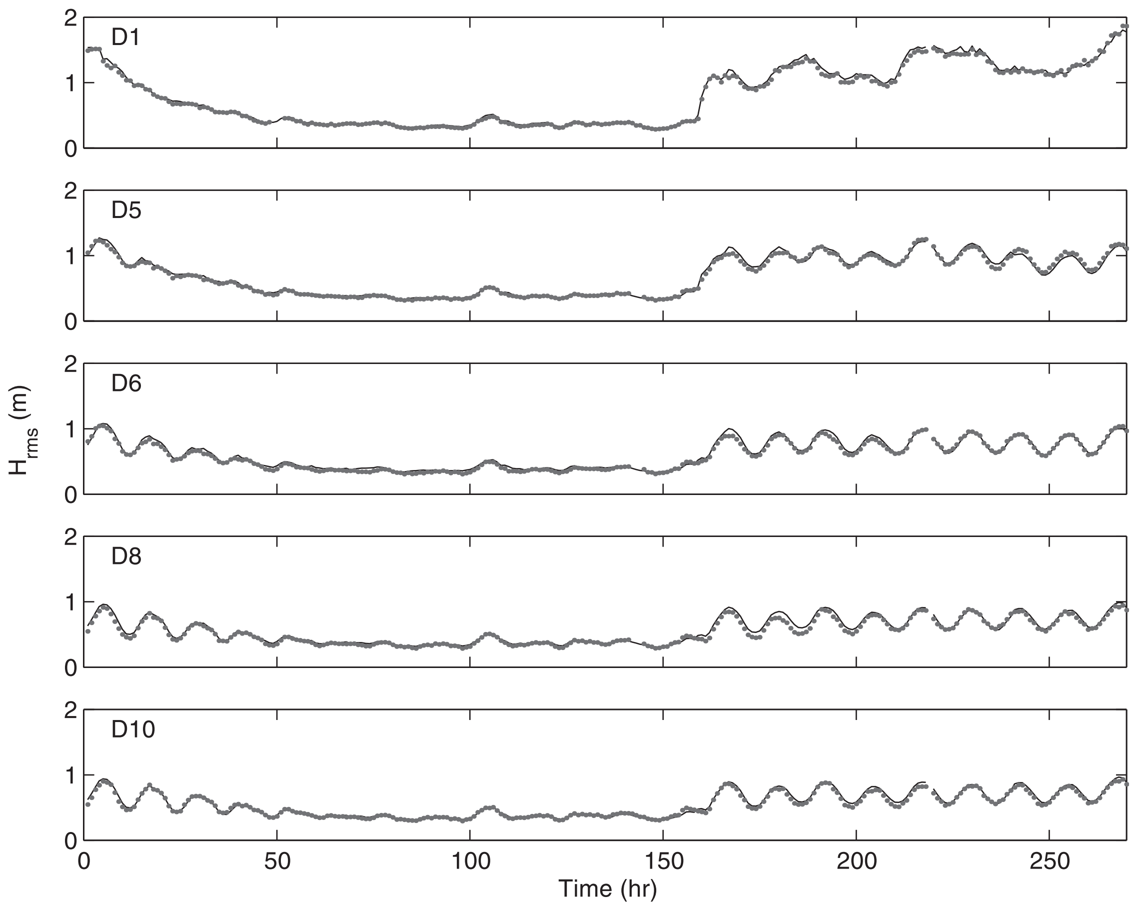

Fig. 4. Measured (symbols) and modelled (lines) H_{rms} from offshore (D1) to onshore (D10) versus time at Duck. For locations see Fig. 1e. Time = 0 corresponds to October 3, 1994, 12:00 EST.

3. Calibration

The calibration of the wave model is approached through an inverse modelling of Eqs. (2), (3) and (4) to yield the cross-shore distribution of γ. The basis of the inverse modelling is a spectrally derived H_{rms} data set collected during the Duck94 experiment at the U.S. Army Corps of Engineers Field Research Facility (FRF) (see, for example, Elgar et al., 1997; Gallagher et al., 1998; Feddersen et al. 1998). The data was obtained at up to 12 cross-shore positions, extending from the shore line across a subtidal bar to 4.5-m depth (Fig. 1). From the available data, an about 570-h portion (September 20, 1994–October 14, 1994) which spanned a wide range of conditions was selected, including both high-energy sea waves and low-energy swell, and for which depth profiles, surveyed with an amphibious vehicle, were regularly available. The first 300-h part (September 20, 1994–October 3, 1994) is used for calibration purposes; the remaining data is used for verification of the calibrated wave model. Offshore H_{rms} and T_{p} during the calibration part of the Duck94 campaign, estimated in 8-m water depth from a two-dimensional array of 15 bottom-mounted pressure sensors (Long, 1996), ranged from 0.12 to 1.98 m and 4.1 to 9.8 s, respectively. All H_{rms} at Duck, as well as all H_{rms} used later on in this paper, are based on spectral analysis rather than wave counting analysis.

Through each cross-shore transect of H_{rms}, a cubic spline was fitted to yield a smooth curve of H_{rms}

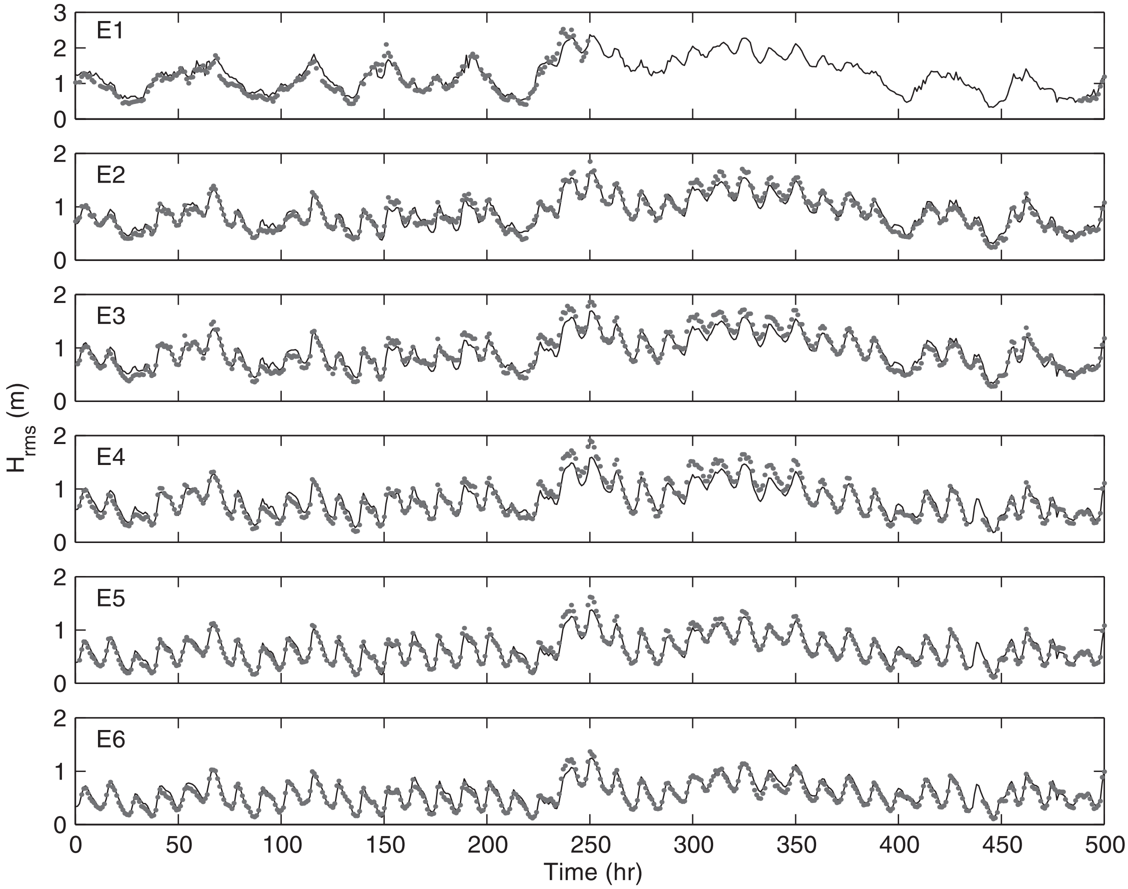

Fig. 5. Measured (symbols) and modelled (lines) H_{rms} from offshore (E1) to onshore (E6) versus time at Egmond. For locations, see Fig. 3a. Time = 0 corresponds to October 15, 1998, 09:00 MET.

transformation at a 1-m grid (e.g., Fig. 1a). Spline parts between the two most offshore (D1 and D2) and onshore (D11 and D12) sensors were not retained as the fitted H_{rms} transformations were often non-realistic. For each grid point, c_g and $\bar{\theta}$ were subsequently estimated using the offshore T_p, $\bar{\theta}$ and ζ, resulting in an estimate of the cross-shore evolution of the wave energy flux, $(1/8)\rho g c_g H_{rms}^2 \cos\bar{\theta}$. The cross-shore gradient of the wave energy flux equals the dissipation due to breaking D (Eq. (2), Fig. 1b). From D, the cross-shore evolution of H_b (Eq. (3), Fig. 1c) and subsequently, γ (Eq. (4), Fig. 1d) were computed, for which a non-linear fitting technique based on the Gauss–Newton method was adopted. To avoid spurious results, γ values based on $D < 15$ N/ms were discarded from further analysis. In total the selected calibration data resulted in about 5500 reliable γ estimates.

It is apparent from Fig. 1 that a cross-shore varying γ is needed to obtain accurate H_{rms} predictions. An attempt was made to relate γ to the local bed slope β (Sallenger and Holman, 1985; Thornton and Guza, 1986), $\beta/(kh)$ (Raubenheimer et al., 1996; Sénéchal et al., 2001), $\beta/(H_{rms}/L)$ (Van Rijn and Wijnberg, 1996), and also to kh and H_{rms}/L separately, where $L = 2\pi/k$ and β was estimated from the observed depth profiles as the difference in vertical elevation over a distance L. The strongest correlation is the increase in γ with

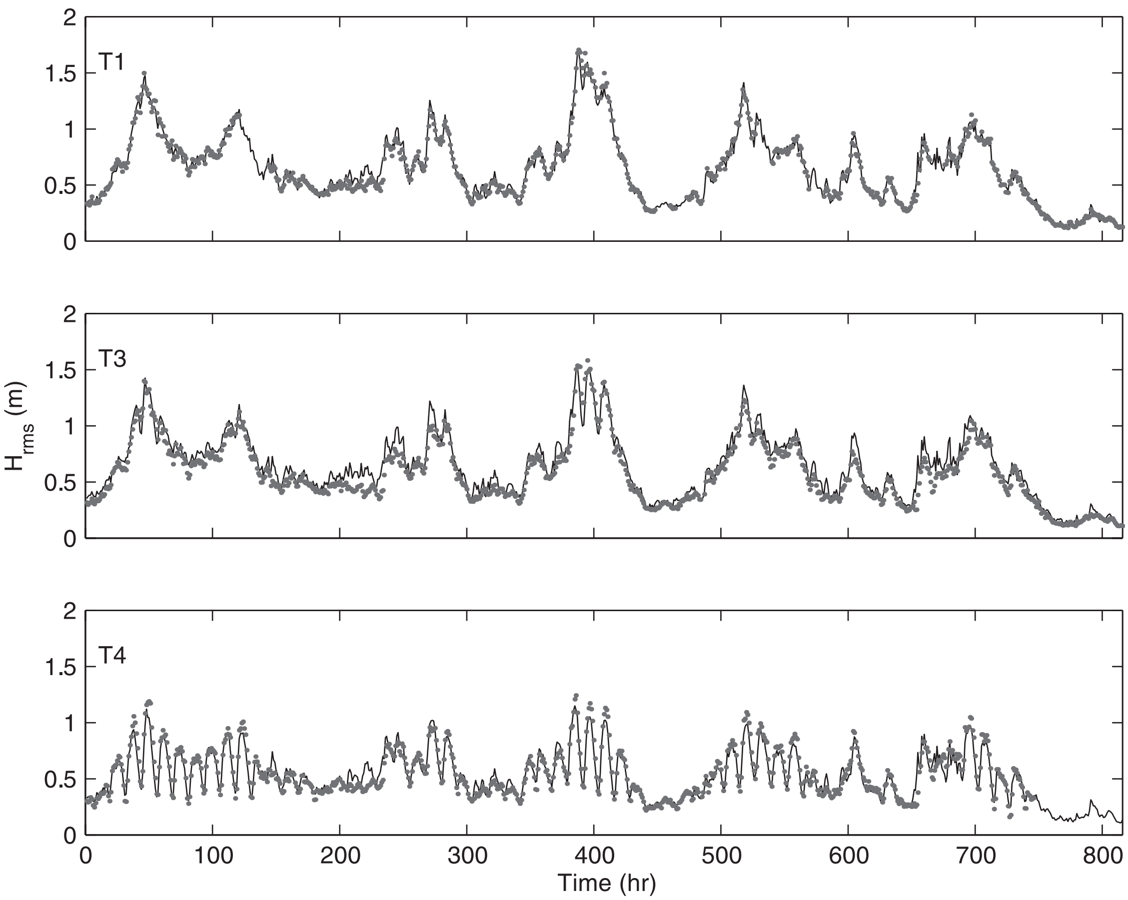

Fig. 6. Measured (symbols) and modelled (lines) H_{rms} from offshore (T1) to onshore (T4) versus time at Terschelling. For locations, see Fig. 3b. Time = 0 corresponds to May 25, 1994, 09:00 MET.

increasing kh (Fig. 2), with the least-squares linear fit given by

$$\gamma = 0.76kh + 0.29, \tag{5}$$

(correlation coefficient $r = 0.97$ for the kh range of $\approx 0.25-0.75$). Only a weak dependence of γ on β, $\beta/(kh)$, and $\beta/(H_{\mathrm{rms}}/L)$ was observed ($|r| \leq 0.21$). Henceforth, we will denote γ estimated with Eq. (5) as γ_{var}. In shallow water, Eq. (5) corresponds to $\gamma_{\mathrm{var}} \sim h^{0.5}$.

At this point, it is illustrative to discuss on which part of the cross-shore profile H_{rms} prediction will be affected most by the implementation of γ_{var} in Eq. (4). In 'deep' water, γ_{var} will be somewhat larger than γ_{BS85}, resulting, however, in comparable H_{rms} predictions. In some depths, γ_{var} and γ_{BS85} will be equal. This depth, denoted h_{c}, increases with increasing offshore H_{rms} and T_{p}. In depths shallower than h_{c}, γ_{var} will be less than γ_{BS85} and, as a consequence, H_{rms} decay with cross-shore distance will be larger. When, in multiple bar systems, h_{c} is found near the inner bar, H_{rms} predictions on outer bars are largely independent on whether γ_{var} or γ_{BS85} is used, but across the inner trough H_{rms} based on γ_{var} will be less than H_{rms} based on γ_{BS85}. This change in the cross-shore evolution of H_{rms} is qualitatively consistent with the observations (Section 1) that H_{rms} predictions in especially inner bar troughs need to be improved.

4. Field verification

The wave model with γ_{var} implemented in Eq. (4) was verified against three extensive H_{rms} data sets, collected at (1) the single-barred beach at Duck, (2) the double-barred beach at Egmond, Netherlands, and (3) the triple-barred beach at Terschelling, Netherlands. An overview of offshore wave conditions is presented in Table 1. Cross-shore profiles with instrumented locations at Egmond and Terschelling are shown in Fig. 3. Values of h_{c} indicate that the effect of γ_{var} on H_{rms} predictions will be most pronounced on and shoreward of the bar at Duck ($h_{\mathrm{c}} \sim 2-5$ m) and on the inner bar and trough at Egmond ($h_{\mathrm{c}} \sim 2-10$ m, but mostly <5 m). In contrast, no effect on H_{rms} predictions at Terschelling is anticipated ($h_{\mathrm{c}} < 3$ m). The error reduction by the implementation of γ_{var} is quantified with the Brier Skill Score BSS (Murphy and Epstein, 1989)

$$\mathrm{BSS} = 1 - \frac{\mathrm{MSE}(H_{\mathrm{rms}} \text{ with } \gamma_{\mathrm{var}},\ \text{observed } H_{\mathrm{rms}})}{\mathrm{MSE}(H_{\mathrm{rms}} \text{ with } \gamma_{\mathrm{BS85}}, \text{observed } H_{\mathrm{rms}})}, \tag{6}$$

where MSE is the mean-square error, in general terms defined as $\mathrm{MSE}(x,y) = \langle (x-y)^2 \rangle$ with the angle brackets representing a time average. BSS is positive (negative) when the model accuracy using γ_{var} is

Table 2
Root-mean-square wave height error statistics

	r^2	ϵ_{rms} (m)	m	BSS
Duck				
D1	0.98	0.05	1.02	0.05
D2	0.98	0.04	1.01	0.49
D3	0.97	0.04	1.01	0.54
D4	no data			
D5	0.92	0.05	1.01	− 0.19
D6	0.94	0.04	1.03	0.61
D7	0.96	0.06	1.07	0.63
D8	0.94	0.05	1.06	0.63
D9	0.95	0.03	1.00	0.74
D10	0.96	0.04	1.04	0.72
D11	0.95	0.05	1.07	0.65
D12	0.87	0.04	1.01	0.68
Egmond				
E1	0.91	0.16	1.02	− 0.11
E2	0.92	0.09	0.98	− 0.03
E3	0.92	0.11	0.96	− 0.25
E4	0.93	0.12	0.95	− 0.01
E5	0.93	0.08	0.98	0.63
E6	0.92	0.07	1.03	0.77
Terschelling				
T1	0.98	0.05	1.00	0.07
T2	0.95	0.08	1.05	0.01
T3	0.95	0.09	1.08	− 0.05
T4	0.92	0.06	0.98	0.03
T5	0.95	0.09	1.12	0.09

ϵ_{rms} is the root-mean-square error between modelled and observed H_{rms}, r^2 and m are the correlation coefficient squared and the slope of the best-fit linear lines (forced through the origin) between modelled and observed H_{rms}. BSS is Brier Skill Score.
A value of $m>1$ corresponds to model overprediction of observed H_{rms}. Values at Duck exclude results for hours 40–160 during which waves did not break across the instrument array (see Fig. 4).

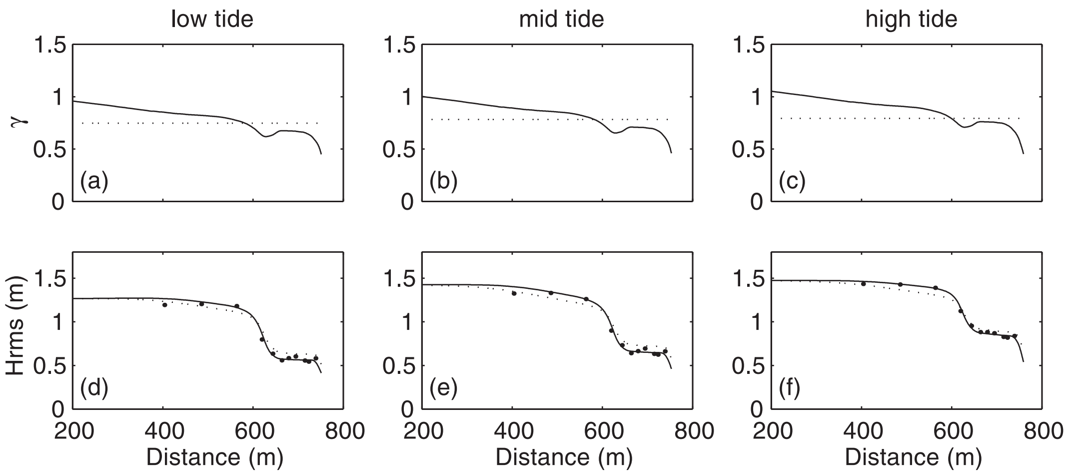

Fig. 7. Modelled (a)–(c) breaker parameter γ and (d)–(f) root-mean-square wave height H_{rms} versus cross-shore distance at Duck. Solid (dotted) lines are model results with γ_{var} (γ_{BS85}). Dots in (d)–(f) are measured H_{rms}. Columns from left to right: low tide (t=236 h), mid tide (t=234 h), high tide (t=229 h). The bar crest is located at x=630 m.

greater (less) than the accuracy using γ_{BS85}. BSS multiplied by 100 is a measure of percentage improvement in accuracy. Details on data acquisition and processing are given in Ruessink et al. (2001) for Egmond and in Ruessink et al. (1998) and Houwman (2000) for Terschelling.

The wave model with γ_{var} yields accurate H_{rms} predictions across the entire profile (Figs. 4–6) with skill $r^2 \geq 0.87$ at all sensors (Table 2). Observed and predicted H_{rms} show the transition from H_{rms} that are closely related to offshore H_{rms} to tidally modulated H_{rms} at the shoreward sensors (Figs. 4–6). Root-mean-square errors ϵ_{rms} for individual sensors vary from 0.03 to 0.16 m (Table 2), with differences between the site being related to the different energetic conditions. Average ϵ_{rms} are 0.05, 0.10 and 0.07

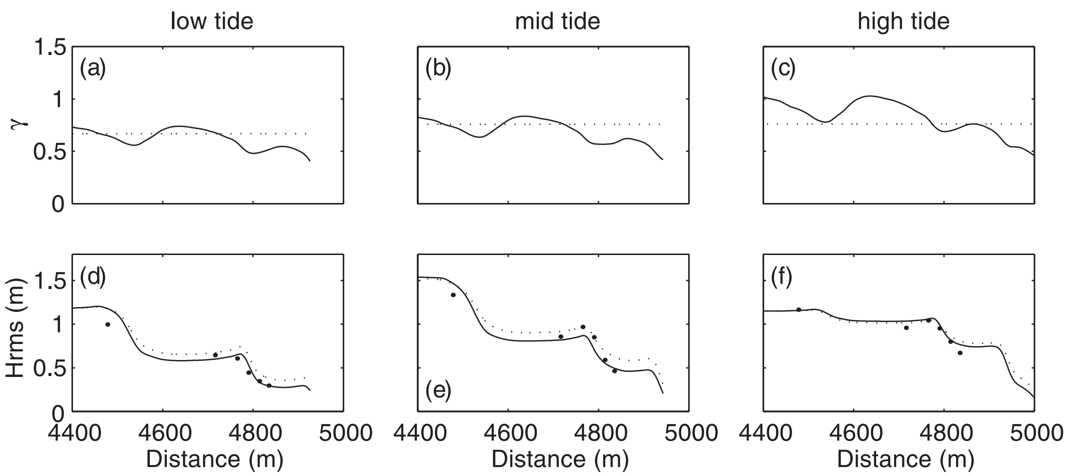

Fig. 8. Modelled (a)–(c) breaker parameter γ and (d)–(f) root-mean-square wave height H_{rms} versus cross-shore distance at Egmond. Solid (dotted) lines are model results with γ_{var} (γ_{BS85}). Dots in (d)–(f) are measured H_{rms}. Columns from left to right: low tide (t=76 h), mid tide (t=52 h), high tide (t=56 h), see also Fig. 6 in Ruessink et al. (2001). The outer and inner bar crests are located at x=4540 and 4800 m, respectively.

m for Duck, Egmond and Terschelling, respectively. Slopes m of best-fit linear lines (forced through the origin) between observed and predicted H_{rms} are close to 1 at all sensors (Table 2). BSS values imply a 50–80% improvement in accuracy (Table 2) in the bar trough at Duck (D7–D10) and inner bar-trough at Egmond (E5–E6), where prediction errors using γ_{BS85} were largest (Ruessink et al., 2001). As expected from the aforementioned h_c values, γ_{var} and γ_{BS85} result in the same predictive skill (i.e., BSS $\approx$ 0) at the outer bar at Egmond (E1) and at all Terschelling sensors (Table 2). We cannot, however, assign much significance to the Duck results since data for these results are from the same site as the data for the γ calibration. Although different data sets from Duck were used for calibration and verification, we would expect a much stronger correlation between the two Duck data sets than between one Duck data set and a data set from another site. The evidence in favour of γ_{var} therefore comes mainly from the Egmond and Terschelling data. Examples of the predicted cross-shore distribution of γ and H_{rms} at low, mid and high tide are shown in Figs. 7 and 8 for Duck and Egmond, respectively.

5. Discussion

In this paper, a new functional form for the breaking-wave parameter γ in Battjes and Janssen (1978)-type parametric wave transformations models was derived empirically through an inverse modelling of a high-resolution (in the cross-shore) H_{rms} data set collected across a subtidal bar at Duck, NC. This new form, a local dependence of γ on kh (Fig. 2, Eq. (5)), results in H_{rms} predictions that are in better agreement with measured H_{rms} than predictions based on the commonly applied parameterization of Battjes and Stive (1985). Particularly, the predicted stronger H_{rms} decay across inner bars causes an up to 80% improvement in model accuracy in inner bar troughs.

Although our work was motivated by the need to improve H_{rms} predictions in the inner bar-trough zone, we would obviously like to see that γ_{var} does not deteriorate H_{rms} predictions in cases for which γ_{BS85} does show good predictive skill, most notably, on planar beaches. To this end, the wave model was additionally run for 11 small-scale, plane-sloping laboratory tests (Table 3, note that Battjes and Stive (1985) used tests 1, 2, 3, 6 and 7 to derive γ_{BS85}). As can be deduced from Fig. 9 and from the error statistics computed for each test using observed and predicted H_{rms} at all measurement points (Table 3), γ_{var} results in about the same or slightly improved H_{rms} predictions (in most cases, BSS>0), implying that γ_{var}, although derived from data collected on a barred beach, is also applicable to planar beaches.

The trend in γ_{var} variation with kh and the absence of a β dependence of γ_{var} contrasts with field observations of the height-to-depth ratio (Raubenheimer et al., 1996; Sénéchal et al., 2001) and model computations based on the one-dimensional depth-averaged non-linear shallow water equations (Raubenheimer et al., 1996). These studies find a positive

Table 3
Laboratory experiments and H_{rms} error statistics

No.	Source	Code	H_{rms} (m)	T_{p} (s)	N	β	r^2	ϵ_{rms} (m)	m	BSS
1	Battjes and Janssen (1978)	BJ2	0.144	1.84	6	1:20	0.99	0.0038	0.99	0.52
2	Battjes and Janssen (1978)	BJ3	0.121	2.48	8	1:20	0.99	0.0028	1.01	0.80
3	Battjes and Janssen (1978)	BJ4	0.142	2.16	8	1:20	0.99	0.0028	0.99	0.85
4	Thompson and Vincent (1984)	–	0.044	2.50	9	1:30	0.98	0.0023	1.02	0.63
5	Thompson and Vincent (1984)	–	0.056	1.25	9	1:30	0.94	0.0028	1.02	0.18
6	Stive (1985)	MS10	0.142	2.93	22	1:40	0.57	0.0206	0.92	– 0.36
7	Stive (1985)	MS40	0.135	1.58	24	1:40	0.97	0.0086	0.97	– 0.21
8	Baldock and Huntley (2002)	J1033C	0.048	1.00	35	1:10	0.99	0.0016	1.02	0.31
9	Baldock and Huntley (2002)	J6033A	0.100	1.67	35	1:10	0.97	0.0046	1.02	0.51
10	Baldock and Huntley (2002)	J6033B	0.075	1.67	35	1:10	0.94	0.0042	1.02	0.37
11	Baldock and Huntley (2002)	J6033C	0.050	1.67	35	1:10	0.70	0.0035	1.02	0.24

N = number of cross-shore measurement points, not including the offshore boundary.

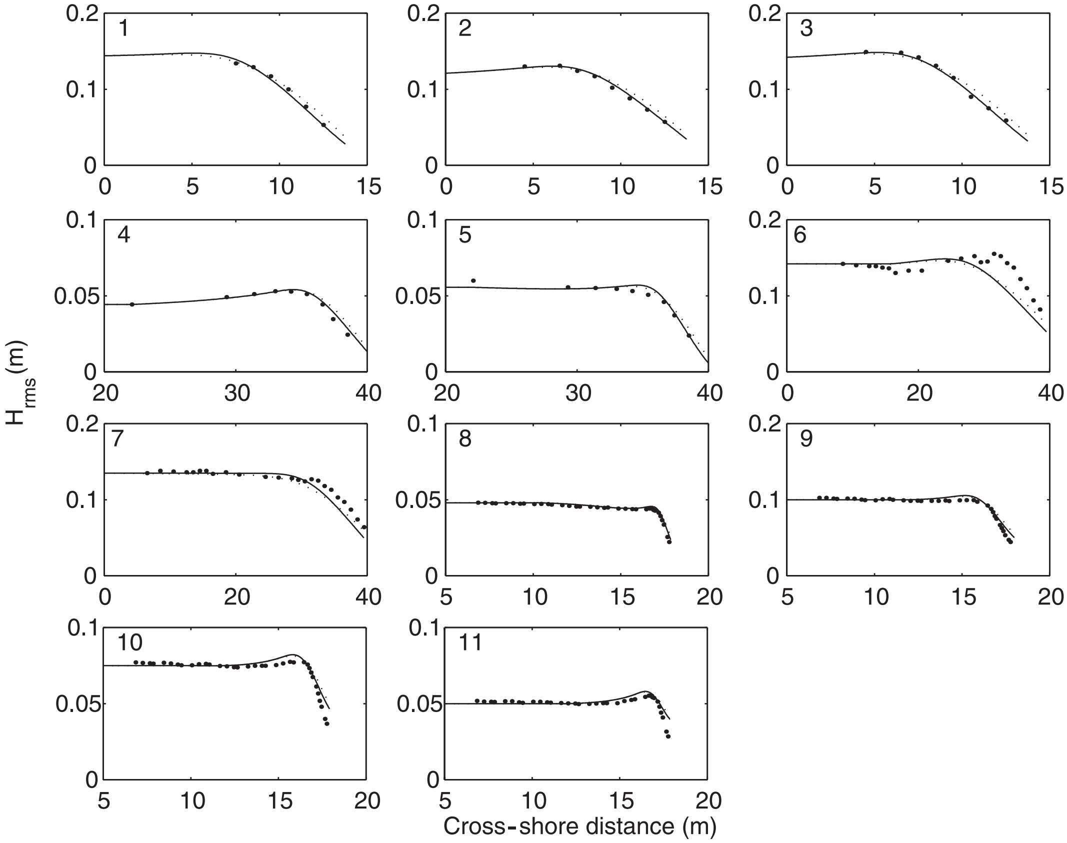

Fig. 9. Modelled (solid line: γ_{var}; dotted line: γ_{BS85}) and measured (symbols) H_{rms} versus cross-shore distance for the 11 planar-beach laboratory cases listed in Table 3.

linear dependence of γ on $\beta/(kh)$, although the slope and intercept of the best-fit linear line differ considerably between Raubenheimer et al. (1996) and Sénéchal et al. (2001). It is stressed that, although both parameters are referred to as γ and are height-to-depth ratios, they are not the same. In the Battjes and Janssen (1978) model γ is related to the maximum wave height H_b and is prescribed empirically, whereas in the field or in Raubenheimer et al.'s model γ is defined as H_{rms}/h based on physical arguments. In addition, a constant α value was applied in Eq. (3); as already suggested by Battjes and Stive (1985), deviations from this constant value are accounted for empirically in γ. Thus, our γ_{var} cannot be compared directly to observed height-to-depth ratios and is best interpreted as the optimum setting of the free model parameter γ. We do not know of any physical mechanism why γ_{var} should have a positive dependence on local kh and should lack a dependence on β.

6. Conclusions

Our inverse modelling results show that that the free model parameter γ in the Battjes and Janssen (1978) wave model is a locally varying parameter that increases linearly with the product of the local wavenumber and waterdepth kh (i.e., Eq. (5)). This contrasts with the present-day implemented functional form of a cross-shore constant γ depending weakly on the offshore wave steepness (Battjes and Stive, 1985). Implementation of the locally varying γ improves H_{rms} predictions by up to 80%, particularly across inner bar-troughs, where errors using the cross-shore constant γ are largest. The proposed new functional form of

γ also results in accurate H_{rms} predictions on planar beaches.

Acknowledgements

This work was carried out as part of the Delft Cluster project Coasts under number 03.01.03. D.J.R. Walstra was partly supported by the Dutch Rijksinstituut voor Kust en Zee through VOP-project Z3412. We thank Steve Elgar, R.T. Guza and Falk Feddersen for providing the data for Duck, and Tom Baldock for providing the data for laboratory tests 8–11. The Egmond and Terschelling data were collected in the framework of the Coast3D and Nourtec projects, funded by the European Commission's research program MAST under contract MAS3-CT97-0086 and MAS2-CT93-0049, respectively.

References

Baldock, T.E., Huntley, D.A., 2002. Long wave forcing by the breaking of random waves on a beach. Proc. R. Soc. Lond. A 258, 2177–2202.

Baldock, T.E., Holmes, P., Bunker, S., Van Weert, P., 1998. Cross-shore hydrodynamics within an unsaturated surf zone. Coast. Eng. 34, 173–196.

Battjes, J.A., Janssen, J.P.F.M., 1978. Energy loss and set-up due to breaking of random waves. Proc. 16th Int. Conf. on Coastal Engineering. ASCE, New York, pp. 570–587.

Battjes, J.A., Stive, M.J.F., 1985. Calibration and verification of a dissipation model for random breaking waves. J. Geophys. Res. 90, 9159–9167.

Elgar, S., Guza, R.T., Raubenheimer, B., Herbers, T.H.C., Gallagher, E., 1997. Spectral evolution of shoaling and breaking waves on a barred beach. J. Geophys. Res. 102, 15797–15805.

Feddersen, F., Guza, R.T., Elgar, S., Herbers, T.H.C., 1998. Alongshore momentum balances in the nearshore. J. Geophys. Res. 103, 15667–15676.

Gallagher, E.L., Elgar, S., Guza, R.T., 1998. Observations of sand bar evolution on a natural beach. J. Geophys. Res. 103, 3203–3215.

Gerritsen, F., 1980. Wave attenuation and wave set-up on a coastal reef. Proc. 17th Int. Conf. on Coastal Eng. ASCE, New York, pp. 444–461.

Houwman, K.T., 2000. Tide, wind- and wave-driven flow processes in the nearshore zone. PhD thesis, Dept. of Physical Geography, Utrecht University, Netherlands.

Long, C.E., 1996. Index and bulk parameters for frequency–direction spectra measured at CERC Field Research Facility, June 1994 to August 1995. Misc. Pap. CERC-96-6, U.S. Army Eng. Waterw. Exp. Stn., Vicksburg, MS.

Murphy, A.H., Epstein, E.S., 1989. Skill scores and correlation coefficients in model verification. Mon. Weather Rev. 117, 572–581.

Raubenheimer, B., Guza, R.T., Elgar, S., 1996. Wave transformation across the inner surf zone. J. Geophys. Res. 101, 25589–25597.

Rivero, F.J., Sánchez-Arcilla, A., Beyer, D., 1994. Comparison of a wave transformation model with LIP-IID data. Proc. Coastal Dynamics '94. ASCE, New York, pp. 518–532.

Roelvink, J.A., 1993. Dissipation in random wave groups incident on a beach. Coast. Eng. 19, 127–150.

Ruessink, B.G., Houwman, K.T., Hoekstra, P., 1998. The systematic contribution of transporting mechanisms to the cross-shore sediment transport in water depths of 3 to 9 m. Mar. Geol. 152, 295–324.

Ruessink, B.G., Miles, J.R., Feddersen, F., Guza, R.T., Elgar, S., 2001. Modeling the alongshore current on barred beaches. J. Geophys. Res. 106, 22451–22463.

Sallenger, A.H., Holman, R.A., 1985. Wave-energy saturation on a natural beach of variable slope. J. Geophys. Res. 90, 11939–11944.

Sénéchal, N., Dupuis, H., Bonneton, P., Howa, H., Pedreros, R., 2001. Observation of irregular wave transformation in the surf zone over a gently sloping sandy beach on the French Atlantic coastline. Oceanol. Acta 24, 545–556.

Southgate, H.N., 1995. Prediction of wave breaking processes at the coastline. In: Rahman, M. (Ed.), Advances in Fluid Mechanics, vol. 6. Computational Mechanics Publications, Southampton, UK.

Southgate, H.N., Wallace, H.M., 1994. Breaking wave persistence in parametric surf zone models. Proc. Coastal Dynamics '94. ASCE, New York, pp. 543–555.

Stive, M.J.F., 1985. A scale comparison of wave breaking on a beach. Coast. Eng. 9, 151–158.

Thompson, E.F., Vincent, C.L., 1984. Shallow water wave height parameters. J. Waterw., Port, Coast. Ocean Eng. 119, 293–298.

Thornton, E.B., Guza, R.T., 1986. Surf zone longshore currents and random waves: field data and models. J. Phys. Oceanogr. 16, 1165–1178.

Van Rijn, L.C., Wijnberg, K.M., 1996. One-dimensional modelling of individual waves and wave-induced longshore currents in the surf zone. Coast. Eng. 28, 121–145.

C Description of Testcases for Dune Erosion Study

Apart from the main criterion (a representative selection of dune erosion experiments) the selection was also determined by:
1. measured initial and final profile,
2. measured wave heights along cross-shore profile,
3. random waves,
4. return flow and concentration measurements,
5. only large scale flume tests are considered (flume larger then 150 m).

These criteria have resulted in the following selection:

Table C.1 Overview of selected large scale flume experiments.

Nr.	Source	Test	Profile Characteristics	Hydraulic Conditions
#01	M1797-'82	T1	Steep / gully profile	Varying
#02	M1263-'84	T1	Relative steep	Constant
#03		T2	Flatter (reference)	Constant
#04		T3	as T2	Varying / storm surge
#05		T4	Delfland	Varying / storm surge
#06		T5	miscallaneous profile	Constant
#07	GWK-'96/97	A9	Equilibrium / 1:20	Constant
#08		B2	Equilibrium / 1:10	Constant
#09		C2	Equilibrium / 1:5	Constant
#10		H2	Equilibrium / 1:15	Constant

In the following sub-sections the experiments are briefly described. Most text is extracted from documents provided by dr. H.J. Steetzel. Some figures have been taken from earlier studies in which DUROSTA was evaluated. Thus model results included in some figures are from the DUROSTA model.

Experiment #01: M1797, Test T1

In order to determine the impact of an existing dune revetment at a coastal section of the Noorderstrand at Schouwen on the ultimate amount of dune erosion during a specific design storm surge, tests with and without a revetment have been conducted in the Delta flume (WL | Delft Hydraulics, 1982). The outcome of the test without a structure, viz. test T1, is discussed in the following.

The hydraulic conditions, viz. water level $h(t)$, (significant) wave height $H_{sig}(t)$ and (peak) wave period $T_p(t)$ during both tests are shown in Figure C.1.

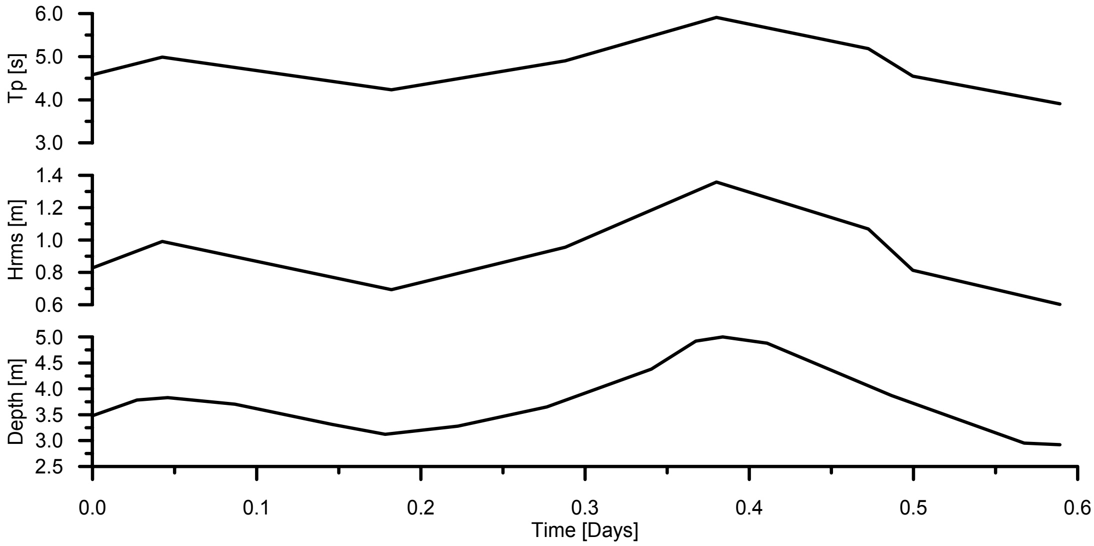

Figure C.1 Hydraulic conditions used in test T1 of the M1797-series.

Figure C.2 shows the initial and final cross-shore profile after *14.1* hours of wave attack for test T1.

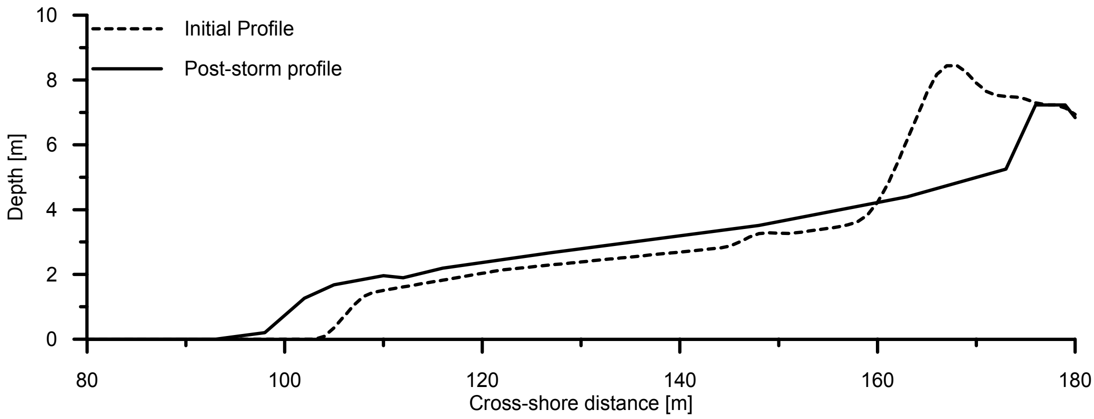

Figure C.2 Initial and measured post-storm profiles for test T1 of the M1797-series.

Experiments #02 - #06: M1263, Test T1- Test T5

This test programme was conducted in order to verify the scale relations and the reliability of the existing dune erosion model DUROSTA (WL | Delft Hydraulics, 1984). In total five different tests were carried out.

Two tests, viz. test T1 and T2, were conducted using constant hydraulic conditions, whereas a third test was performed to investigate the relative effect of the naturally varying water level. In test T4, the storm surge of 1953 was reproduced with a depth scale factor of $n_d = 3.27$, while the last test can be considered as a full scale replica of a moderate storm in nature.

A brief description of all tests is presented below.

Table C.2 Overview of the tests of the M1263–III-series.

test	hydraulic conditions	h (m)	H_{sig} *) (m)		T_p (s)	Brief description
T1	constant	*4.20*	*1.50*	*1.72*	*5.4*	Steep profile (1 : 60)
T2	constant	*4.20*	*1.50*	*1.70*	*5.4*	Less steep (1 : 90); reference test
T3	varying	< *4.20*	< *1.50*	-	< *5.4*	as test T2 with varying conditions
T4	varying	< *4.20*	< *1.85*	-	< *5.0*	'Delfland'-profile for 1953-surge
T5	constant	*5.00*	*2.00*	*2.86*	*7.6*	Arbitrary profile

*) Second number refers to estimated actual condition.

The second wave height is the actual wave height at the location of the wave board, as determined from a large number of wave height measurements in the flume. The procedure followed to obtain this number is presented in (Steetzel, 1990). It will be obvious that this magnitude has been used as a boundary condition for the subsequent verification of the mathematical model.

For the moulding of the profile dune sand with $D_{50} = 225$ mm has been used, having an estimated fall velocity of $w_s = 0.0268$ m/s. More details on the individual tests are summarised hereafter.

An overview of the flume for Test T1 is shown in Figure C.3. The slope of the foreshore is $1{:}60$ which is about three times as steep as the average prototype slope, being $1{:}180$ on the average. The test duration was 10 hours. Wave generation was stopped at $t = 0.1$, 0.3, 1.0, 3.0, 6.0 and 10.0 hours for profile recording by echo sounding in three parallel rays along the flume. The latter result, viz. the post-storm profile present at $t = 10.0$ hours, is also shown in the figure.

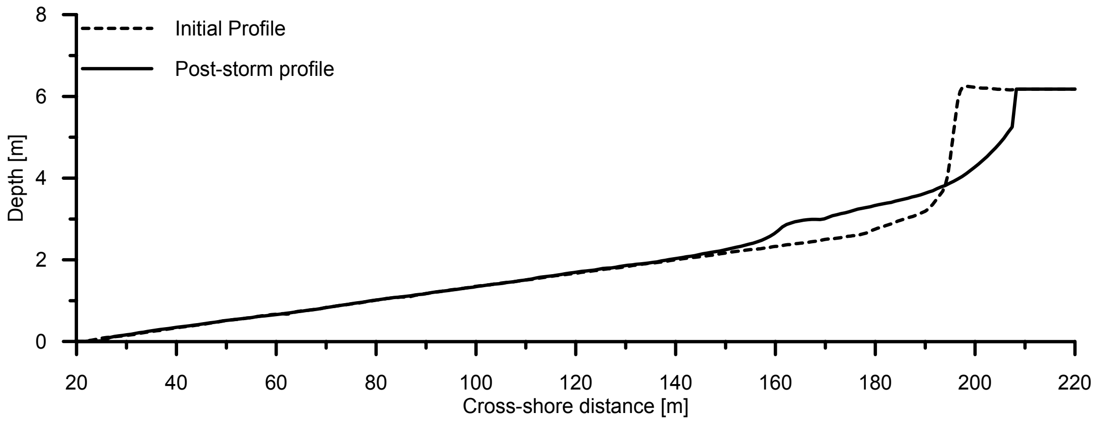

Figure C.3 Overview of profiles for test T1 of the M1263-III-series.

An overview of the final profile at $t = 10.0$ hours is shown in Figure C.4.

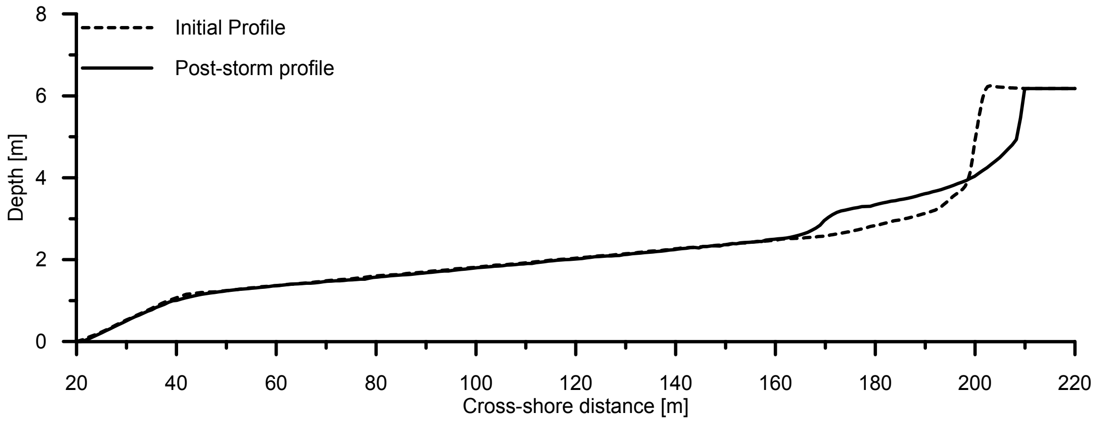

Figure C.4 Overview of profiles for test T2 of the M1263-III-series.

It is noted that the agreement in the final volumes present in the under water profile is the result of the calibration.

The erosion quantities are summarised Table C.3.

Table C.3 Summary of ultimate dune erosion quantities for model tests of the M1263-III-series.

test	time (hrs)	Measurements				
		A_d (m^3/m^1)	A_{er} (m^3/m^1)	A_{ac} (m^3/m^1)	(A_{er} - A_{ac}) (m^3/m^1)	(DA / A_{er}) (%)
T1	*10.0*	*19.8*	*20.7*	*19.1*	*1.6*	*7.7*
T2	*10.0*	*14.8*	*15.1*	*14.1*	*1.0*	*6.6*
T3	*19.25*	*9.6*	*9.7*	*9.3*	*0.4*	*4.1*
T4	*17.0*	*7.6*	*7.6*	*7.3*	*0.3*	*4.0*
T5	*6.0*	*49.4*	*51.3*	*43.8*	*7.5*	*14.6*

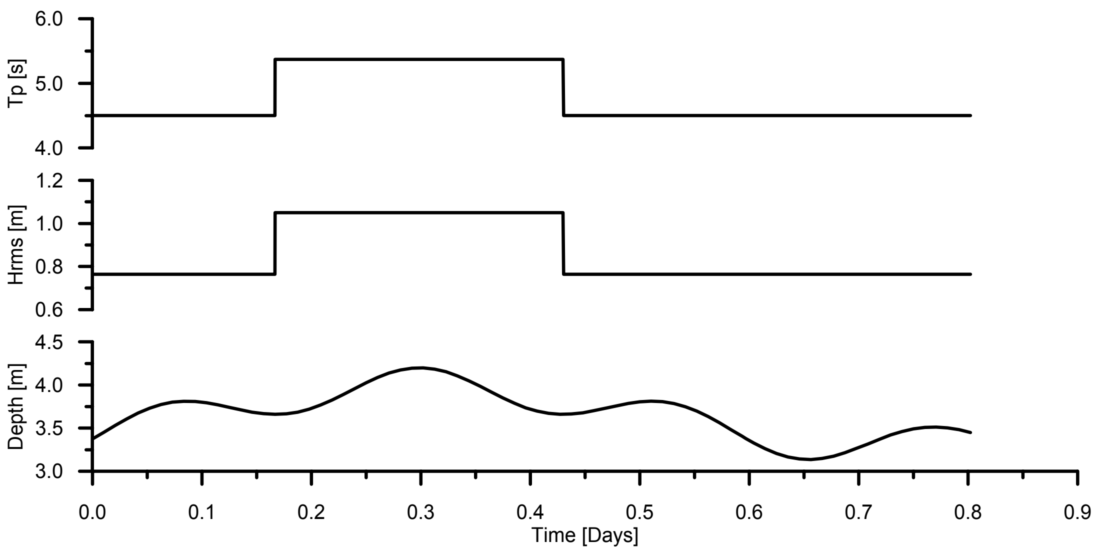

Figure C.5 Hydraulic conditions used for test T3 of the M1263-III-series.

In Test T3, the initial profile of test T2 was tested again but now with a natural storm surge hydrograph and naturally varying wave height and wave period instead of fixed hydraulic conditions. The water level and wave conditions present during this test are shown in Figure C.5.

As can be observed, an additional storm phase has been introduced, ranging from t_6 to t_7. An overview of the flume including the cross-shore profile after 19.25 hours ($= t_7$) is shown in Figure C.6.

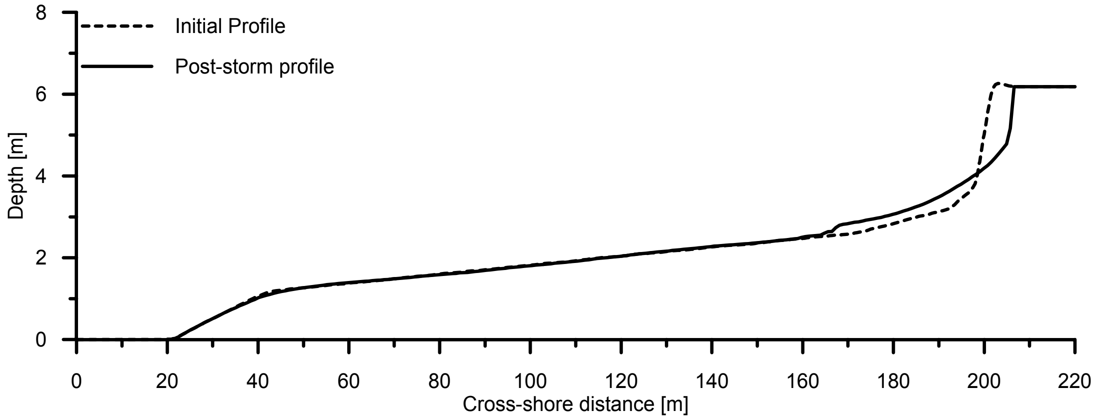

Figure C.6 Overview of profiles for test T3 of the M1263-III-series.

From the physical model tests it was concluded that the effect of a period of about 2.0 to 2.5 hours of constant (maximum) surge conditions is equivalent to the effect of a naturally varying storm surge hydrograph.

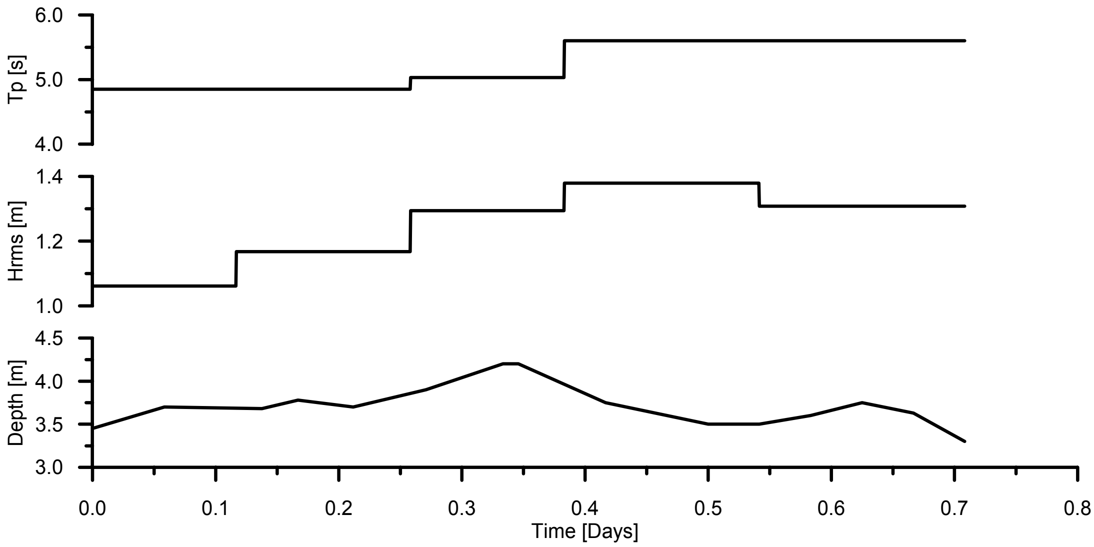

Figure C.7 Hydraulic conditions used for test T4 of the M1263-III-series.

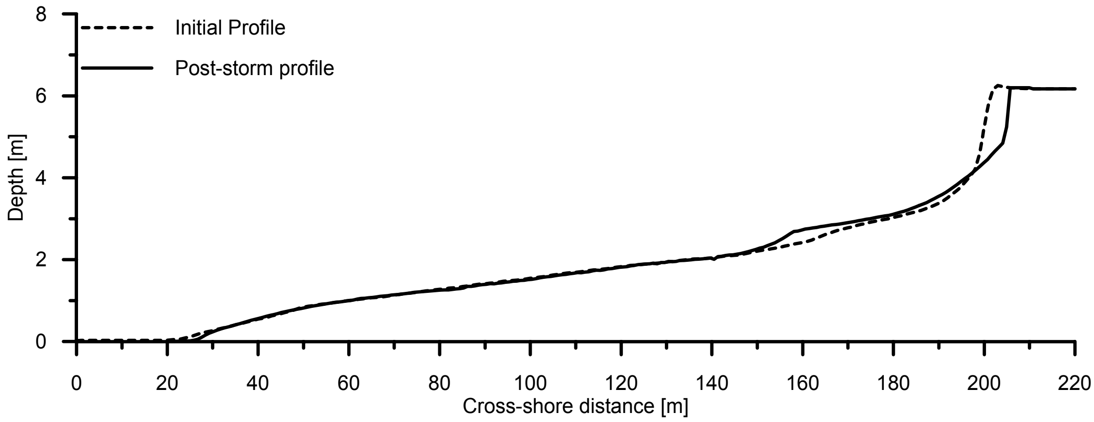

Figure C.8 Overview of profiles for test T4 of the M1263-III-series.

The hydraulic conditions present during Test T4 are shown in Figure C.7, whereas an overview of the initial 'Delfland'-profile is shown in Figure C.8.

It is noted that the (relative) apparent sediment loss for test T1 through T4 reduces systematically due to an overall increased compaction of the sand in the flume.

In the last test, viz. Test T5, a 'full scale' reproduction of the conditions during a moderate storm surge in situ was investigated. An overview of the flume, including the profiles after 1.0 and 6.0 hours, is shown in Figure C.9.

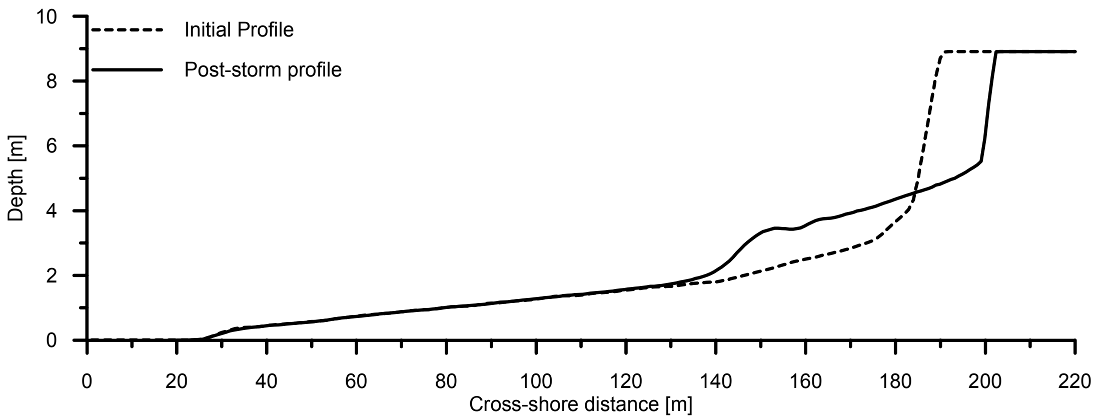

Figure C.9 Overview of profiles for test T5 of the M1263-III-series.

The amounts of erosion involved are summarised in Table C.3. Since a significant amount of extra sand was added for this test, the apparent sediment loss did increase dramatically.

Experiments #07 - #10: GWK1998, Tests A9, B2, C2 and H2

Within the framework of the SAFE-project, tests have been performed in the Large Wave Flume of the Leichtweiss-Institute in Hanover to investigate the development of beach profiles under storm conditions (Dette et al., 1998a and 1998b).

In the LWF-tests, data on beach profile change have been generated as a function of waves and water levels. For this purpose the slope of the beach above the normal water level was defined as the dominant variable. The first phase of the experiments focused on beach profiles developing under normal wave and water level conditions, whereas the second phase concentrates on changes of the profiles due to a storm surge at raised water levels with the aim to study erosion of the initially dry beach by storm surges.

Initial beach slopes used during the tests range from 1:20 (test series A), 1:10 (B), 1:5 (C) and 1:15 (H) above a underwater equilibrium profile. First the beach is attacked by waves with H_s = 0.65 m, representing normal weather conditions. These conditions are continued for a time period between 5.00 and 11.33 hours. During this interval the beach profile slowly adjusts to this hydraulic condition, but large profile changes do not occur. During the second part of the experiment the water level is raised 1 meter and larger waves with H_s = 1.20 m are generated, representing storm surge conditions.